3-21-2014

# Contribution of Lipophilic Secondary Metabolites to the Toxicity of Strains of Freshwater Cyanobacterial Harmful Algal Blooms, Identified Using the Zebrafish (Danio rerio) Embyo as a Model for Vertebrate Development

Asha D. Jaja-Chimedza
ajaja001@fiu.edu

**DOI:** 10.25148/etd.FI14071128

FLORIDA INTERNATIONAL UNIVERSITY

Miami, Florida

# CONTRIBUTION OF LIPOPHILIC SECONDARY METABOLITES TO THE TOXICITY OF STRAINS OF FRESHWATER CYANOBACTERIAL HARMFUL ALGAL BLOOMS, IDENTIFIED USING THE ZEBRAFISH (*DANIO RERIO*) EMBRYO AS A MODEL FOR VERTEBRATE DEVELOPMENT

A dissertation submitted in partial fulfillment of the

requirements for the degree of

DOCTOR OF PHILOSOPHY

in

CHEMISTRY

by

Asha Jaja-Chimedza

2014

To: Interim Dean Michael R. Heithaus
College of Arts and Sciences

This dissertation, written by Asha Jaja-Chimedza, and entitled Contribution of Lipophilic Secondary Metabolites to the Toxicity of Strains of Freshwater Cyanobacterial Harmful Algal Blooms, Identified Using the Zebrafish (*Danio rerio*) Embyo as a Model for Vertebrate Development, having been approved in respect to style and intellectual content, is referred to you for judgment.

We have read this dissertation and recommend that it be approved.

_____
Miroslav Gantar

_____
Kevin O'Shea

_____
Kathleen Rein

_____
Stanislaw Wnuk

_____
John Berry, Major Professor

Date of Defense: March 21, 2014

The dissertation of Asha Jaja-Chimedza is approved.

_____
Interim Dean Michael R. Heithaus
College of Arts and Sciences

_____
Dean Lakshmi N. Reddi
University Graduate School

Florida International University, 2014

DEDICATION

To Science…

ACKNOWLEDGMENTS

A special thanks to my advisor, Dr. John Berry without whom this project would never have been possible. As well as serving as my supervisor and advisor he also encouraged me, challenged me and deprived me of many hours of sleep. Thank you to my committee members, Dr. Miroslav Gantar, Dr. Kevin O'Shea, Dr. Kathleen Rein, and Dr. Stanislaw Wnuk for constantly pushing me to achieve my best.

A big thank you to Dr. Gantar and his lab for constantly providing me with the cyanobacterial cultures needed to carry out my project. I would also like to thank Dr. Patrick Gibbs at the University of Miami, RSMAS for his expertise and assistance with the zebrafish maintenance, breeding, and bioassay. Thank you very much to Dr. William Louda at Florida Atlantic University for his expertise in carotenoid chemistry and the analysis and identification of one of the carotenoids. I would also like to thank those persons within Dr. Gardinali's and Dr. Jaffe's lab who assisted with the analysis of my samples on their various instruments.

To my family who were extremely supportive and patient with me throughout this process, never allowing me to give anything less than my best efforts, pushing me to go that extra mile, and constantly asking me "when are you going to be done?", thank you very much To my friends and co-workers, I thank you all.

A final thanks to the funding sources; NIH-NIEHS Grant Funding R21 Exploratory/Developmental Grant (ES014037).

ABSTRACT OF THE DISSERTATION

CONTRIBUTION OF LIPOPHILIC SECONDARY METABOLITES TO THE TOXICITY OF STRAINS OF FRESHWATER CYANOBACTERIAL HARMFUL ALGAL BLOOMS, IDENTIFIED USING THE ZEBRAFISH (*DANIO RERIO*) EMBRYO AS A MODEL FOR VERTEBRATE DEVELOPMENT

by

Asha Jaja-Chimedza

Florida International University, 2014

Miami, Florida

Professor John Berry, Major Professor

Cyanobacteria (blue-green algae) are known to produce a diverse repertoire of biologically active secondary metabolites. When associated with so-called harmful algal blooms, particularly in freshwater systems, a number of these metabolites have been associated - as toxins, or commonly cyanotoxins - with human and animal health concerns. In addition to the known water-soluble toxins from these genera (i.e. microcystins, cylindrospermopsin, and saxitoxins), our studies have shown that there are metabolites within the lipophilic extracts of these strains that inhibit vertebrate development in zebrafish embryos. Following these studies, the zebrafish embryo model was implemented in the bioassay-guided purification of four isolates of cyanobacterial harmful algal blooms, namely *Aphanizomenon*, two isolates of *Cylindrospermopsis*, and *Microcystis*, in order to identify and chemically characterize the bioactive lipophilic metabolites in these isolates.

We have recently isolated a group of polymethoxy-1-alkenes (PMAs), as potential toxins, based on the bioactivity observed in the zebrafish embryos. Although PMAs have been previously isolated from diverse cyanobacteria, they have not previously been associated with relevant toxicity. These compounds seem to be widespread across the different genera of cyanobacteria, and, according to our studies, suggested to be derived from the polyketide biosynthetic pathway which is a common synthetic route for cyanobacterial and other algal toxins. Thus, it can be argued that these metabolites are perhaps important contributors to the toxicity of cyanobacterial blooms. In addition to the PMAs, a set of bioactive glycosidic carotenoids were also isolated because of their inhibition of zebrafish embryonic development. These pigmented organic molecules are found in many photosynthetic organisms, including cyanobacteria, and they have been largely associated with the prevention of photooxidative damage. This is the first indication of these compounds as toxic metabolites and the hypothesized mode of action is via their biotransformation to retinoids, some of which are known to be teratogenic. Additional fractions within all four isolates have been shown to contain other uncharacterized lipophilic toxic metabolites. This apparent repertoire of lipophilic compounds may contribute to the toxicity of these cyanobacterial harmful algal blooms, which were previously attributed primarily to the presence of the known water-soluble toxins.

TABLE OF CONTENTS

CHAPTER PAGE

LIST OF TABLES

TABLES PAGE

LIST OF FIGURES

FIGURES PAGE

# CHAPTER 1

INTRODUCTION

### 1.1. Cyanobacteria Harmful Algal Blooms

Cyanobacteria, despite being commonly referred to as 'blue-green algae', are prokaryotic photosynthetic bacteria that are ubiquitous in nature with fossil records dating back more than 3 billion years being one of the oldest life forms on earth. Cyanobacteria are natural inhabitants of rocks, soil, and all water sources, where they can occur as free-living planktonic cells or form symbiotic phototrophic biofilm. The surface waters of both marine and freshwater systems, tends to host the growth of cyanobacteria whenever the conditions of light, temperature, and nutrients (nitrogen and phosphorus) are conducive, where they can aggregate to form visible masses known as "blooms", primarily observed during the hot summer months. In addition to forming these "surface scum" in freshwater and brackish water reservoirs, cyanobacteria can also form "dense benthic mats" in marine and freshwater reservoirs. These blooms are then called "harmful algal blooms" (HAB; more specifically cyanoHABs) when they are associated with the production of toxic secondary metabolites which causes serious health problems in humans and animals (Paerl *et al.*, 2011).

Some of the most commonly occurring cyanobacterial blooms in freshwater sources belong to genera such as *Anabaena*, *Aphanizomenon*, *Cylindrospermopsis*, *Nodularia*, *Microcystis, Plantothrix (Oscillatoria)*, and *Plectonema (Lyngbya)*. These cyanoHABs produce many different toxins that cause various health effects ranging from mild skin irritations to more severe neurotoxicological effects and even death. Exposure routes to these toxins include swimming or other recreational activities in contaminated water sources, ingestion of contaminated drinking water, or consumption of foods in which there has been bioaccumulation of the toxins. As a result of the large amounts of

nutrients (nitrates and phosphates) being released into freshwater systems by various anthropogenic activities, there has been an increase in the eutrophication and hypertrophication of these systems. In addition, it is thought that with the changing of the global climate (increasing atmospheric $CO_2$ and temperature) the conditions are more favorable to the growth and proliferation of these HABs (Paerl *et al.*, 2011). As such these cyanoHABs are a major environmental and health problem around the world, particularly because of the production of various toxins including the known commonly studied toxins and those toxins which still remain unknown.

### 1.2. Cyanobacterial Secondary Metabolites (or Cyanobacterial Toxins)

As a result of the long evolutionary history of cyanobacteria, they have developed morphological, physiological, and ecological adaptability to geochemical and ecological changes in their environment. Cyanobacteria produce various types of secondary metabolites (usually genera-, species-, and strain-specific) which allow them to persist under harsh conditions such as high herbivory and extreme nutrient and light conditions (Yadav *et al.*, 2011). These secondary metabolites can be classified into groups according to the functions of the compounds, having both positive and negative effects, such as antiviral compounds, grazer/feeding deterrents, antimicrobial compounds, anticancer compounds, protease inhibitors, photoprotective compounds, and cyanotoxic compounds (Yadav *et al.*, 2011). Cyanobacterial toxins are referred to as such because of the negative health effects that are associated with their exposure to humans and animals.

Table 1.1 provides a list of the various known cyanobacterial toxins according to their chemical composition and also includes their toxicological classification, and the

genera from which they are produced. The toxicological classification is also included for each of the cyanotoxins based on their action on principal target organs and includes hepatotoxins, neurotoxins, dermatotoxins, and endotoxins. Even though these toxins might have the same target organ, they are structurally different and as such have different mechanism of action with some toxins producing the similar effects (e.g., neurotoxins causing respiratory paralysis).

Table 1. 1: Cyanobacterial Toxins, Their Toxicological Classification, Toxin Producing Genera, and Mode of Action

| Class of Cmpds | Toxin/Toxin Group | T.C. | Toxin-producing genera | Mode of Action |
|---|---|---|---|---|
| Cyclic Peptides | Microcystins | Hepatotoxins | *Microcystis, Anabaena, Oscillatoria, Nostoc, Anabaenopsis, Planktothrix*, others | Inhibits serine/threonine protein phosphatases 1 and 2A |
| | Nodularins | Hepatotoxins | *Nodularia* | Inhibits serine/threonine protein phosphatases 1 and 2A |
| Alkaloids | Anatoxin-a, Homoanatoxin-a | Neurotoxins | *Anabaena*, *Aphanizomenon, Oscillatoria, Microcystis*, *Phormidium, Cylindrospermum*, *Raphidiopsis*, | Neuromuscular blocking agent |
| | Anatoxin-a(s) | Neurotoxins | *Anabaena* | Inhibits neurotransmission |
| | Saxitoxins | Neurotoxins | *Aphanizomenon*, *Anabaena*, *Lyngbya*, *Cylindrospermopsis* | Blocks sodium channels in nerve cells |
| | Cylindrospermopsin | Hepatotoxins | *Anabaena, Aphanizomenon, Cylindrospermopsis, Raphidiopsis* | Inhibits protein synthesis |
| | Lyngbyatoxin | Dermatoxin | *Lyngbya* | Inflammatory and tumor promoting via activation of protein kinase C |
| | Aplysiatoxin | Dermatoxin | *Lyngbya, Oscillatoria* | Activation of protein kinase C |
| Others | β-methylamino-L-alanine (BMAA) | Neurotoxins | *Nostoc, Fischerella, Symploca, Synechococcus, Trichodesmium* and many others | Glutamate receptor agonist, induction of oxidative stress, and other unknown mechanisms |
| | Lipopolysaccharides | Endotoxins | *Microcystis*, *Oscillatoria* | Stimulation of inflammatory responses |

Note: Updated from Codd et al, 1999; Stewart et al, 2006.
T.C. – toxicological classification

### *1.2.1. Hepatotoxic Cyclic Peptides*

**Microcystin** (MCYST) is one of the most commonly studied cyanotoxins and is a part of a family of cyclic heptapeptides with over 70 different variants currently isolated from various cyanobacterial strains (Yadav *et al.*, 2011). These variants of MCYST are usually seen by the different amino acids at the $R_1$ and $R_2$ positions (Figure 1.1), with the most commonly isolated MCSYTs being microcystin-LR, -RR, and -YR in the $R_1$ and $R_2$ positions respectively, where L is leucine, R is arginine, and Y is tyrosine (Izaguirre *et al.,* 2007, Jungblut & Neilan, 2006). Microcystin was first isolated from the freshwater cyanobacterium *Microcystis aeruginosa* and has subsequently been isolated from other cyanobacterial genera including *Anabaena, Oscillatoria, Nostoc, Anabaenopsis, Planktothrix*, and others (Prieto *et al.*, 2006; Izaguirre *et al.,* 2007; Sangolkar *et al.,* 2006; Carmichael, 1992).

Microcystins are potently toxic, and exposure to these toxins has been associated with animal and human poisoning, and in severe cases, has led to death in vertebrate animals and humans (Wiegand *et al.,* 2005). They are known to cause liver damage through the inhibition of type 1 and 2A serine/threonine protein phosphatases, which leads to excessive phosphorylation of cytoskeleton filaments (Dai *et al.*, 2007). They also promote the growth of tumors in the liver and colon, and can produce allergic and gastrointestinal reactions through long term exposure to low levels (Dai *et al.,* 2007).

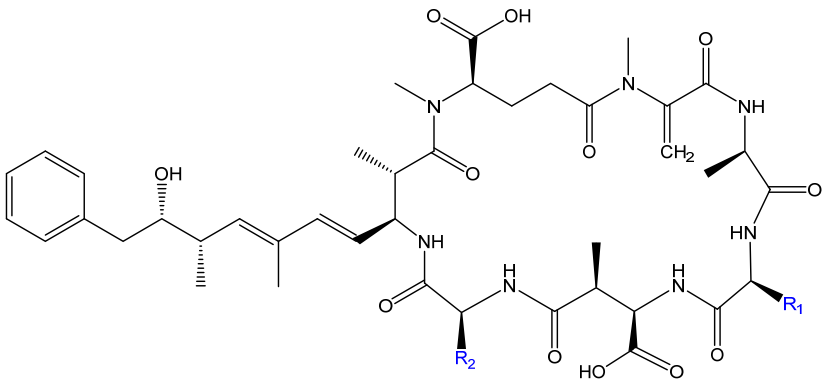


Figure 1. 1: General structure of microcystin showing the variable R-groups (R1, R2).

**Nodularins** (NOD) are another class of nonribosomal hepatotoxic cyclic peptides that are similar in structure to that of microcystins with less structural variation within the family, and slightly higher water solubility (Figure 1.2). Nodularin is produced by the cyanobacterium, *Nodularia spumigena*, which is commonly found as blooms in the brackish waters of the Baltic Sea. Nodularins are closetly related to MCYSTs (possessing the same Adda moiety) and also act by inhibiting the serine/threonine protein phosphatases type 1 and type 2A (Ohta *et al.,* 1994, Pflugmacher *et al.,* 1998). Nodularin producing *N. spumigena* has been linked to deaths of both domestic and wild animals in regions such as Australia, New Zealand, and the Baltic Sea (Moffitt and Neilan 2004).

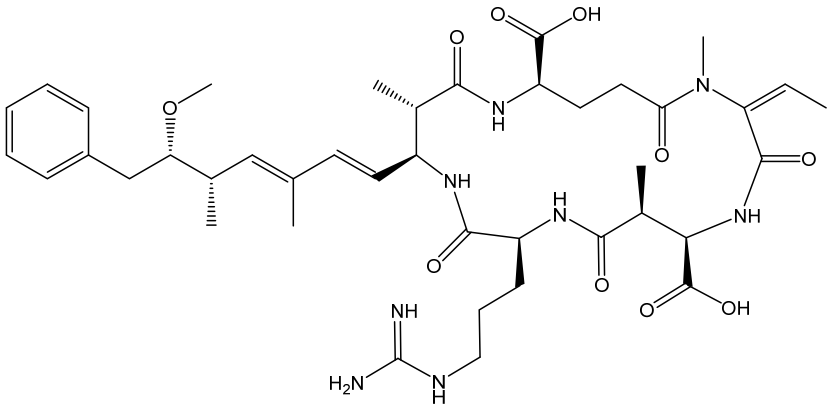


Figure 1. 2: Structure of nodularin

*1.2.2. Neurotoxic Alkaloids*

**Anatoxin-a** (ATX) along with its methylene homologue, homoanatoxin-a (Figure 1.3) are neurotoxic alkaloids that are commonly found in the cyanobacterial genera, *Anabaena* and *Oscillatoria* and have been frequently implicated in the poisoning of birds and mammals (Stewart *et al.*, 2008). Anatoxin-a is a potent nicotinic agonist for the acetylcholine receptor, acting as a postsynaptic, depolarizing, neuromuscular blocking agent (James *et al.,* 1997). Exposure to ATX can cause paralysis of the peripheral skeletal and respiratory muscles, tremors, convulsions, and death (Rogers *et al.,* 2005).

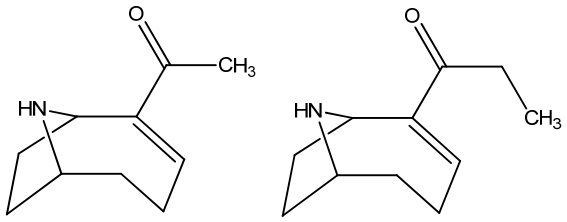


Figure 1. 3: Structure of anatoxin-a (left) and homoanatoxin-a (right)

**Anatoxin-a(s)** (ATS), (s) for salivation, is a naturally occurring organophosphate that is associated with the cyanobacteria *Anabaena flos-aquae*. Despite its name, ATS is a phosphate ester of a cyclic N-hydroxyguanidine and is therefore unrelated to ATX (Figure 1.4). The neurotoxic effects associated with ATS are caused by the irreversible inhibition of acetylcholinesterase, preventing neurotransmission (Devic *et al.,* 2002). The symptoms associated with this toxin include hypersalivation, ataxia, diarrhea, tremors, dyspnea, and cyanosis. It is also responsible for the intoxication of domestic animals (Dittmann and Wiegand, 2006).

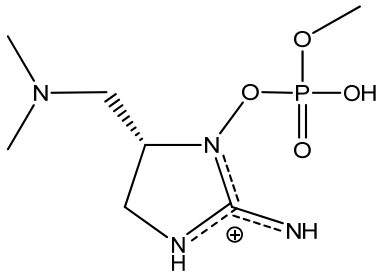


Figure 1. 4: Structure of anatoxin-a(s)

**Saxitoxin** (STX) is a water-soluble neurotoxic alkaloid (Figure 1.5) that along with its analogues, are classified as paralytic shellfish toxins (PSTs) as a result of their involvement in paralytic shellfish poisoning (PSP). There are currently over 20 structural variants of the toxin and they are classified as non-sulfated, singly-sulfated, doubly sulfated, and decarbamoylated, and possessing varying degrees of toxicity. Saxitoxins can be found in both marine (produced by dinoflagellates) and freshwaters (produced by cyanobacteria) being produced by organisms belonging to two different kingdoms. In freshwater, STXs have been isolated from the cyanobacteria *Cylindrosermopsis*, *Anabaena*, *Aphanizomenon*, *Lyngbya*, and *Plantothrix* and in marine environments from the dinoflagellates *Alexandrium*, *Gymnodinium* and *Pyrodinium* (Dittman *et al.*, 2013; Lefebvre *et al.*, 2004). Saxitoxins exhibit their toxicity by reversibly binding to voltage-gated sodium channels resulting in neurotoxic effects including nausea, numbness, ataxia, and paralysis which can lead to death as a result of respiratory failure (Lefebvre *et al.*, 2004).

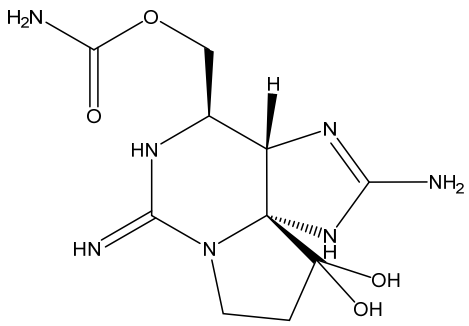


Figure 1. 5: Structure of saxitoxin

*1.2.3. Cytotoxic Alkaloids*

**Cylindrospermopsin** (CYN) is characterized as a hepatotoxic, water-soluble cyclic guanidinium alkaloid which also causes general cytotoxic and neurotoxic effects (Figure 1.6; Ohtani *et al.*, 1992). Cylindrospermopsin was originally isolated from the cyanobacterium belonging to the genera *Cylindrospermopsis* but subsequently found in other freshwater cyanobacterial genera such as *Anabaena*, *Aphanizomenon*, *Lyngbya*, *Raphidiopsis*, and *Umezakia* (Harada *et al.*, 1994; Banker *et al.*, 1997; Li *et al.*, 2001; Seifert *et al.*, 2007). Predominantly, occurrence of CYN has been reported in the tropical and subtropical regions in water reservoirs such as lakes, rivers, and ponds; however reports have indicated their presence in more temperate environments (Neilan *et al.*, 2003; Fastner *et al.*, 2007).

The toxicity of CYN was originally determined because of an outbreak of symptoms of gastroenteritis among more than 100 children from an Aboriginal community on Palm Island in Queensland, Australia. The cause of the illness was subsequently linked to a contaminated water supply (Solomon Dam) containing a dense algal bloom, which contained a strain of *C. raciborskii*. Even though CYN has been

termed a hepatotoxin as a result of its main in vivo effect, it has been shown to target other organs including the lungs, heart, kidneys, adrenal glands, and others (López-Alonso *et al.*, 2013). Considerable efforts have been made to identify the specific toxicity of CYN however these effects are still unclear. The toxicity of CYN is thought to be associated with the inhibition of protein synthesis and glutathione production (Runnegar *et al.*, 2002; Humpage *et al.*, 2005).

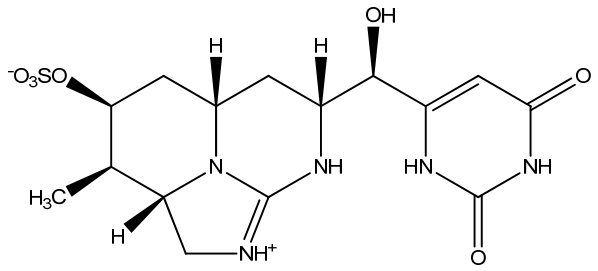


Figure 1. 6: Structure of cylindrospermopsin

*1.2.4. Dermatotoxic Alkaloids*

**Lyngbyatoxin-a** (LTX) is an indole-containing alkaloid, produced by the marine cyanobacterium *Lyngbya majuscula* which is typically found in coastal and estuarine waters of tropical and subtropical environments (Fiure 1.7; Dittman *et al.*, 2013) Lyngbyatoxin is a highly potent skin irritant that is known to cause the condition, Swimmer's Itch, by specific activation of protein kinase C (PKC). Human exposure with the cyanobacteria causes the development of erythema and blisters and has also been found to be highly toxic to fish and other grazer species (Cardellina *et al.*, 1979).

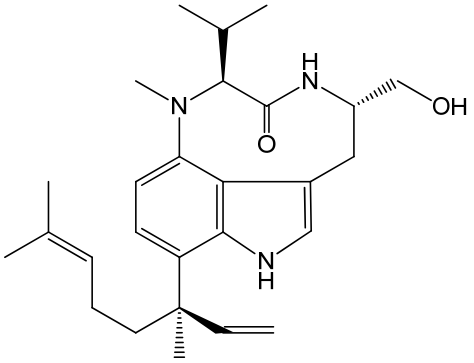


Figure 1. 7: Structure of lyngbyatoxin

**Aplysiatoxin** (APX) (and debromoaplysiatoxin) are phenolic bislactones that along with LTX are thought to be the cause of contact dermatitis associated with *L. majuscula* (Figure 1.8; Moore *et al.*, 1984). In addition to cyanobacteria, APXs have also been detected in the red alga *Gracularia coronopifolia* (Ito & Nagai, 1998). Toxicity of APX also occurs through ingestion and causes symptoms such as vomiting, diarrhea, and bleeding in the small intestine with the suggested mode of action being an activator of protein kinase C (Ito and Nagai, 2000).

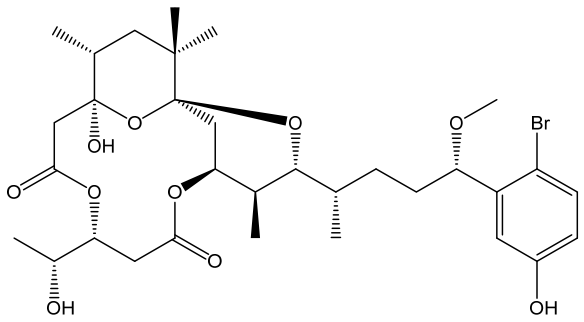


Figure 1. 8: Structure of aplysiatoxin

*1.2.5. Other Cyanobacterial Toxins*

**β-methylamino-L-alanine** (BMAA) is a non-proteinogenic amino acid (Figure 1.9) that was originally isolated from cycads and subsequently isolated from an endophytic cyanobacterium (genus *Nostoc*) that resided in the specialized roots of the Guam cycad plants (Banack *et al.*, 2007). It has since been found in other taxonomic groups of cyanobacteria, both free-living and bloom forming strains. The amino acid is thought to be associated with neurodegenerative diseases such as dementia and amyotrophic lateral sclerosis (ALS) however further research is essential to identifying its mode of action and health risks from environmental exposure (Chiu *et al.*, 2011; Okle *et al.*, 2013).

The mechanism of action of BMAA is still being investigated however there are studies that have indicated that it acts as a glutamate receptor agonist, such as NMDA, AMPA, ionotropic and metabotropic glutamate receptors. It has also been suggest to increasing oxidative stress by the inhibition of the cysteine/glutamate antiporter system which prevents the uptake of cysteine thereby causing depletion in glutathione (Chiu *et al.*, 2011). Continued research is being done to get a better understanding of the mode of action of this neurotoxin and how it relates to neurodegeneration.

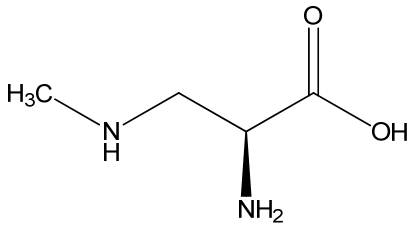


Figure 1. 9: Structure of BMAA

**Lipopolysaccharides** (LPS) are characteristic structural components of the outer membrane of Gram-negative bacteria, including cyanobacteria. The structure of LPS is comprised of four segments covalently linked: lipid A moiety (acylated glycolipid), a core oligosaccharide (made up of an inner and outer segment) and an O-specific chain (carbohydrate polymer on the surface). Cyanobacterial LPSs are thought to be different, both in structure and function, from Gram-negative bacteria, where one study showed that cyanobacterial LPSs lacks significant endotoxin activity due to the structural differences in the lipid A moiety (Stewart *et al.*, 2006). There are limited studies on LPS as cyanobacterial toxins; however some studies have shown that health effects associated with these LPSs have a wide range and can include gastro-intestinal illness, skin rashes, allergy, respiratory disease, headache, fever, and other health incidents (Stewart *et al.,* 2006).

### 1.3. Biosynthetic Pathways of Cyanobacterial Secondary Metabolites

The structures of majority of the cyanobacterial secondary metabolites are peptides, peptide-like structures or polyketides. The common biosynthetic pathways associated with the production of cyanobacterial secondary metabolites are the non-ribosomal peptide synthetase (NRPS) for the peptidic structures, and polyketide synthase (PKS) pathways for the polyketide structures. There is also a hybrid NRPS/PKS pathway that is also involved in the production of the peptidic metabolites (Dittman *et al.*, 2013).

Secondary metabolites that have cyclic or branched-cyclic structures, or small peptides with unusual or modified amino acids typically indicated the involvement of a non-ribosomal biosynthetic pathway. The NRPS biosynthetic pathway can be standalone

or can occur in hybrid enzyme complexes, often with the PKS pathway as a result of the structural and mechanistic similarities of the biosynthetic pathway. Non-ribosomal peptide synthetases are made up of large modular, multi-enzyme complex, in which each module has a role in different stages of the synthesis such as activation, thiolation, modification, and condensation of an amino acid substrate. The organization and order of the NRPS modules within the complex follows the co-linearity rule where it corresponds with that of the amino acid sequence within the peptide product (Dittman *et al.*, 2001).

The other biosynthetic pathway that is commonly observed in cyanobacteria is the PKS pathway which, similar to NRPS, involves a family of modular enzymes which are organized as functional units. Each PKS unit catalyzes specific reactions in the elongation of the polyketide chain with each unit comprising of at least a ketosynthase (KS), acyl transferase (AT) and acyl carrier protein (ACP) domain. The carbon backbone of the polyketides is biosynthesized by decarboxylative condensation of acyl coenzyme A (Acyl-CoA) subunits, typically using acetate as building blocks. Further modification to the backbone can then be made by various subsequent enzyme "modules" (e.g., ketoreductases (KR), dehydrogenases (DH)) into the final biosynthetic product (Snyder *et al.*, 2003).

### *1.3.1. Non-Ribosomal Peptide Synthetase/Polyketide Synthase (NRPS/PKS)*

Most of the biosynthetic pathways involved in cyanobacterial toxin production seem to involve a hybrid NRPS/PKS pathway, including the well-studied hepatotoxic cyclic peptide MCYST and its related pentapeptide NOD, the hepatotoxic alkaloid CYN, and the neurotoxic alkaloid, ATX. The biosynthetic route for the cyclic peptides

(MCYST and NOD) was thought to be similar and feeding experiments as well as their unusual structure suggested that biosynthesis was of non-ribosomal origin (Moore *et al.*, 1991).

The MCYST biosynthetic gene cluster (*mcyS*) is 55kb and comprises of ten genes (McyA-J) with two bidirectional operons (*mcyA-C* and *mcyD-J*). The larger operon (*mcyD-J*) encodes for two NRPS/PKS hybrid (McyE and G) modules and a PKS (McyD) modules involved in the formation of the Adda moiety. This operon also encodes for enzymes involved in the modification (McyF, J, and I) and transport (McyH) of MCYST. Operon *mcyA-C* encodes for three NRPS modules (McyA-C) which is involved in the extension to the heptapeptide as well as subsequent cyclization (Tillett *et al.*, 2000 and Pearson *et al.*, 2010). The course of reactions for MCYST biosynthesis is the same across different genera of cyanobacteria with some variation in domain specificities (Dittman *et al.*, 2013). The proposed biosynthetic pathway for NOD is similar to that of MCYST and the assignments of the enzymes were made on the basis of the homology with the MCYST enzymes combined with bioinformatics analysis. The NOD gene cluster (*ndaS*) is 48kb and consisting of nine open reading frames (ORFs; *ndaA-I*) and are also assembled with a bidirectional operon. The mixed NRPS/PKS (NdaC, D, and F) modules are involved in the formation of the Adda side chain and the two NRPS (NdaA and B) modules are involved in adding the other amino acids for completion of the cyclic pentapeptide (Pearson *et al.*, 2010; Dittman *et al.*, 2013).

The putative biosynthesis genes for CYN were identified in *A. ovalisporum*, with the gene products involved being an amidinotransferase (AoaA), a NRPS/PKS hybrid (AoaB), and a PKS (AoaC) along with other unidentified enzymes (Shalev-Alon *et al.*,

2002). The complete CYN biosynthesis gene cluster from *C. raciborskii* (*cyr*) was subsequently revealed by genome walking to be 43kb and encodes for 15 ORFs and includes all the necessary functions for the biosynthesis, regulation, and transport of the toxin. The corresponding homologs of AoaA, B, and C are CyrA, B, and C respectively. The first step in the biosynthesis involves the formation of the guanidinoacetate catalyzed by CyrA followed by activation via CyrB is thought to be involved in the second step. Subsequent steps involve the elongation and modifications by PKS modules (CyrC, D, E, and F). The ring formations are thought to occur spontaneously, leaving the other gene products for the final biosynthesis, tailoring and transport of the toxin (Mihali *et al.*, 2008).

Biosynthesis of ATX was thought to involve the PKS pathway as a result of feeding experiments that indicated that the carbon skeleton was derived from acetate and glutatmate (Hemcheidt *et al.*, 1995). The ATX biosysnthesis gene cluster (*ana*) encodes for seven proteins (AnaA-G) with the proposed biosynthetic route being in two stages. The first stage in the biosynthesis begins with proline as the starter unit activated by AnaC (a NRPS-type adenylation protein) then subsequently loaded on AnaD (an ACP). The second stage then involves elongation, cyclization, and modification on the PKS (AnaE, F, and G) modules. This proposed biosynthetic route was suggested based on feeding experiments and bioinformatics analysis (Mejean *et al.*, 2010; Mann *et al.*, 2011).

### *1.3.2. Non-ribosomal Peptide Synthetase*

The LTX biosynthesis gene cluster (*ltx*) consists of four genes (ltxA-D) making it the smallest cluster identified in the known cyanobacterial toxin biosynthesis. Feeding

studies of teleocidin (a closely related toxin in *Streptomyces* sp.) helped to identify LTX biosynthesis, revealing the incorporation of L-valine and L-tryptophan into the indolactam ring. The proposed structure involves the condensation of N-methyl-L-Val and L-Trp by LtxA (NRPS) followed by its release by reductive cleavage. LtxB (a cytochrome P450 monooxygenase) is involved with the formation of the indolactam ring with LtxC (phetnytransferase) involved in the generating the quaternary carbon by adding a geranyl group to the indolactam core (Huynh *et al.*, 2010).

### *1.3.3. Other Biosynthetic Pathways*

The biosynthetic route for STX does not follow the typical NRPS or PKS pathway. Radioisotope feeding experiments suggested that arginine, acetate, and methionine methyl were involved in the biosynthesis with subsequent confirmation using a reverse genetics approach (Kellmann & Neilan, 2007). The STX gene cluster (*stx*) was first identified in *C. raciborskii* as a 35kb gene locus with homologous clusters being found in other genera ranging in size from 25.7-36 kb. The toxin profile expressed by these clusters depends on the presence and the organization of the *stx* genes. The initiation of STX biosynthesis is thought to involve the methylation of acetate and a Claisen condensation reaction with arginine by an unusual PKS-like enzyme, StxA. Subsequent reactions include three heterocyclizations and tailoring reactions, which give rise to different isoforms of the toxin (Kellmann *et al.*, 2008).

The biosynthetic pathways for the neurotoxic, BMAA and the dermatotoxin, APX have yet to be elucidated.

### 1.4. Zebrafish Embryo Model

Zebrafish (*Danio rerio*) are small freshwater fish that have been an integral part of laboratory studies for the past few decades especially as it relates to the effects of various chemicals on developmental processes and identifying the cellular and molecular mechanisms involved. There are many attributes of the zebrafish that makes its use suitable as a developmental model such as their small size, ease of husbandry, high fecundity, transparent chorion, and rapid embryonic development. Zebrafish mating and breeding can occur almost all year round producing a large number of eggs (hundreds and sometimes thousands) with one breeding. The embryos are very small (about 1mm in diameter) and at 7 days post fertilization (dpf) can grow up to about 4 mm in length which allows for the use of multiple embryos with each exposure and use in high-throughput exposures, using minimal amounts of toxicant. Additionally, embryos can survive on its yolk for up to 7dpf, so exposure studies can be done without the complication of added food. The embryos develop in a transparent chorion making the examination and monitoring of the developmental features easily achieved using a dissecting light-microscope. Zebrafish undergo rapid embryonic development (See Figure 1.10) with most of the internal organs being fully developed by 96 hours post fertilization (hpf), which therefore produces a quick response with exposure studies. Even though zebrafish are not the only teleost fish that possess these characteristics, the added advantage to using the zebrafish above these other teleost fish lies in the completely elucidation of the genome which allows them to be used for additional studies, including genetic studies.

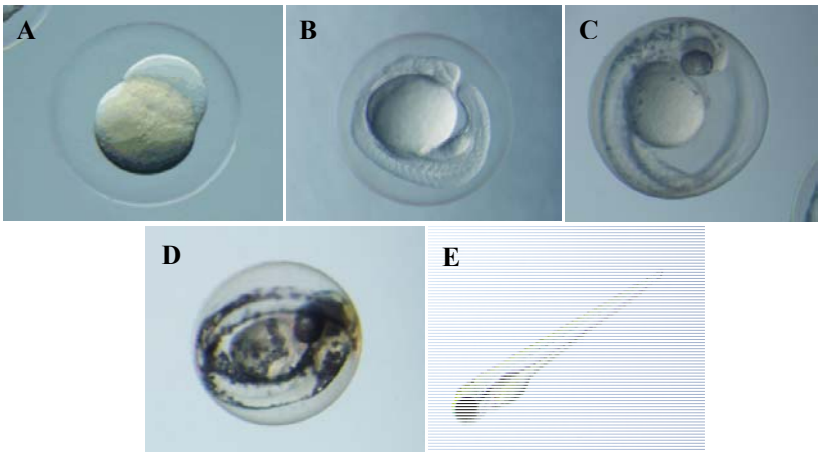


Figure 1. 10: Stages of development of the zebrafish embryo taken using an Olympus camera attached to a dissecting microscope: A - Newly fertilized embryo, B - 1dpf, C - 2dpf, D – 3dpf, E - newly hatched embryo.

The zebrafish has been implemented as a model for various studies as a result of their applicable attributes to different areas of study. One of these has been the use of zebrafish as a model of vertebrate development (Oberemm *et al.,* 1997; Papendorf *et al.,* 1997; Veldman *et al.,* 2008). It has also been an ideal genetic system for the study of developmental and human disease (Dodd *et al.,* 2000; Zhu & Zon, 2002), including neurological diseases (Best *et al.,* 2008) and developmental neurotoxicology (Linney *et al.,* 2004). More recently, the zebrafish has been used for drug screening and discovery, especially in the area of cardiovascular drug discovery (Rocke *et al.,* 2009). The zebrafish model has also been used for toxicological studies of various natural occurring toxins, specifically in the identification and characterization of developmental toxins from marine dinoflagellates and cyanobacteria (Berry *et al.*, 2007) as well as the toxic effects of cylindrospermopsin (Berry *et al.*, 2009). They have also been used to study selected detoxifying enzymes in response to various toxins, such as microcystin (Wiegand *et al.*,

1999), lipopolysaccharides in conjunction with microcystin (Best *et al.*, 2002), and natural organic matter on microcystin toxicity (Cazenave *et al.*, 2006).

### *1.4.1. As a model for vertebrate development and toxicological studies*

Much research has been carried out using the zebrafish as a model for toxicological studies of various natural occurring toxins. The zebrafish embryo model has been previously used in the study of several of the known toxins from cyanobacteria (e.g. Lefebvre *et al.*, 2004; Wang *et al.*, 2005; Berry *et al.*, 2009). Wang *et al.* (2005) carried out a study to analyze the effects of microcystin on zebrafish embryos. During the study, it was observed that microcystin was not taken up by the embryo, and as such microinjections of embryos were required, after which the effects of the toxin became apparent. A similar study was done with cylindrospermopsin, showing that microinjection was also required in order to observe the effects of the toxin (Berry *et al.*, 2009). Even though these toxins are water-soluble in nature, there seems to be some prevention in the uptake of these toxins in the embryo. Within the same study, Berry *et al.* (2009) tested the lipophilic extracts of eight different isolates of cyanobacteria, including cylindrospermopsin-producing *C. raciborskii* and *A. ovalisporum* and non-cylindrospermopsin producing *C. raciborskii*, and showed that there were developmental effects on the zebrafish embryos. These studies showed that the compounds responsible for the bioactivity were unrelated to the known toxins from those strains of cyanobacteria, which is evident because of the apparent lipophilic nature of the bioactive extract, and as bioactivity was seen in non-cylindrospermopsin producing strains of cyanobacteria.

*1.4.2. Bioassay-guided fractionations using zebrafish embryos*

The zebrafish embryo has been previously used in the bioassay-guided fractionations of bioactive metabolites from various sources as a model for vertebrate development as it relates to inhibition of development and as a model for natural product discovery (Crawford *et al.*, 2011; Liu *et al.*, 2011; Han *et al.*, 2012) as it relates to inhibition of angiogenesis. This model has also been implemented in the screening of small molecules for the discovery of cardiovascular drugs (Novodvorsky *et al.*, 2013).

## 1.5. Research Objectives

Cyanobacteria are known to produce a diverse repertoire of biologically active secondary metabolites. When associated with so-called "harmful algal blooms", particularly in freshwater systems, a number of these metabolites have been associated - as "toxins", or commonly "cyanotoxins" - with human and animal health concerns (Valério *et al.*, 2010; Carmichael, 2008; Ferrão-Filho and Kozlowsky-Suzuki, 2011). It is notable, although perhaps not surprising, that all of these recognized toxins are generally polar and water-soluble metabolites. Previous studies have identified the presence of uncharacterized toxic lipophilic metabolites in toxic and non-toxic strains of cyanoHABs which may give rise to the toxigenicity of the species (e.g. Falch *et al.*, 1995; Nogueira *et al.*, 2006; Berry *et al.*, 2009).

Recently, Berry *et al.* (2009) showed that lipophilic extracts (not containing CYN or STX) from *C. raciborskii* and *A. ovalisporum* inhibit the development of zebrafish embryos. Additionally, a screening was done with the lipophilic extracts of other cyanobacterial isolates, including a few cyanoHABs, which also showed the bioactivity

of the previously identified isolates as well as bioactivity with other cyanobacterial isolates (Table 1.1). Over thirty (30) isolates of cyanobacteria and green algae were obtained and the lipophilic extracts were screened at a representative low and high dosage for bioactivity using the zebrafish embryo bioassay. The extracts from ten isolates of cyanobacteria and green algae showed mortality and inhibition of development at sub-lethal dosages up to 5dpf (Table 1.1). The lipophilic extracts from the cyanobacteria isolates that showed bioactivity were *Aphanothece* 80-12a, *Pseudanabaena* 108-1, *Microcystis* 81-11, *Aphanizomenon* APH, and two isolates of *C. raciborskii* 121-1 and AQS, four of which belong to genera that are considered cyanoHABs. The lipophilic extracts from the green algae that showed bioactivity were *Chlamydomonas* 80-1, *Kirchneriella* 104-7, and two different isolates of *Scenedesmus* 79-1 and 80-15.

Table 1. 2: Cyanobacteria and green algae chloroform extracts that were used in the screening against the zebrafish embryos, indicating the ones that showed bioactivity by inhibiting their development.

| **Isolates** | **Chloroform Extracts / µL** | |
|---|---|---|
| | **10** | **100** |
| **Cyanobacteria** | | |
| *Aphanothece* 103-7 | | X |
| ***Aphanizomenon* APH** | X | X |
| ***C. raciborskii* 121-1** | X | X |
| ***C. raciborskii* AQS** | X | X |
| ***Microcystis* 81-11** | X | X |
| *Pseudanabaena* 108-1 | X | X |
| **Green Algae** | | |
| *Chlamydomonas* 80-1 | X | X |
| *Kirchneriella* 104-7 | X | X |
| *Scenedesmus* 79-1 | X | X |
| *Scenedesmus* 80-15 | | X |

Note: Isolates in bold are from genera that are considered cyanoHABs.

*1.5.1. Specific Aims*

In continuity to these preliminary findings, the current study was developed to focus on the identification of these lipophilic bioactive metabolites that contribute to the toxicity of these cyanoHABs. The study therefore implemented the use of the zebrafish embryo bioassay as a model for vertebrate development to guide the isolation of these compounds for subsequent characterization of these 'toxic' lipophilic metabolites. As such, the specific aims were as follows:

a) Isolate and characterize bioactive compounds within the lipophilic extract of known toxigenic strains of freshwater cyanobacteria, namely *Microcystis* spp., *Cylindrospermopsis raciborskii*, and *Aphanizomenon ovalisporum*. The collection sites for the isolates are indicated in the table below.

Table 1. 3: Cyanobacterial isolates used in this study and their sources of origin.

| **Cyanobacterial Isolate** | **Source of Origin** |
|---|---|
| *A. ovalisporum* | Lake Kinneret, Israel |
| *C. raciborskii* 121-1 | Catemaco, Mexico |
| *C. raciborskii* AQS | Townsville, Australia |
| *M. aeruginosa* 81-11 | Bay of Quinte, Lake Ontario |

b) Develop an analytical method to effectively identify and quantify the bioactive compounds and evaluate the occurrence, and possible bioaccumulation, of these compounds in freshwater sources.

   i. A modification to this objective was to evaluate the occurrence of the bioactive compounds in different genera and species of cyanobacteria, since locating freshwater sources known to have these identified and characterized bioactive compounds would be difficult.

ii. An addition to this objective involved doing feeding experiments with $^{13}C$-labeled acetate to test the hypothesis that biosynthesis of the polymethoxy-1-alkenes (PMAs) is via the polyketide biosynthetic pathway.

c) Toxicological characterization of the purified compounds was focused on the developmental defects of the zebrafish including mortality, hatching rates, and inhibition of development.

**References**


1. Banack, S. A.; Johnson, H. E.; Cheng, R.; Cox, P. A. Production of the neurotoxin BMAA by a marine cyanobacterium.*Marine drugs* **2007***, 5*, 180-196.
2. Banker, R.; Carmeli, S.; Hadas, O.; Teltsch, B.; Porat, R.; Sukenik, A. Identification of cylindrospermopsin in Aphanizomenon ovalisporum (Cyanophceae) isolated from Lake Kinneret, Israel. J. Phycol. **1997**, 33, 613–616.
3. Berry, J.; Gantar, M.; Gibbs, P.; Schmale, M. The zebrafish (Danio rerio) embryo as a model system for identification and characterization of developmental toxins from marine and freshwater microalgae. Comp. Biochem. Physiol. C Pharmacol. Toxicol. **2007**, 145, 61–72.
4. Berry, J.; Gibbs, P.; Schmale, M.; Saker, M. Toxicity of cylindrospermopsin, and other apparent metabolites from Cylindrospermopsis raciborskii and Aphanizomenon ovalisporum, to the zebrafish (Danio rerio) embryo. Toxicon **2009**, 53, 289–299.
5. Best J.D.; Alderton, W.K. Zebrafish: An in vivo model for the study of neurological diseases. *Neuropsychiatr Dis Treat* **2008**, 4(3), 567-76
6. Best, J.H.; Pflugmacher, S.; Weigand, C.; Eddy, F.B.; Metcalf, J.S.; Codd, G.A. Effects of enteric bacterial and cyanobacterial lipopolysaccharides, and of microcystin-LR, on glutathione S-transferase activities in zebrafish (*Danio rerio*). *Aquat. Toxicol* **2002**, 60, 223-231
7. Cardellina, J. H.,2nd; Marner, F. J.; Moore, R. E. Seaweed dermatitis: structure of lyngbyatoxin A. *Science* **1979***, 204*, 193-195.

8. Carmichael, W.W. A world overview—One-hundred-twenty-seven years of research on toxic cyanobacteria—Where do we go from here? *Adv. Exp. Med. Biol.* **2008**, *619*, 105–125.

9. Carmichael, W. Cyanobacteria secondary metabolites: the cyanotoxins. *J Appl Bacteriol* **1992**, 72(6), 445-459

10. Cazenave, J.; Bistoni, M.; Zwirnmann, E.; Wunderlin, D.; Wiegand, C. Attenuating effects on natural organic matter on microcystin toxicity in Zebrafish (Danio rerio) embryos. *Envir Toxicol* **2006,** 21(1), 22-32

11. Chiu, A. S.; Gehringer, M. M.; Welch, J. H.; Neilan, B. A. Does α-amino-β-methylaminopropionic acid (BMAA) play a role in neurodegeneration? *International journal of environmental research and public health* **2011***, 8*, 3728-3746.

12. Codd, G.; Bell, S.; Kaya, K.; Ward, C.; Beattie, K.; Metcalf, J. Cyanobacterial toxins, exposure routes and human health. *Eur J Phycol* **1999**, 34, 405-415

13. Crawford, A. D.; Liekens, S.; Kamuhabwa, A. R.; Maes, J.; Munck, S.; Busson, R.; Rozenski, J.; Esguerra, C. V.; de Witte, P. A. Zebrafish bioassay-guided natural product discovery: isolation of angiogenesis inhibitors from East African medicinal plants. *PloS one* **2011***, 6*, e14694.

14. Dai, R.; Liu, H.; Qu, J.; Hou, Y. Cyanobacteria and their toxins in Guanting Resevoir of Beijing, China. *J Hazard Mater* **2008,** 153(1-2), 470-477

15. Devic, E.; Li, D.; Dauta, a.; Henriksen, P.; Codd, G.; Marty, J.; Fournier, D. Detection of Anatoxin-a(s) in Environmental Samples of Cyanobacteria by Using a Biosensor with Engineered Acetylcholinesterases. *App Environ Micro* **2002**, 68, 4102-4106

16. Dittmann, E.; Fewer, D. P.; Neilan, B. A. Cyanobacterial toxins: biosynthetic routes and evolutionary roots. *FEMS Microbiol. Rev.* **2013***, 37*, 23-43.

17. Dittmann, E.; Neilan, B.; Börner, T. Molecular biology of peptide and polyketide biosynthesis in cyanobacteria. *Appl. Microbiol. Biotechnol.* **2001***, 57*, 467-473.

18. Dodd, A.; Curtis, P.; Williams, L.; Love, D. Zebrafish: bridging the gap between development and disease. *Hum Molec Genet* **2000**, 9, 2443-2449

19. Falch, B. S.; König, G. M.; Wright, A. D.; Sticher, O.; Angerhofer, C. K.; Pezzuto, J. M.; Bachmann, H. Biological activities of cyanobacteria: Evaluation of extracts and pure compounds. *Planta Med.* **1995***, 61*, 321-328.

20. Fastner, J.; Rücker, J.; Stueken, A.; Preussel, K.; Nixdorf, B.; Chorus, I.; Koehler, A.; Wiedner, C. Occurrence of the cyanobacterial toxin cylindrospermopsin in northeast Germany. *Environ. Toxicol.* **2007***, 22*, 26-32.

21. Ferrão-Filho, A.; Kozlowsky-Suzuki, B. Cyanotoxins: Bioaccumulation and effects on aquatic animals. *Mar. Drugs* **2011**, 9, 2729–2772.

22. Han, L.; Yuan, Y.; Zhao, L.; He, Q.; Li, Y.; Chen, X.; Liu, X.; Liu, K. Tracking antiangiogenic components from Glycyrrhiza uralensisFisch. based on zebrafish assays using high-speed countercurrent chromatography. *Journal of separation science* **2012***, 35*, 1167-1172.

23. Harada, K.; Ohtani, I.; Iwamoto, K.; Suzuki, M.; Watanabe, M. F.; Watanabe, M.; Terao, K. Isolation of cylindrospermopsin from a cyanobacterium< i> Umezakia natans</i> and its screening method. *Toxicon* **1994***, 32*, 73-84.

24. Hemscheidt, T.; Rapala, J.; Sivonen, K.; Skulberg, O. M. Biosynthesis of anatoxin-a in Anabaena flos-aquae and homoanatoxin-a in Oscillatoria formosa. *Journal of the Chemical Society, Chemical Communications* **1995**, 1361-1362.

25. Humpage, A. R.; Fontaine, F.; Froscio, S.; Burcham, P.; Falconer, I. R. Cylindrospermopsin genotoxicity and cytotoxicity: role of cytochrome P-450 and oxidative stress. *Journal of Toxicology and Environmental Health, Part A* **2005***, 68*, 739-753.

26. Huynh, M. U.; Elston, M. C.; Hernandez, N. M.; Ball, D. B.; Kajiyama, S.; Irie, K.; Gerwick, W. H.; Edwards, D. J. Enzymatic production of (−)-indolactam V by LtxB, a cytochrome P450 monooxygenase. *J. Nat. Prod.* **2010***, 73*, 71-74.

27. Ito, E.; Nagai, H. Bleeding from the small intestine caused by aplysiatoxin, the causative agent of the red alga Gracilaria coronopifolia poisoning. *Toxicon* **2000***, 38*, 123-132.

28. Ito, E.; Nagai, H. Morphological observations of diarrhea in mice caused by aplysiatoxin, the causative agent of the red alga Gracilaria coronopifolia poisoning in Hawaii. *Toxicon* **1998***, 36*, 1913-1920.

29. Izaguirre, G.; Jungblut, A.D.; Neilan, B. Benthic cyanobacteria (Oscillatoriaceae) that produce microcystin-LR, isolated from four reservoirs in southern California. *Water Research* **2007**, 41, 492-498

30. James, K.; Sherlock, I.; Stack, M. Anatoxin-a in Irish freshwater and cyanobacteria, determined using a new fluorimetric liquid chromatographic method. *Toxicon* **1997**, 35, 963-971

31. Jungblut, AD.; Neilan, B. Molecular identification and evolution of the cyclic peptide hepatotoxins, microcystin and nodularin, synthetase genes in three orders of cyanobacteria. *Arch Microbiol* **2006,** 185, 107–114

32. Kellmann, R.; Mihali, T. K.; Jeon, Y. J.; Pickford, R.; Pomati, F.; Neilan, B. A. Biosynthetic intermediate analysis and functional homology reveal a saxitoxin gene cluster in cyanobacteria. *Appl. Environ. Microbiol.* **2008***, 74*, 4044-4053.

33. Kellmann, R.; Neilan, B. A. Biochemical characterization of paralytic shellfish toxin biosynthesis *in vitro*. *J. Phycol.* **2007***, 43*, 497-508.

34. Lefebvre, K. A.; Trainer, V. L.; Scholz, N. L. Morphological abnormalities and sensorimotor deficits in larval fish exposed to dissolved saxitoxin. *Aquatic Toxicology* **2004***, 66*, 159-170.

35. Li, R.; Carmichael, W. W.; Brittain, S.; Eaglesham, G. K.; Shaw, G. R.; Liu, Y.; Watanabe, M. M. First report of the cyanotoxins cylindrospermopsin and deoxycylindrospermopsin from Raphidiopsis curvata (Cyanobacteria). *J. Phycol.* **2001***, 37*, 1121-1126.

36. Linney, E.; Upchurch, L.; Donerly, S. Zebrafish as a neurotoxicological model. *Neurotoxicol Teratol* **2004**, 26(6), 709-718

37. Liu, S.; Leach, S. D. Zebrafish models for cancer. *Annual Review of Pathology: Mechanisms of disease* **2011***, 6*, 71-93.

38. López-Alonso, H.; Rubiolo, J. A.; Vega, F.; Vieytes, M. R.; Botana, L. M. Protein synthesis inhibition and oxidative stress induced by cylindrospermopsin elicit apoptosis in primary rat hepatocytes. *Chem. Res. Toxicol.* **2013***, 26*, 203-212.

39. Mann, S.; Lombard, B.; Loew, D.; Méjean, A.; Ploux, O. Insights into the reaction mechanism of the prolyl–acyl carrier protein oxidase involved in anatoxin-a and homoanatoxin-a biosynthesis. *Biochemistry (N. Y. )* **2011***, 50*, 7184-7197.

40. Méjean, A.; Mann, S.; Vassiliadis, G.; Lombard, B.; Loew, D.; Ploux, O. In vitro reconstitution of the first steps of anatoxin-a biosynthesis in Oscillatoria PCC 6506: from free L-proline to acyl carrier protein bound dehydroproline. *Biochemistry (N. Y. )* **2009***, 49*, 103-113.

41. Mihali, T. K.; Kellmann, R.; Muenchhoff, J.; Barrow, K. D.; Neilan, B. A. Characterization of the gene cluster responsible for cylindrospermopsin biosynthesis. *Appl. Environ. Microbiol.* **2008***, 74*, 716-722.

42. Moffitt, M. C.; Neilan, B. A. Characterization of the nodularin synthetase gene cluster and proposed theory of the evolution of cyanobacterial hepatotoxins. *Appl. Environ. Microbiol.* **2004***, 70*, 6353-6362.

43. Moore, R. E.; Blackman, A. J.; Cheuk, C. E.; Mynderse, J. S.; Matsumoto, G. K.; Clardy, J.; Woodard, R. W.; Craig, J. C. Absolute stereochemistries of the aplysiatoxins and oscillatoxin A. *J. Org. Chem.* **1984***, 49*, 2484-2489.

44. Moore, R. E.; Chen, J. L.; Moore, B. S.; Patterson, G. M.; Carmichael, W. W. Biosynthesis of microcystin-LR. Origin of the carbons in the Adda and Masp units. *J. Am. Chem. Soc.* **1991***, 113*, 5083-5084.

45. Neilan, B.; Saker, M.; Fastner, J.; Törökné, A.; Burns, B. Phylogeography of the invasive cyanobacterium Cylindrospermopsis raciborskii. *Mol. Ecol.* **2003***, 12*, 133-140.

46. Nogueira, I. C.; Lobo-da-Cunha, A.; Vasconcelos, V. M. Effects of Cylindrospermopsis raciborskii and Aphanizomenon ovalisporum (cyanobacteria) ingestion on Daphnia magna midgut and associated diverticula epithelium. *Aquatic Toxicology* **2006***, 80*, 194-203.

47. Novodvorsky, P.; Da Costa, M. M.; Chico, T. J. Zebrafish-based small molecule screens for novel cardiovascular drugs.*Drug Discovery Today: Technologies* **2013***, 10*, e109-e114.

48. Oberemm, A.; Fastner, J.; Steinberg, C. Effects of microcystin-LR and cyanobacterial crude extracts on embryo-larval development of zebrafish (*Danio rerio*). *War Res* **1997** 31(11), 2918-2921

49. Ohta, T.; Sueoka, E.; Iida, N.; Komori, A.; Suganuma, M.; Nishiwaki, R.; Tatematsu, M.; Kim, S.; Carmichael, W.; Fujiki, H. Nodularin, a potent inhibitor of protein phosphatases 1 and 2A, is a new environmental carcinogen in male F344 rat liver. *Caner Res* **1994**, 54(24), 6402-6406

50. Ohtani, I.; Moore, R. E.; Runnegar, M. T. Cylindrospermopsin: a potent hepatotoxin from the blue-green alga Cylindrospermopsis raciborskii. *J. Am. Chem. Soc.* **1992***, 114*, 7941-7942.

51. Okle, O.; Rath, L.; Galizia, C. G.; Dietrich, D. R. The cyanobacterial neurotoxin beta-N-methylamino-l-alanine (BMAA) induces neuronal and behavioral changes in honeybees. *Toxicol. Appl. Pharmacol.* **2013***, 270*, 9-15.

52. Paerl, H. W. Coastal eutrophication and harmful algal blooms: Importance of atmospheric deposition and groundwater as" new" nitrogen and other nutrient sources. *Limnol. Oceanogr.* **1997***, 42*, 1154-1165.

53. Papendorf, O.; König, G.M.; Wright, A.D.; Chorus, I.; Oberemm, A. Mueggelone, a novel inhibitor of fish development from the fresh water cyanobacterium Aphanizomenon flos-aquae. *J Nat Prod* **1997**, 60(12), 1298-300

54. Pearson, L.; Mihali, T.; Moffitt, M.; Kellmann, R.; Neilan, B. On the chemistry, toxicology and genetics of the cyanobacterial toxins, microcystin, nodularin, saxitoxin and cylindrospermopsin. *Marine Drugs* **2010***, 8*, 1650-1680.

55. Pflugmacher, S.; Wiegand, C.; Oberremm, A.; Beattie, K.; Krause, E.; Codd, G.; Steinberg, C. Identification of an enzymatically formed glutathione conjugate of the cyanobacterial hepatotoxin microcystin-LR: the first step of detoxication. *Biochim Biophys Acta* **1998**, 1425(3), 527-533

56. Prieto, A.; Jos, A.; Pichardo, S.; Moreno, I.; Camean, A. Differential oxidative stress responses to microcystins LR and RR in intraperitoneally exposed tilapia fish (*Oreochromi*s sp.). *Aquat. Toxicol* **2006**, 77, 314-321

57. Rocke, J.; Lees, J.; Packham, I.; Chico, T.; The zebrafish as a novel tool for cardiovascular drug discovery. *Recent Patents Cardiovasc Drug Discov* **2009,** 4, 1-5

58. Rogers, E.; Hunter, S.; Moser, V.; Phillips, P.; Herkovits, J.; Munoz, L.; Hall, L. Potential developmental toxicity of anatoxin-a, a cyanobacterial toxin. *J. Appl. Toxicol* **2005**, 25, 527–534

59. Runnegar, M. T.; Xie, C.; Snider, B. B.; Wallace, G. A.; Weinreb, S. M.; Kuhlenkamp, J. In vitro hepatotoxicity of the cyanobacterial alkaloid cylindrospermopsin and related synthetic analogues. *Toxicological Sciences* **2002***, 67*, 81-87.

60. Sangolkar, L.; Maske, S.; Chakrabarti, T. Methods for determining Microcystins (peptide hepatotoxins) and microcystin producing cyanobacteria. *Water Res* **2006**, 40(19), 3485-3496

61. Seifert, M.; McGregor, G.; Eaglesham, G.; Wickramasinghe, W.; Shaw, G. First evidence for the production of cylindrospermopsin and deoxy-cylindrospermopsin by

the freshwater benthic cyanobacterium,< i> Lyngbya wollei</i>(Farlow ex Gomont) Speziale and Dyck. *Harmful Algae* **2007***, 6*, 73-80.

62. Shalev-Alon, G.; Sukenik, A.; Livnah, O.; Schwarz, R.; Kaplan, A. A novel gene encoding amidinotransferase in the cylindrospermopsin producing cyanobacterium Aphanizomenon ovalisporum. *FEMS Microbiol. Lett.* **2002***, 209*, 87-91.

63. Snyder, R.; Gibbs, P.; Palacios, A.; Abiy, L.; Dickey, R.; Lopez, J.; Rein, K. Polyketide synthase genes from marine dinoflagellates. *Marine Biotechnology* **2003***, 5*, 1-12.

64. Stewart, I.; Falconer, I. R. Cyanobacteria and cyanobacterial toxins. *Oceans and human health: risks and remedies from the seas* **2008**, 271-296.

65. Stewart, I.; Webb, P.; Schluter, P.; Shaw, G. Recreational and occupational field exposure to freshwater cyanobacteria – a review of anecdotal and case reports, epidemiological studies and the challenges for epidemiologic assessment. *Environmental Health: A Global Access Science Source* **2006**, 5:6

66. Tillett, D.; Dittmann, E.; Erhard, M.; von Döhren, H.; Börner, T.; Neilan, B. A. Structural organization of microcystin biosynthesis in Microcystis aeruginosa PCC7806: an integrated peptide–polyketide synthetase system. *Chem. Biol.* **2000***, 7*, 753-764.

67. Valério, E.; Chaves, S.; Tenreiro, R. Diversity and impact of prokaryotic toxins on aquatic environments: A review. Toxins 2010, 2, 2359–2410.

68. Veldman, MB.; Lin, S. Zebrafish as a developmental model organism for pediatric research. [Review]. *Ped Res* **2008**, 64(5), 470-476

69. Wang, P.J.; Chien, M.S.; Wu, F.J.; Chou, H.N.; Lee, S.J. Inhibition of embryonic development by microcystin-LR in zebrafish, Danio rerio. Toxicon 2005, 45, 303–308.

70. Wiegand, C.; Pflugmacher, S. Ecotoxicological effects of selected cyanobacterial secondary metabolites a short review. *Toxicol Appl Pharm* **2005**, 203, 201-218

71. Wiegand, C.; Pflugmacher, S.; Oberemm, A.; Meems, N.; Beattie, K.; Steinberg, C.; Codd, G. Uptake and effects of microcystin-LR on detoxication enzymes of early life stages of the zebrafish (*Danio rerio*). *Environ Toxicol* **1999**, 14, 89-95

72. Yadav, S.; Sinha, R.; Tyagi, M.; Kumar, A. Cyanobacterial secondary metabolites. *International Journal of Pharma & Bio Sciences* **2011***, 2*.

73. Zhu H.; Zon, LI. Use of zebrafish models for the analysis of human disease. *Curr Protoc Hum Genet* **2002**, Ch.15, Unit 15.3

# CHAPTER 2*

POLYMETHOXY-1-ALKENES FROM *APHANIZOMENON OVALISPORUM* AND *CYLINDROSPERMOPSIS RACIBORSKII* INHIBIT VERTEBRATE DEVELOPMENT IN ZEBRAFISH (*DANIO RERIO*) EMBRYOS

(*This chapter has been modified from Jaja-Chimedza *et al.*, 2012, *Marine Drugs*.)

## 2.1. Introduction

Cyanobacteria ("blue-green algae") are known to produce a diverse repertoire of biologically active secondary metabolites (Valério *et al.*, 2010). When associated with so-called "harmful algal blooms", particularly in freshwater systems, a number of these metabolites have been associated - as "toxins", or commonly "cyanotoxins" - with human and animal health concerns (Valério *et al.*, 2010; Carmichael, 2008; Ferrão-Filho and Kozlowsky-Suzuki, 2011). As health concerns have largely been associated with exposure to drinking water contaminated with these toxins (except BMAA), it is notable, although perhaps not surprising, that all of these recognized toxins are generally polar and water-soluble metabolites. Previous evaluation of crude, non-polar (i.e., chloroform) extracts from strains of both *C. raciborskii* and *A. ovalisporum* identified developmental toxicity, clearly unrelated to the presence of CYN, and specifically associated with apparent lipophilic metabolites from extracts of all of the isolates evaluated (Berry *et al.*, 2009).

*C. raciborskii* has been specifically associated with the production of the hepatotoxic alkaloid, cylindrospermopsin (CYN), as well as the neurotoxic saxitoxin (STX) and its analogues. *Aphanizomenon*, as a genus, and particularly the species, *A. flos-aquae*, is a recognized producer of CYN, as well as the neurotoxic saxitoxin and anatoxin-a. Although *A. ovalisporum* is not known to produce either saxitoxin or anatoxin-a, studies of the Lake Kinneret isolate (Banker *et al.*, 1997; Banker *et al.*, 2000) identified both CYN and its 7-epimer (i.e., 7-epi-CYN). Interestingly, and relevant to the present study, during the isolation of the latter CYN congener, a series of isotactic

polymethoxy-1-alkenes (**4-6**; Figure 2.1) were concurrently identified, purified and chemically characterized.

Indeed, in the present study, bioassay-guided fractionation, as described below, led to the isolation, and chemical characterization of these previously identified polymethoxy-1-alkenes (PMAs), i.e., **4-6**, as well as three additional members (**1-3**) of the apparent homologous series (Figure 2.1), as lipophilic developmental toxins from the Lake Kinneret strain of *A. ovalisporum*. Although three of the six PMAs reported here have been isolated previously from this strain (Banker *et al.*, 2000) - as well as at least two other genera (i.e., *Scytonema*, *Tolypothrix*) of the cyanobacterial order Nostocales (Mynderse and Moore, 1979; Mori *et al.*, 1991a and 1991b) - in studies spanning more than three decades, they have not previously been associated with toxicity. In addition to their isolation, and chemical characterization, we report here on their developmental toxicity in the zebrafish embryo model, and specifically, the apparent synergistic activity of congeners in the series.

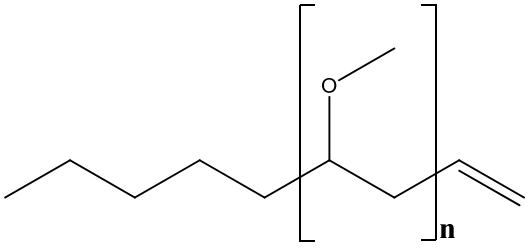


**1** n = 7
**2** n = 8
**3** n = 9
**4** n = 10
**5** n = 11
**6** n = 12

Figure 2. 1: Structure of polymethoxy alkenes (1-6) isolated in the current and previous studies.

## 2.2. Results and Discussion

### *2.2.1. Purification of PMAs by Bioassay-Guided Fractionation*

Biomass from unialgal cultures of *A. ovalisporum* was twice extracted in $CHCl_3$, and pooled extracts were confirmed to inhibit zebrafish embryo development as previously documented (Berry *et al.*, 2009). The pooled crude extracts were subsequently fractionated (see Experimental Section) by silica gel column chromatography and reverse-phase HPLC, affording a bioactive fraction containing a total of six components (**1**-**6**; Figure 2.2). LC-MS of the active fraction identified nominal masses of the presumptive molecular ions ($M + H^+$) for compounds 1–6 of *m/z* 505 (**1**), 563 (**2**), 621 (**3**), 679 (**4**), 737 (**5**) and 795 (**6**), in addition to apparent, i.e., M + 23, sodium adducts ($M + Na^+$) and M + 39, potassium adducts ($M + K^+$) of each (Figure 2.3). An incremental mass difference of 58 amu, corresponding to $-CH_2CH(OCH_3)-$ units, between each of the six compounds, as well as collision induced fragmentations, corresponding to sequential losses of 32 amu ($-OCH_3$ lost as $CH_3OH$) for each compound, was consistent with a homologous series of PMAs, as previously observed for the strain (Banker *et al.*, 2000) as well as other cyanobacteria (Mynderse and Moore, 1979; Mori *et al.*, 1991a and 1991b). Each of the six peaks was collected for subsequent chemical and toxicological characterization (as described below).

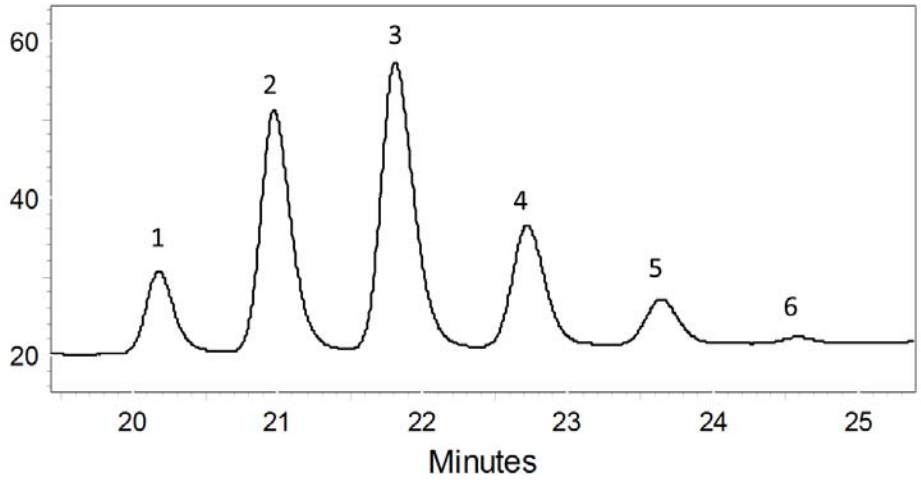


Figure 2. 2: Chromatogram showing PMAs (1-6) isolated by HPLC from A. ovalisporum. See experimental section for details.

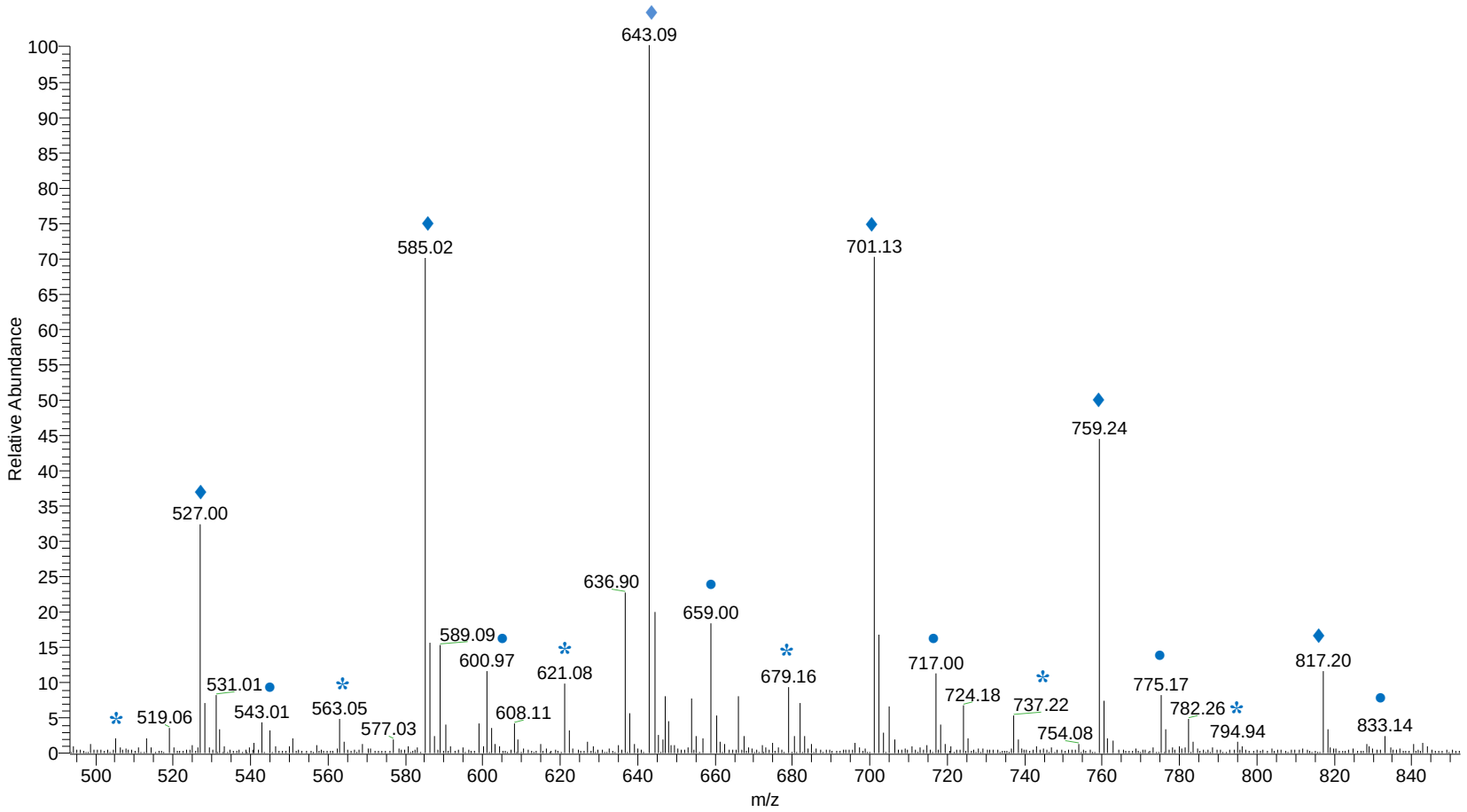


Figure 2. 3: Low resolution LC-MS of the PMA mixture from *A. ovalisporum* showing all 6 PMAs isolated from the HPLC with the * indicating the $[M+H]^+$ peaks, ♦ indicating the $[M+Na]^+$ peaks, and • indicating the $[M+K]^+$ peaks.

*2.2.2. Structure Elucidation of the PMAs from A. ovalisporum*

Compound **3** was the most abundant of the purified compounds and was isolated as a white amorphous solid. A molecular formula of $C_{34}H_{68}O_9$ was suggested by high-resolution MS (HRMS; *m/z* 621.4920 $[M + H]^+$), and subsequently confirmed by $^1H$ and $^{13}C$-NMR studies (see below). MS/MS of the presumptive molecular ion (*m/z* 621.5) in the triple quadrupole instrument identified nine sequential losses of 32 amu consistent with nine methoxy groups (as $CH_3OH$) from the molecule (Figure 2.4). $^1H$ NMR (Table 1), likewise, revealed eight signals at δ 3.1641 (s, 3H), 3.2105 (s, 3H), 3.218 (s, 3H), 3.2432 (s, 3H), 3.2514 (s, 3H), 3.2708 (s, 3H), 3.2745 (s, 3H) and 3.2798 (s, 6H), consistent with nine methoxy groups, with two of the methoxy groups being equivalent (Figure 2.5b).

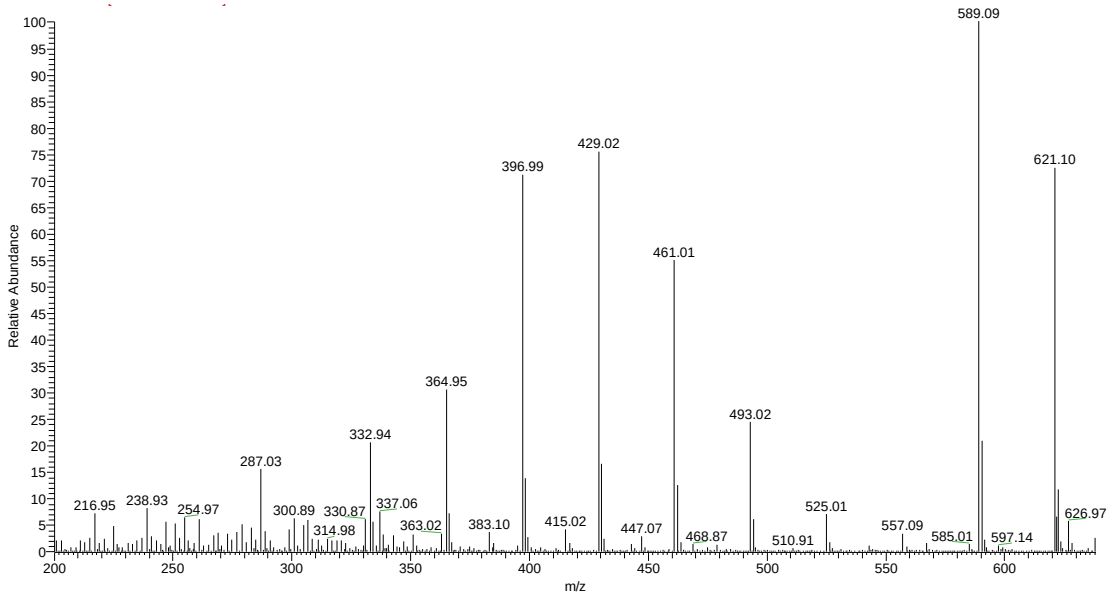


Figure 2. 4: LC-MS (low-resolution) of purified PMA 3 showing the sequential loss of *m/z* 32 corresponding to the loss of methoxy groups.

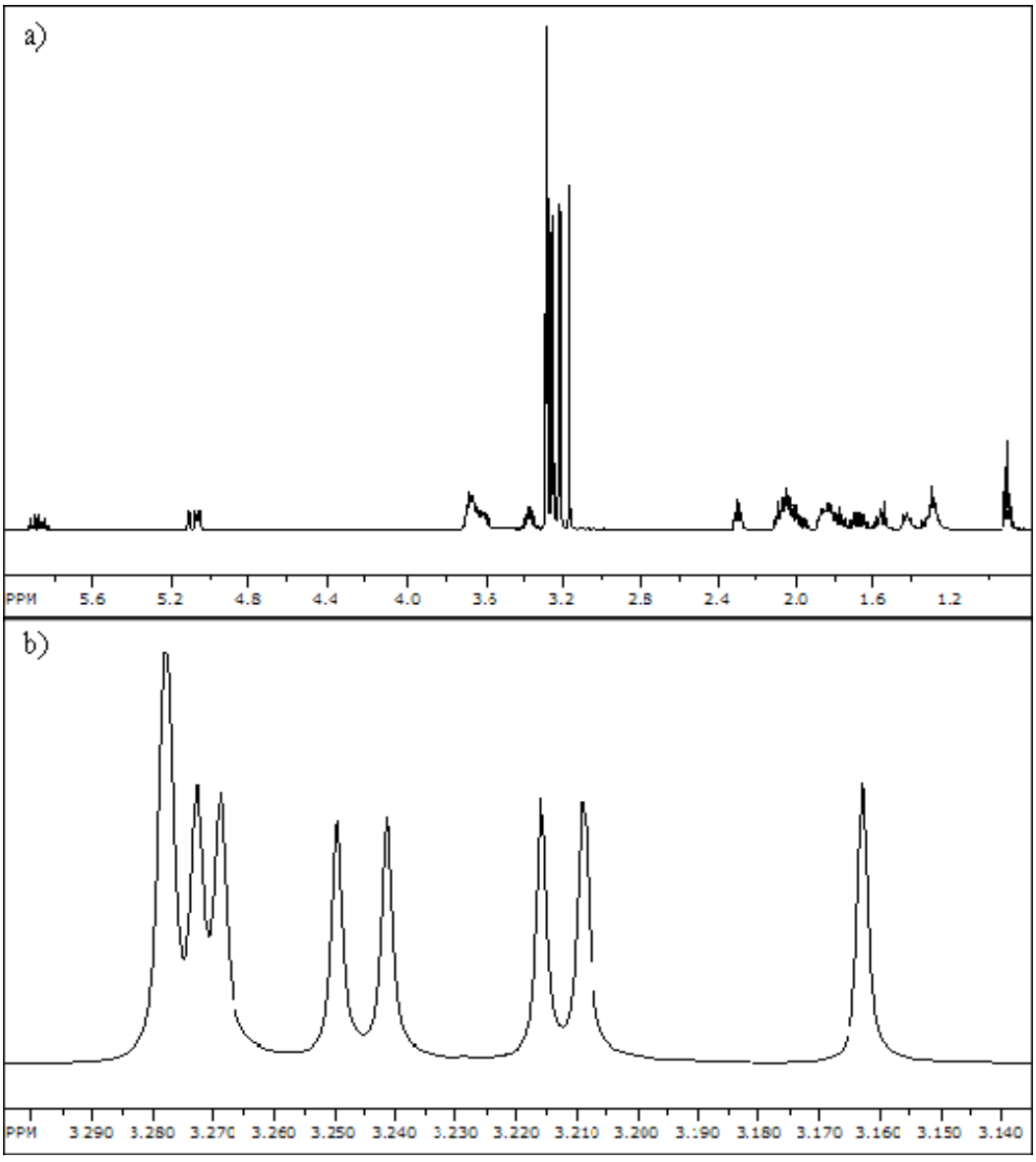


Figure 2. 5: $^{1}$H-NMR of PMA **3** from A. ovalisporum; a) the total 1H-NMR spectrum and b) the signals observed for the methoxy protons showing 8 singlets corresponding to 9 methoxy groups (27H) with two of the methoxy groups being equivalent.

Proton signals were observed at $\delta_H$ 5.09 (H-1E), 5.13 (H-1Z) and 5.93 (H-2), integrating to 3H, suggesting the presence of a terminal alkene, and a signal at $\delta_H$ 2.30, integrating to 2H, which suggests the presence of a methylene group attached to the terminal alkene determined based on the COSY correlation (see below). A triplet was

observed at $\delta_H$ 0.91, integrating to 3H which was assigned to the methyl group (C-25). Two sets of overlapping multiplets at δ 3.37 (m, 2H) and 3.65 (m, 7H) (Table 2.1) were assigned as oxymethine hydrogens geminal to the methoxy groups as well as overlapping multiplets at δ 2.04 (m, 8H), 1.80 (m, 6H), 1.67 (m, 2H), 1.56 (m, 2H), 1.43 (m, 2H) and 1.30 (m, 4H), which integrated to a total of 24 protons. Based on distinct chemical shifts, and the assumption that **3** was a PMA, 16 of these were tentatively assigned to the protons vicinal to methoxy groups (δ 2.04, 1.80 and 1.67), and the remaining eight protons (δ 1.56, 1.43 and 1.30) were assigned to methylenes at C-21 to C-24 positions (Figure 2.6). Tentative proton assignments, and the proposed molecular formula, were confirmed by $^{13}$C-NMR and DEPT, as well as subsequent COSY, HMQC and HMBC experiments, as described below.

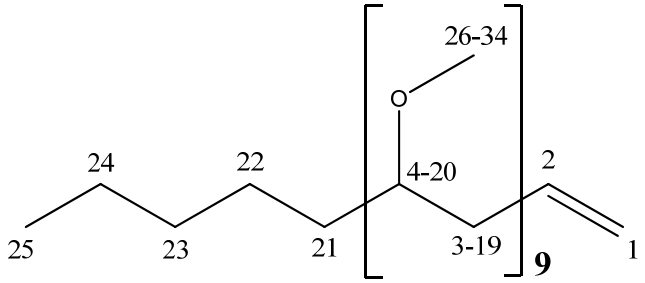


Figure 2. 6: Proposed structure of PMA **3** with carbons numbered.

Table 2. 1: $^{1}H$ ($C_6D_6$, 400.13 MHz) and $^{13}C$ ($C_6D_6$, 100.61 MHz) NMR Data for 4,6,8,10,12,14,16,18,20-nonamethoxy-1-pentacosene from A. ovalisporum (**3**).

| C # | $\delta_C$ | $\delta_H$ (mult, *J* in Hz; #H) | COSY | HMBC |
|---|---|---|---|---|
| 1 | 117.01 | 5.13 (dd,17,2; 1H)* | H-2 | $H_2$-3 |
| | | 5.09 (dd,10,2; 1H)* | H-2 | $H_2$-3 |
| 2 | 135.26 | 5.93 (ddt,17,10,7; 1H) | H-1, $H_2$-3 | $H_2$-3 |
| 3 | 38.66 | 2.30 (m; 2H) | H-2, H-4 | $H_2$-1, $H_1$-2 |
| 4 | 77.61 | 3.37 (m; 1H) | H-3, $H_2$-5 | $H_3$-26 |
| 5, 7 ,9…19 | 38.35-38.97 | 1.67-2.04 (m; 16H) | See text | See text |
| 6, 8, 10…18 | 75.92-76.11 | 3.65 (m; 7H) | See text | See text |
| 20 | 78.13 | 3.37 (m; 1H) | $H_2$-21, $H_2$-19 | $H_3$-34 |
| 21 | 33.96 | 1.56 (m; 2H) | $H_2$-20, $H_2$-22 | See text |
| 22 | 25.09 | 1.43 (m; 2H) | $H_2$-21, $H_2$-23 | See text |
| 23 | 32.51 | 1.30 (m; 2H) | $H_2$-22, $H_2$-24 | See text |
| 24 | 23.08 | 1.30 (m; 2H) | $H_2$-23, $H_2$-25 | See text |
| 25 | 14.27 | 0.91 (t, 7.1; 3H) | $H_2$-24 | $H_2$-24, $H_2$-23 |
| 26-34 | 56.93-56.16 | 3.16-3.28 (s; 27H) | | H-4,6…H-20 |

*Due to poor resolution, further splitting could not have been determined beyond the doublet of doublet.

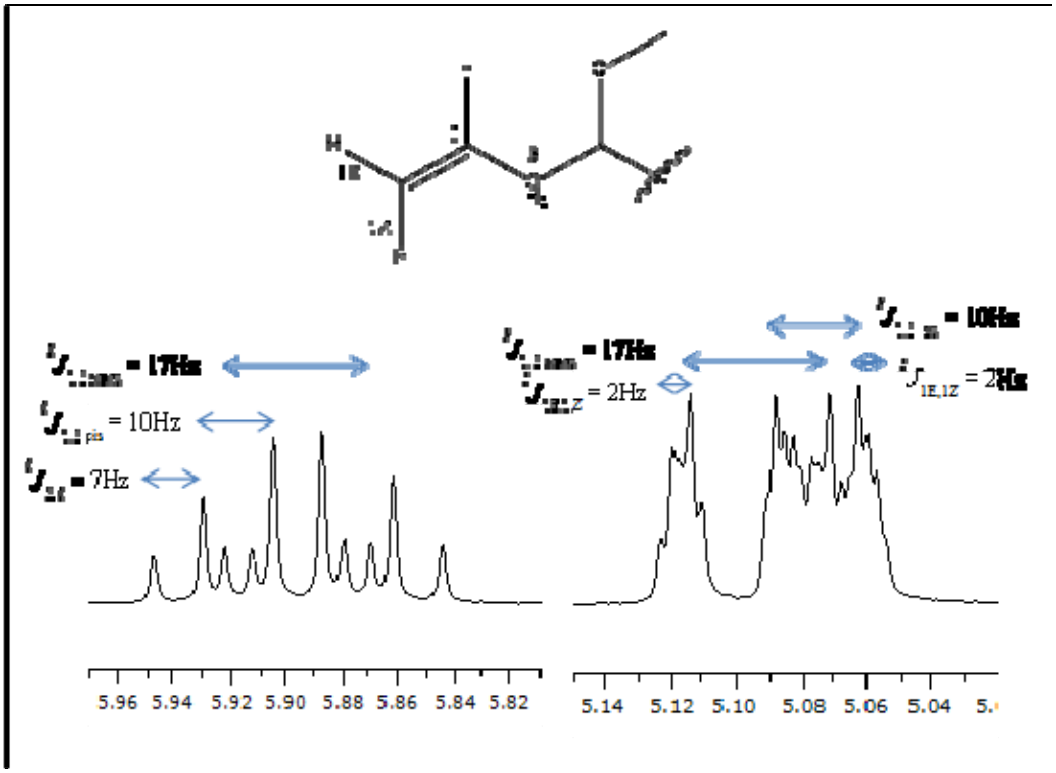


Figure 2. 7: $^{1}H$-NMR of PMA **3** showing the terminal alkene

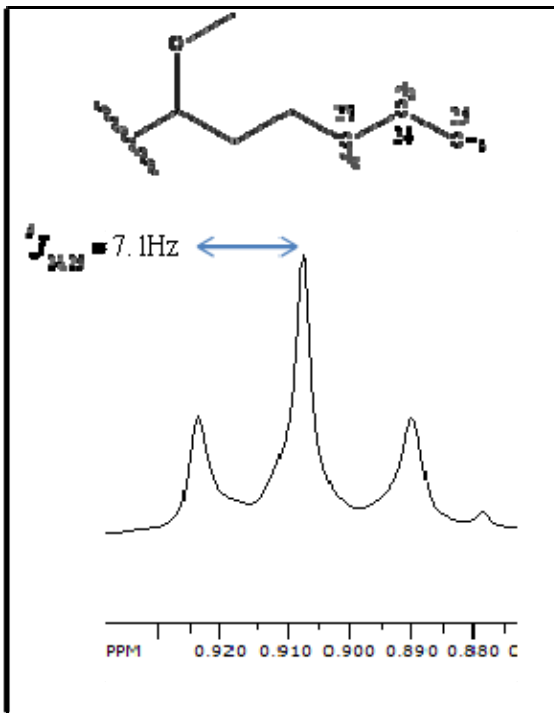


Figure 2. 8: $^{1}$H-NMR of PMA **3** showing the terminal methyl group.

The DEPT-135 experiment helped to support the assignments of the protons from the $^{1}$H-NMR by indicating differentiating the presence of 'CH' and '$CH_3$' carbons (positive signals) from '$CH_2$' carbons (negative signals) (Figure 2.9). The experiment showed a positive carbon signal at δ 135.26 and a negative signal at δ 117.01 supporting the assignment of the terminal alkene, as well as a negative signal at δ 38.66 supporting the assignment of the allylic protons. A positive signal was observed at δ 14.27 which also supports the presence of a methyl group. Overlapping positive signals were observed between δ 56.93-56.16 and overlapping positive signals at δ 75.92-78.13 corresponding to the methoxy carbons (-$OCH_3$) and the oxymethine carbons (-**C**H$OCH_3$) respectively. Negative signals were also observed at δ 23.08, 25.09, 32.51, and 33.96 indicating methylene carbons which were assigned a chain of four $CH_2$ connected to the terminal

methyl carbon (-$CH_2CH_2CH_2CH_2CH_3$). The 1D $^{13}$C-NMR did not show additional carbon signals, suggesting that no quaternary carbons were present in the structure (Appendix *A2.1.3*D).

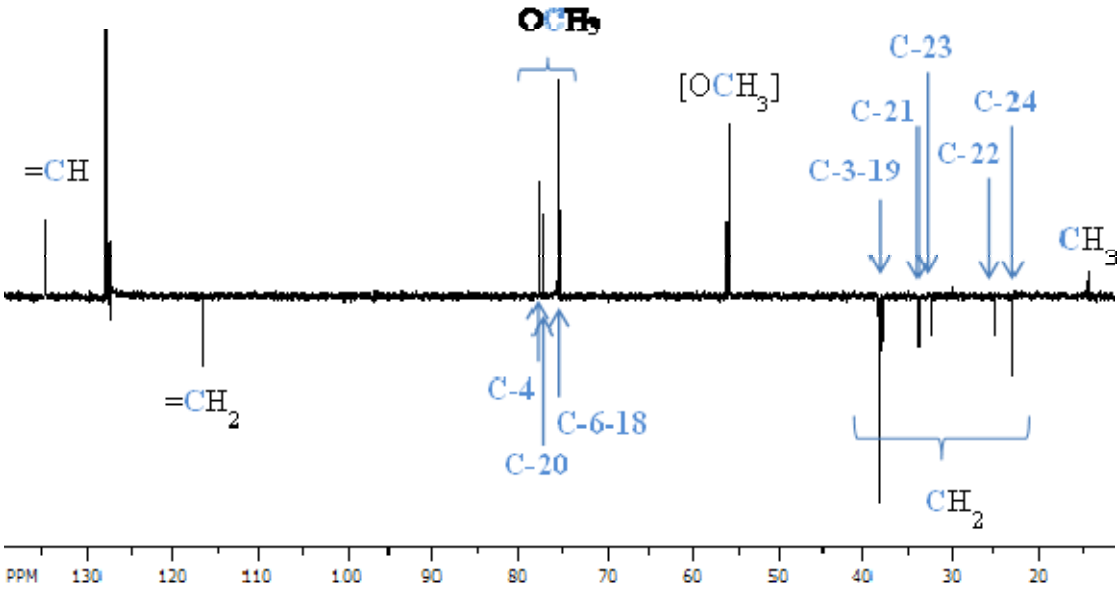


Figure 2. 9: DEPT-135 experiment differentiating the 'CH' and '$CH_3$' carbons (positive signals) from the '$CH_2$' carbons (negative signals).

COSY experiments, in conjunction with HMQC and HMBC, revealed the apparent linear structure of **3**. Protons of the single methyl group ($H_3$-25, δ 0.91) were found to correlate by COSY to two pairs of hydrogens (δ 1.30) that were revealed, by HMQC correlations, to be bonded to two methylene carbons (as confirmed by DEPT-135). HMBC correlation of both methylene carbons to protons of the methyl group further enabled assignment of C-25, -24 and -23. COSY correlation of C-23/24 protons to a single pair of methylene protons (assigned as C-22), and subsequent correlation to a single adjacent pair of methylene protons (assigned as C-21) - as well as COSY correlation of C-21 hydrogens to a pair of oxymethine protons (δ 3.37) - enabled

assignments of hydrogens on C-25 through C-20. Similarly, at the alkene terminal, COSY correlation was observed between alkene hydrogens and a single pair of methylene protons that was consequently assigned to C-3. Although methylene protons on both C-21 and C-3 correlated to the same two overlapping oxymethine proton signals (assigned C-20 and C-4, respectively), correlation of these protons to C-22 methylene and C-1/2 terminal alkene protons, respectively, allowed these two pairs of methylene hydrogens to be clearly distinguished.

The data from the heteronuclear 2D experiments (HMQC and HMBC) obtained for compound **3**, were used to confirm the assignments of the chemical shifts and the connectivities within the structure. The HMBC data showed the correlation between the signal at δ 0.91 ($CH_3$ protons) and the signals at δ 23.08 and 32.51 confirming the assignments of C-24 and C-23 respectively as previously established from the HMQC. The methylene signals at δ 1.30-1.56 did not show any correlation, possibly due to the low concentration of the sample. Correlations were also observed for the signal at δ 2.30 (allylic $CH_2$) with the signals at δ 77.61, 117.01, and 135.26 confirming the methylene connectivity to the terminal alkene as well as assigning the signal at δ 77.61 as C-4. Overlapping signals at δ 3.16-3.28 (methoxy protons) were coupled to the signals at δ 75.92-76.11 (oxymethine carbons) and δ 38.35-38.97 (methylene carbons) which shows the 2 and 3 bond coupling between the heteroatoms confirming the assignments of the alternating methoxy groups. The other set of overlapping signals of the methylene protons at δ 1.67-2.04 were coupled to the signals at δ 75.92-76.11 (oxymethine carbons) and δ 38.35-38.97.

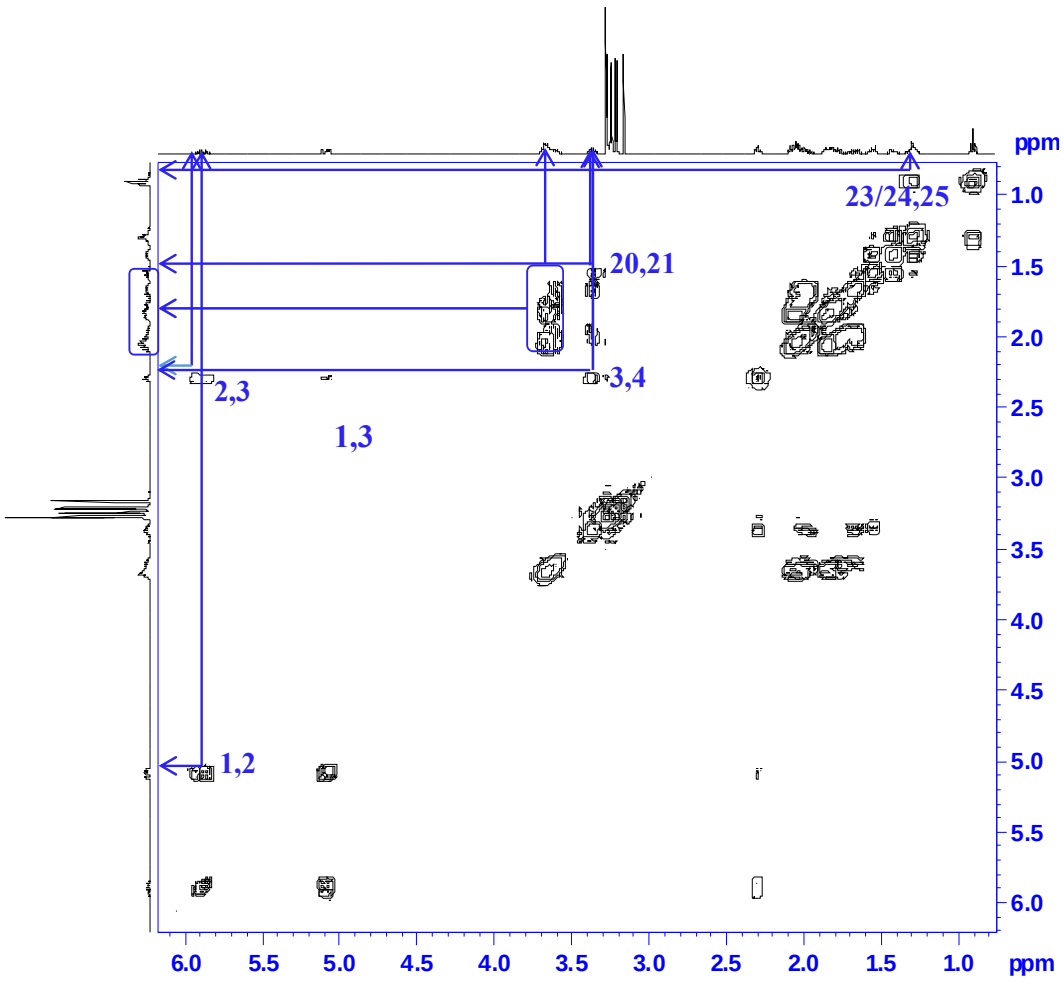


Figure 2. 10: Total COSY spectrum of PMA **3** from *A. ovalisporum*.

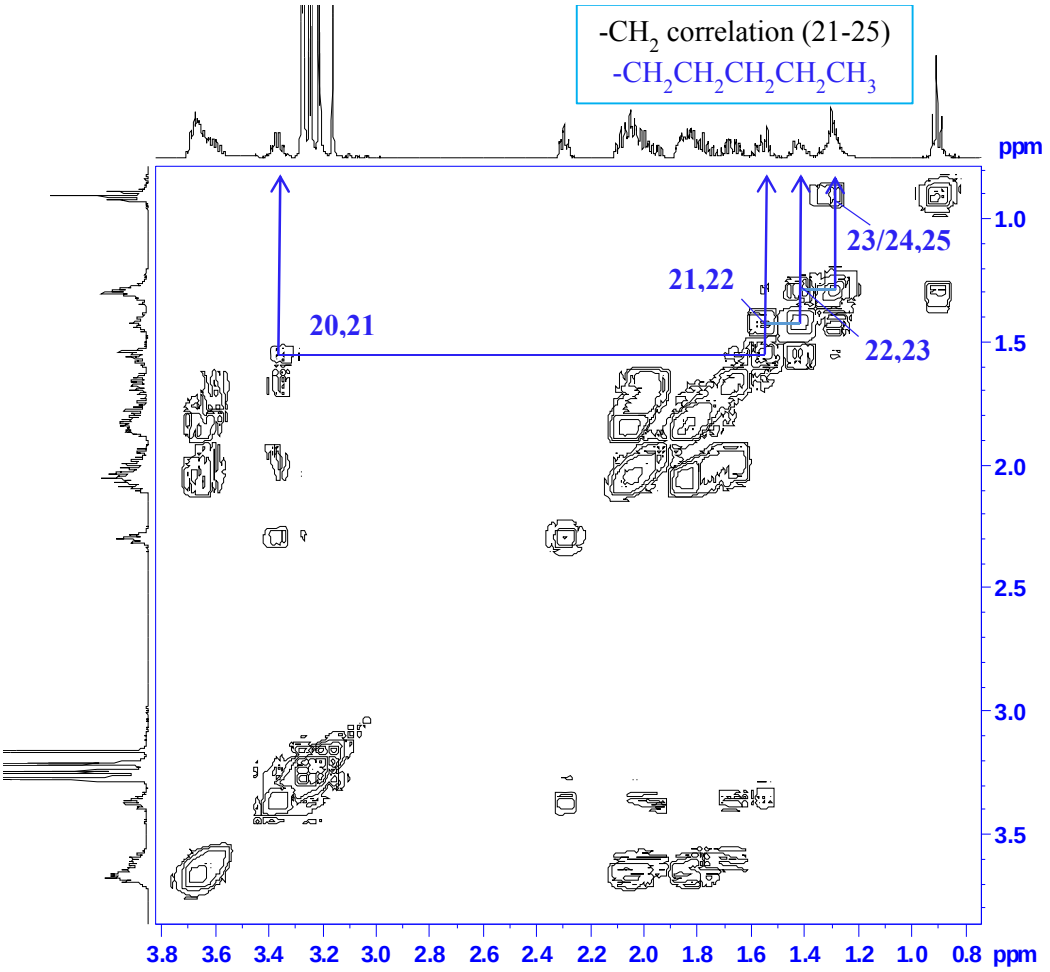


Figure 2. 11: COSY spectrum of PMA **3** from *A. ovalisporum* showing the methylene correlations.

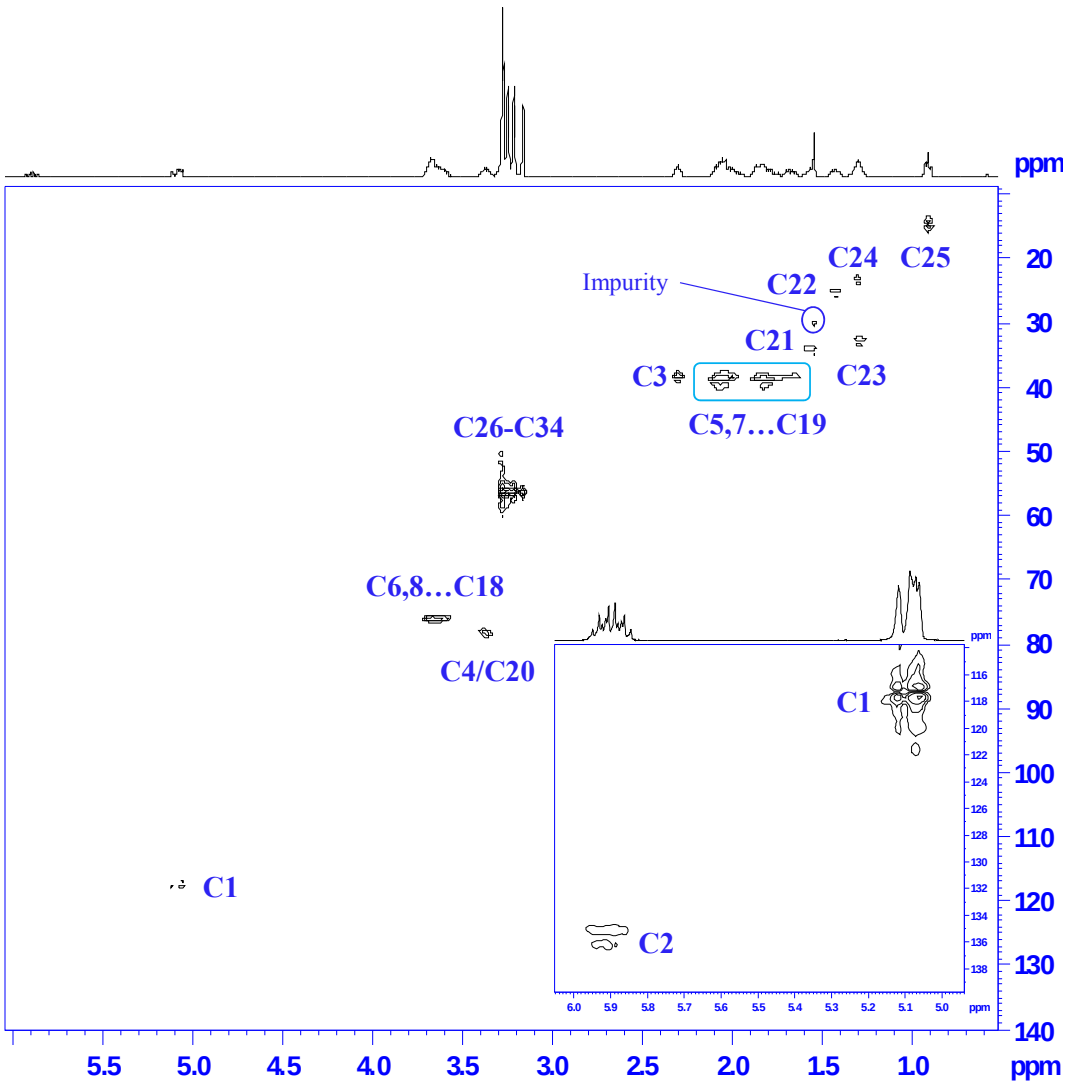


Figure 2. 12: HMQC of PMA 3 from A. ovalisporum with terminal alkene zoomed in.

Finally, a stretch of nine alternating methoxy-bearing carbons and the methylene carbons between (C-4 to C-20; Figure 2.6) were identified based on correlations in COSY and HMBC. HMBC correlations between proposed methoxy carbons (nine in total) and seven remaining oxymethine protons, along with mass fragmentation (i.e., loss of 32 amu) consistent with $–OCH_3$ functional groups, further confirmed their identity as methoxy-bearing carbons. Chemical shifts, in both $^{1}H$- and $^{13}C$-NMR spectra, assigned to protons and carbons of the remaining methylenes and oxymethines, overlapped considerably, and did not consequently allow resolution of these signals for direct correlations. However, COSY and HMBC correlation of the total integrated signals for the methylene and oxymethine protons (i.e., 16 and 9, respectively) and corresponding carbons (i.e., 8 and 9, respectively) confirmed that methoxy-bearing carbons alternated with methylenes.

Accordingly, **3** was determined to be 4,6,8,10,12,14,16,18,20-nonamethoxy-1-pentacosene. As such, this compound would represent a structural isomer of 4,6,8,10,12,14,16,18,22-nonamethoxy-1-pentacosene previously isolated from the same strain by Banker *et al.* (2000). Although a new PMA variant for this particular strain, **3** was, in fact, previously isolated by Mynderse and Moore (1979) from *Tolypothrix conglutinata* var. *colorata* - specifically as the similarly most abundant (~80%) of three congeners isolated from this strain - as well as by Mori *et al.* (1991a) from *Scytonema burmanicum*. In this case, as in other prior studies (Banker *et al.*, 2000; Mori *et al.*, 1991a and 1991b), the methoxy groups of the PMA were determined, based on NMR studies, to be isotactic (i.e., on the same side of the alkene chain). Based on the nearly identical $^{1}H$- and $^{13}C$-NMR observed here, **3** was proposed to be, likewise, isotactic.

Although quantities of each of the less abundant PMAs purified, including the more major (i.e., **2** and **4**) and minor (i.e., **1**, **5** and **6**; see Figure 2.2) congeners, did not generally allow for $^{13}$C-NMR and related NMR analysis (i.e., HMQC, HMBC), structures were assigned based on comparison to the $^{1}$H-NMR and associated assignments based on COSY of **3** (as described above), as well as MS/MS (i.e., losses of 32 amu corresponding each methoxy group). Furthermore, comparison of this data (i.e., $^{1}$H-NMR, COSY, MS) to that previously published and available for characterization of PMAs, and specifically, studies by Mynderse and Moore (1979) and Mori *et al.* (1991a and 1991b), were used to support these structural assignments. A clear correlation (e.g., nearly identical $^{1}$H-NMR chemical shifts, identical molecular ions and subsequent fragmentation patterns) between spectroscopic data obtained for **2** and **4**-**6** in the present study, as well as those previously reported (Mynderse and Moore, 1979; Banker *et al.*, 2000; Mori *et al.*, 1991a), support our structural determinations for these less abundant variants. On the other hand, although **1** has not been previously identified from any other source, consistency in the NMR and MS data for this congener, compared to the other purified in the present study, strongly support the proposed structure of this variant. Similar to **3**, the stereochemistry - and specifically the assignment as isotactic methoxy groups - was, likewise, concluded based on the similarities observed in the NMR data for these congeners and those previously characterized (Banker *et al.*, 2000; Mori *et al.*, 1991a and 1991b). Accordingly, **1** and **2** were identified as isotactic 4,6,8,10,12,14,16-heptamethoxy-1-uncosene and 4,6,8,10,12,14,16,18-octamethoxy-1-tricosene, respectively. The former variant (**1**) has not been previously isolated (to the authors' knowledge) from cyanobacteria, however, the latter (**2**) was previously isolated from *T. conglutinata*

(Mynderse and Moore, 1979). On the other hand, **4**-**6** were identified as 4,6,8,10,12,14,16,18,20,22-decamethoxy-1-heptacosene, 4,6,8,10,12,14,16,18,20,22,24-undecamethoxy-1-nonacosene and 4,6,8,10,12,14,16,18,20,22,24,26-dodecamethoxy-1-hentriacontene, respectively, and each has been previously isolated from the Lake Kinneret isolate of *A. ovalisporum* (Banker *et al.*, 2000) and other cyanobacteria (Mori *et al.*, 1991a and 1991b). Additional members of the apparent homologous series, including penta- and hexa-methoxylated variants, although not seen here, have been previously isolated from species of *Scytonema* (Mori *et al.*, 1991a and 1991b).

*2.2.3. Structure Elucidation of the PMAs from C. raciborskii*

Purification of the PMAs from *C. raciborskii* was done according to the procedure as describe for *A. ovalisporum*. Five of the six PMAs isolated from *A. ovalisporum* were identified in *C. raciborskii*, based on the high-resolution LC-MS data (Figure 2.14), however only four of the PMAs (**2**-**5**) were purified by HPLC (Figure 2.13). The resulting chemical characterization was similar to the PMAs isolated from *A. ovalisporum* and the other cyanobacterial stains previously shown to produce these compounds (Mynderse and Moore, 1979; Mori *et al.*, 1991a and 1991b; Rao and Faulkner, 2002; Jaja-Chimedza *et al.*, 2012). All four compounds obtained from the purification were white amorphous solids. High-resolution mass spectral data for all four compounds were obtained; $[M+H]^+$ 563.4488 (**2**), 621.4900 (**3**), 679.5312 (**4**), and 737.5733 (**5**), which allowed for the determination of the molecular formulas $C_{31}H_{62}O_8$ (**2**), $C_{34}H_{68}O_9$ (**3**), $C_{37}H_{74}O_{10}$ (**4**), $C_{40}H_{80}O_{11}$ (**5**), which were further confirmed by NMR analyses.

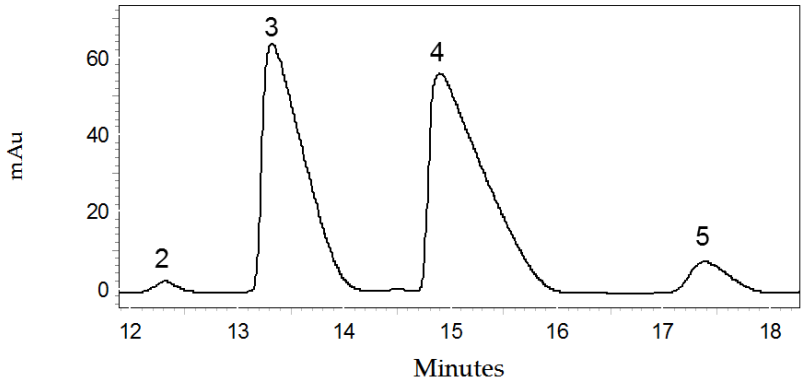


Figure 2. 13: HPLC Chromatogram of the four PMAs purified from *C. raciborskii* with UV detection at 200 nm.

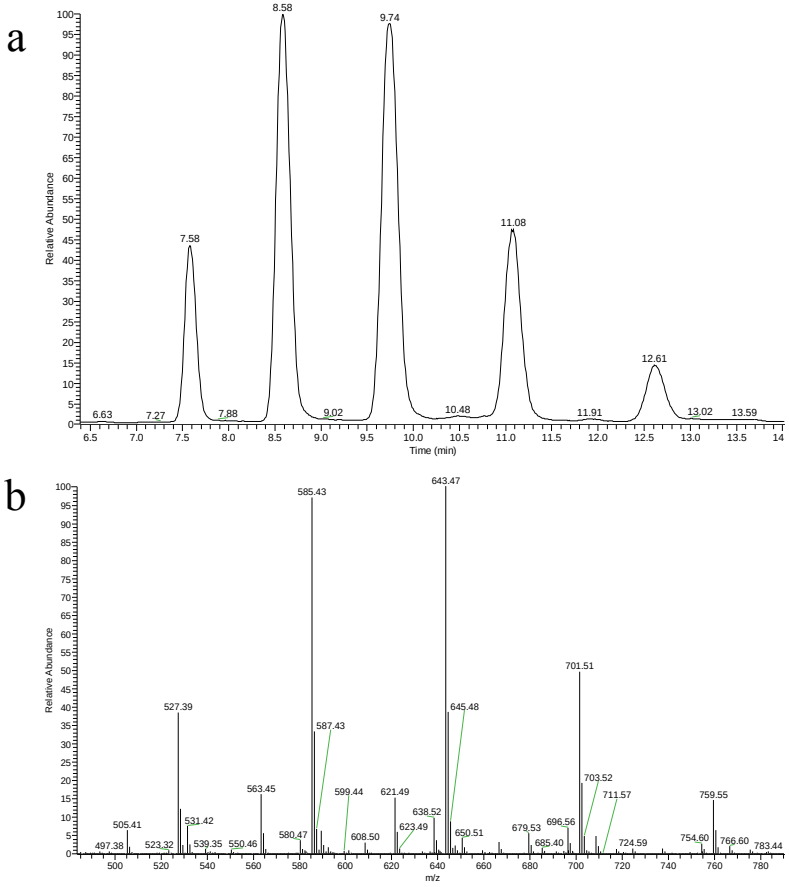


Figure 2. 14: High resolution LC-MS analysis of a crude fraction of *C. raciborskii* showing the presence of five PMAs (**1**-**5**); a) chromatogram of the PMAs and b) mass spectral data of the PMAs.

Fragmentation of the molecular ion of each of the compounds showed a sequential loss of *m/z* 32 corresponding to the number of methoxy groups associated with the compound, indicating the presence of a polymethoxylated structure. Mass spectral data also showed that the masses of the four polymethoxy-1-alkenes differed from the next by a mass of 58, corresponding to the $-CH_2CH(OCH_3)-$ unit (See Figure 2.14). This is consistent with that observed from the polymethoxy-1-alkenes isolated from other cyanobacterial strains (Mynderse and Moore, 1979; Mori *et al.*, 1991a and 1991b; Banker *et al.*, 2000; Jaja-Chimedza *et al.*, 2012) and sponge (Rao and Faulkner, 2002).

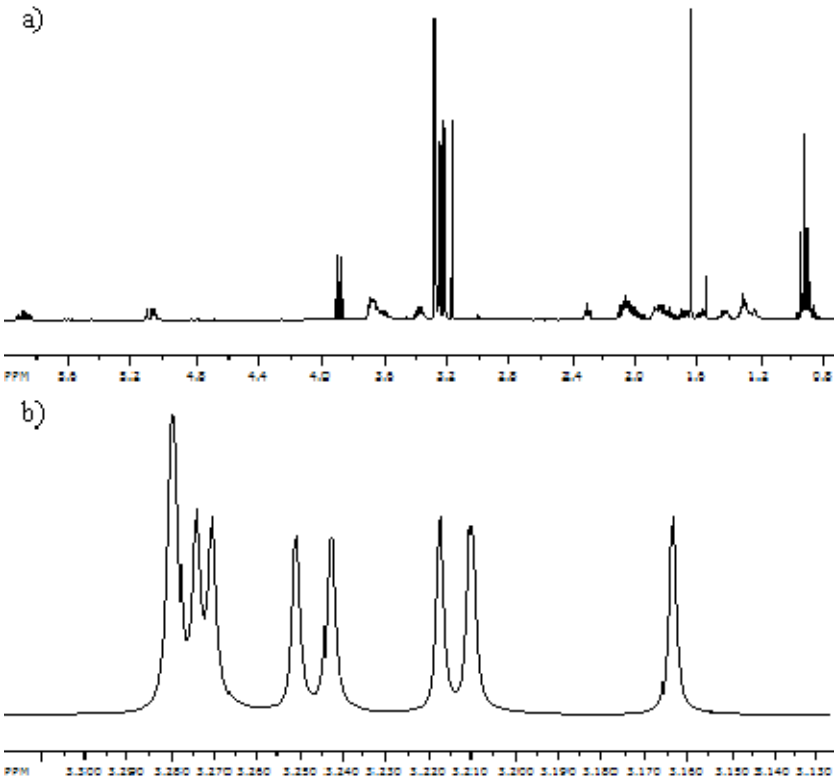


Figure 2. 15: $^1$H-NMR of PMA **3** from *C. raciborskii*; a) the total $^1$H-NMR spectrum and b) the signals observed for the methoxy protons showing 8 singlets corresponding to 9 methoxy groups (27H) with two of the methoxy groups being equivalent.

The NMR data showed signals and splitting patterns were similar to those observed for the PMAs isolated from the other strains of cyanobacteria. $^{1}$H and COSY NMR spectroscopic data were obtained for all the compounds with the exception of PMA **2** due to the low amount of the compound purified (57μg). Chemical shifts and connectivities were similar for all three compounds and so analysis of compound **3** will represent what was observed for the other two PMAs. The $^{1}$H-NMR showed 8 signals at δ 3.1637 (s, 3H), 3.2101 (s, 3H), 3.2174 (s, 3H), 3.2427 (s, 3H), 3.2508 (s, 3H), 3.2705 (s, 3H), 3.2742 (s, 3H), and 3.2792 (s, 6H) corresponding to 9 methoxy groups. The NMR signals for the terminal alkenes were observed at δ 5.07 (1H-1E), 5.10 (1H-1Z), and 5.90 (ddt, 1H-2), which was coupled to the signal at δ 2.30 (2H-3) for the methylene hydrogens (m; 2H). The methylene signal was then coupled to a signal δ 3.37 corresponding to one of the oxymethine hydrogens (2H), designated H-4. The signals observed at δ 0.91 (t; 3H), 1.30 (m; 4H), 1.42 (m; 2H), and 1.56 (m; 2H), corresponds to the terminal methyl group and subsequent methylene groups respectively, making up the alkyl chain (-$CH_2CH_2CH_2CH_2CH_3$) at the end of the molecule, based on the couplings observed from the COSY experiment. The methylene signal at δ 1.56 (m; 2H) was then coupled to an oxymethine signal at δ 3.37, designated H-20. The oxymethine multiplets at δ 3.37 and 3.64 (8H) were coupled to the overlapping multiplets from δ 1.67 – 2.03 (16H).

Table 2. 2: $^{1}H$ ($C_6D_6$, 400.13MHz) and $^{13}C$ ($C_6D_6$, 100.61MHz) NMR data for 4,6,8,10,12,14,16,18,20-nonamethoxy-1-pentacosene (**3**) from *C. raciborskii*.

| **C #** | **$\delta_C$** | **$\delta_H$ (mult, *J* in Hz; #H)** | **COSY** | **HMBC** |
|---|---|---|---|---|
| 1 | 117.35 | 5.10 (dd, 17,2; 1H) | H-2 | $H_2$-3 |
| | | 5.07 (dd, 10,2; 1H) | H-2 | $H_2$-3 |
| 2 | 135.56 | 5.90 (ddt,17,10,7; 1H) | H-1, $H_2$-3 | $H_2$-3 |
| 3 | 38.35 | 2.30 (m; 2H) | H-2, H-4 | $H_2$-1, $H_1$-2 |
| 4 | 77.89 | 3.37 (m; 1H) | H-3, $H_2$-5 | $H_3$-26 |
| 5, 7 ,9…19 | 38.54-38.97 | 1.67-2.03 (m; 16H) | See text | See text |
| 6, 8, 10…18 | 75.92-76.11 | 3.64 (m; 7H) | See text | See text |
| 20 | 78.42 | 3.37 (m; 1H) | $H_2$-21, $H_2$-19 | $H_3$-34 |
| 21 | 34.26 | 1.56 (m; 2H) | $H_2$-20, $H_2$-22 | See text |
| 22 | 25.40 | 1.42 (m; 2H) | $H_2$-21, $H_2$-23 | See text |
| 23 | 32.82 | 1.30 (m; 2H) | $H_2$-22, $H_2$-24 | See text |
| 24 | 23.40 | 1.30 (m; 2H) | $H_2$-23, $H_2$-25 | See text |
| 25 | 14.60 | 0.91 (t, 7.1; 3H) | $H_2$-24 | $H_2$-24, $H_2$-23 |
| 26-34 | 56.24-56.47 | 3.16-3.28 (s; 27H) | | H-4,6…H-20 |

The heteronuclear 2D experiments, HMQC and HMBC data were obtained for compound **3** which were used to confirm the assignments of the chemical shifts and determine the long range connectivities between the protons and carbons respectively (See Table 1). The HMBC data showed the connectivities of the methoxy proton signals at δ 3.16-3.28 coupled to signals at δ 75.92-78.42, the oxymethine signals at δ 3.37-3.64 coupled to the signals at δ 56.24-56.47 and the methylene protons at δ 1.67-2.03 coupled to signals at δ 75.92-78.42. Specific correlations were observed for the methylene protons at δ 2.30 coupled to the terminal alkene signals (δ 5.07, 5.10, and 5.90) and the signal at δ 77.89 (designated C-4). The terminal methyl signal at δ 0.91 was coupled to the signals at δ 23.40 and 32.82 confirming the designations of C-24 and C-23 respectively. The NMR and mass spectral data obtained correlates with those observed for other PMAs identified

in other strains of cyanobacteria (Mynderse and Moore, 1979; Mori *et al.*, 1991; Jaja-Chimedza *et al.*, 2012).

The PMAs isolated in this study, with the exception of PMA **1**, were previously isolated from other strains of cyanobacteria, however not enough material was purified to obtain relative or absolute stereochemistry. However, the absolute stereochemistry of the PMAs isolated from the cyanobacteria, *Scytonema*, were determined by carrying out a direct comparison with the optically active synthetic compounds (Mori *et al.*, 1991a and 1991b). Based on the synthesis, it was determined that the PMA from *S. burmanicum* and *S. ocellatum* (Mori *et al.*, 1991a), specifically the nonamethoxy-1-pentacosene, was slightly different in structure from the PMA from *S. ocellatum* (Mori *et al.*, 1991b) with the location of one of the methoxy groups (C-34) being on C-22 instead of C-20 (Figure 2.16). Other PMAs with a similar structure were also isolated from *S. ocellatum* with one of the methoxy groups being located on a different carbon atom. These two structures however differed slightly in their chemical shifts as well as their optical rotation (done in $CHCl_3$ at $25^oC$, $c$ = +4.73 for 4,6,8,10,12,14,16,18,20-nonamethoxy-1-pentacosene and $c$ = +11.20 for 4,6,8,10,12,14,16,18,22-nonamethoxy-1-pentacosene). The NMR data obtained for PMA **3** in this study supports the assignment of 4,6,8,10,12,14,16,18,20-nonamethoxy-1-pentacosene, however not enough sample was obtained to do optical rotation for further confirmation based on the synthesis of these compounds in the previous studies.

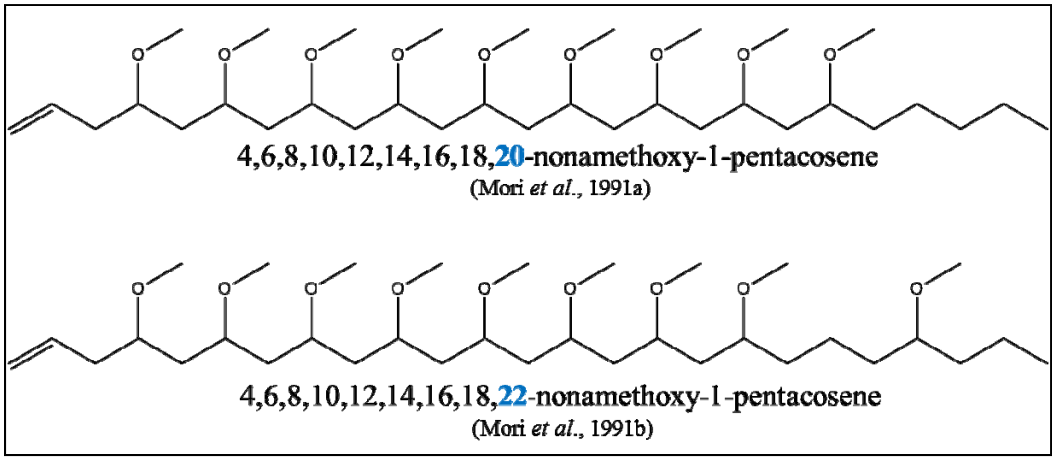


Figure 2. 16: Two different forms of nonamethoxy-1-pentacosene isolated from different species of *Scytonema* previously determined by synthesis (Mori *et al.*, 1991a and 1991b)

A model of the 3D structure of PMA **3** (based on the proposed structure as determine above) was generated using Chem3D Pro 12.0 Ink which shows the structure resembling a cork screw with the methoxy groups sticking out of the carbon backbone (Figure 2.17).

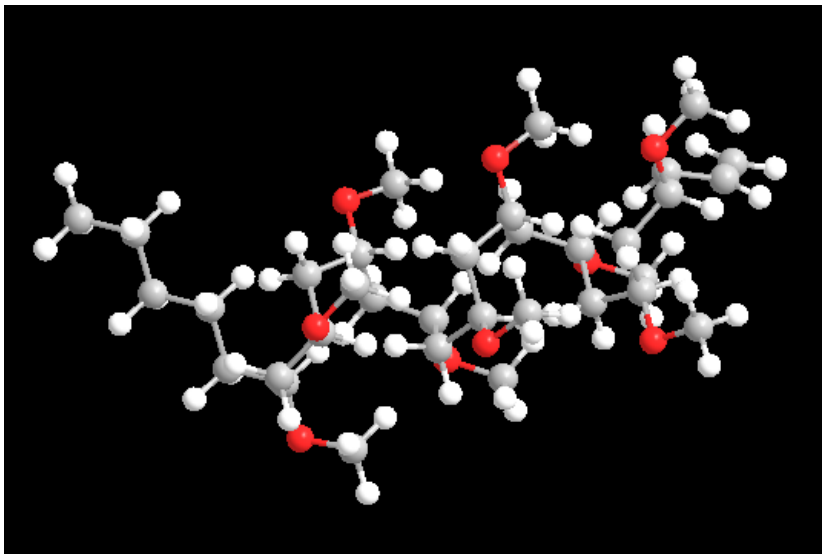

Figure 2. 17: A model of the 3D structure of PMA **3** from Chem3D Pro 12.0 Ink.

## 2.3. Experimental Section

### *2.3.1. Culturing of the Cyanobacteria*

The isolates of *A. ovalisporum*, (designated APH 127-1) and *C. raciborskii* (designated CAQS) were grown, as previously described (Berry *et al.*, 2007; Berry *et al.*, 2009; Gantar *et al.*, 2008), in 3-L flasks in BG11 medium under cool-white fluorescent light (intensity 30 $\mu Em^{-2} \cdot s^{-1}$) with aeration. The cells/biomass were harvested after three to four weeks by centrifugation and freeze-dried.

### *2.3.2. Extraction and Isolation of Polymethoxy-1-alkenes*

Isolation and purification of the polymethoxy-1-alkenes was carried out by a bioassay-guided fractionation using the zebrafish embryo model. Freeze-dried biomass of *A. ovalisporum* and *C. raciborskii* was extracted in chloroform in a 10:1 ratio overnight. The filtered extract was initially fractionated by flash chromatography on a normal phase silica-gel glass column (Silica Gel 60Å, Commercial 40–63 μm) with a stepwise gradient of ethyl acetate in hexane; a bioactive fraction (as identified with the zebrafish embryo toxicity assay; see Chapter 4) eluted with 100% ethyl acetate. This bioactive (i.e., 100% ethyl acetate) fraction was further separated by reverse-phase HPLC (Phenomenex Luna 5 μm C18 100 Å LC Column 250 × 4.6 mm; solvent gradient of 50:50 acetonitrile/water to 100% acetonitrile for 37 min at a flow rate of 1ml/min) with UV detection (i.e., 200 nm absorbance). The crude mixture of all six polymethoxy-1-alkenes eluted with retention times between 21 and 24 min. This mixture of polymethoxy-1-alkenes was confirmed to be toxic in the zebrafish embryo model (see Chapter 4), and individual

PMAs were purified by HPLC-UV (isocratic 65:35 acetonitrile/water) with the compounds eluting in order of increasing size (see Figure 2.2 and 2.3).

*2.3.3. Characterization of Polymethoxy-1-alkenes from A. ovalisporum*

Purified compounds were characterized by NMR and mass spectrometry. $^{1}$H- and $^{13}$C/DEPT-135 NMR, as well as two-dimensional homonuclear (i.e., COSY) and heteronuclear (i.e., HMQC and HMBC) analyses, were done on a Bruker AVANCE 400 MHz instrument. Mass spectrometry was performed on a Thermo TSQ Quantum Access ESI/triple quadrupole instrument coupled to a Thermo Accela UHPLC; high-resolution mass spectrometry data was done on a Thermo LTQ ESI-Orbitrap.

**4,6,8,10,12,14,16-Heptamethoxy-1-uncosene (1)**: HRESIMS *m/z* 505.4067 ($C_{28}H_{56}O_7$, $[M + H]^+$, Δmmu of -3.18); $^{1}$H NMR (400 MHz, benzene-$d_6$) δ 0.91 (t, 3H, *J* = 7.1 Hz), 1.30 (m, 4H), 1.43 (m, 2H), 1.56 (m, 2H), 1.67 (m, 2H), 1.81 (m, 4H), 2.02 (m, 6H), 2.30 (m, 2H), 3.16 (s, 3H), 3.21 (s, 3H), 3.22 (s, 3H), 3.24 (s, 3H), 3.25 (s, 3H), 3.27 (s, 3H), 3.27 (s, 3H), 3.37 (m, 2H), 3.64 (m, 5H), 5.07 (dd, 1H, *J* = 10,2 Hz), 5.09 (dd, 1H, *J* = 17, 2 Hz), 5.90 (ddt, 1H, *J* = 17, 10, 7 Hz).

**4,6,8,10,12,14,16,18-Octamethoxy-1-tricosene (2)**: HRESIMS *m/z* 563.4222 ($C_{31}H_{62}O_8$, $[M + H]^+$, Δmmu of -3.56); $^{1}$H NMR (400 MHz, benzene-$d_6$) δ 0.91 (t, 3H, *J* = 7.1 Hz), 1.30 (m, 4H), 1.42 (m, 2H), 1.56 (m, 2H), 1.67 (m, 2H), 1.81 (m, 5H), 2.03 (m, 7H), 2.30 (m, 2H), 3.16 (s, 3H), 3.21 (s, 3H), 3.22 (s, 3H), 3.24 (s, 3H), 3.25 (s, 3H), 3.27 (s, 3H),

3.27 (s, 3H), 3.28 (s, 3H), 3.37 (m, 2H), 3.64 (m, 6H), 5.07 (dd, 1H, $J$ = 10, 2 Hz), 5.09 (dd, 1H, $J$ = 17, 2 Hz), 5.90 (ddt, 1H, $J$ = 17, 10, 7 Hz).

**4,6,8,10,12,14,16,18,20-Nonamethoxy-1-pentacosene (3)**: HRESIMS *m/z* 621.4900 ($C_{34}H_{68}O_9$, $[M + H]^+$, Δmmu of -3.95); $^1$H NMR (400 MHz, benzene-$d_6$) δ 0.91 (t, 3H, $J$ = 7.1 Hz), 1.30 (m, 4H), 1.43 (m, 2H), 1.56 (m, 2H), 1.67 (m, 2H), 1.80 (m, 6H), 2.04 (m, 8H), 2.30 (m, 2H), 3.1641 (s, 3H), 3.2105 (s, 3H), 3.218 (s, 3H), 3.2432 (s, 3H), 3.2514 (s, 3H), 3.2708 (s, 3H), 3.2745 (s, 3H), and 3.2798 (s, 6H), 3.37 (m, 2H), 3.65 (m, 7H), 5.09 (dd, 1H, $J$ = 10, 2 Hz), 5.13 (dd, 1H, $J$ = 17, 2 Hz), 5.93 (ddt, 1H, $J$ = 17, 10, 7 Hz); $^{13}$C NMR (100 MHz, benzene-$d_6$) δ 14.3, 23.1, 25.1, 32.5, 33.9, 38.0, 38.2, 38.3, 38.6, 38.6 (3C), 38.7 (4C), 55.9, 56.0, 56.0 (3C), 56.0 (2C), 56.1, 56.1, 75.6, 75.7 (2C), 75.7, 75.8, 77.6, 78.1, 117.0, 135.3.

**4,6,8,10,12,14,16,18,20,22-Decamethoxy-1-heptacosene (4)**: HRESIMS *m/z* 679.5312 ($C_{37}H_{74}O_{10}$, $[M + H]^+$, Δmmu of -4.08); $^1$H NMR (400 MHz, benzene-$d_6$) δ 0.91 (t, 3H, $J$ = 7.1 Hz), 1.30 (m, 4H), 1.44 (m, 2H), 1.58 (m, 2H), 1.68 (m, 2H), 1.81 (m, 7H), 2.03 (m, 9H), 2.30 (m, 2H), 3.16 (s, 3H), 3.21 (s, 3H), 3.22 (s, 3H), 3.24 (s, 3H), 3.25 (s, 3H), 3.27 (s, 3H), 3.27 (s, 3H), 3.28 (s, 9H), 3.37 (m, 2H), 3.64 (m, 8H), 5.07 (dd, 1H, $J$ = 10, 2 Hz), 5.10 (dd, 1H, $J$ = 17, 2 Hz), 5.90 (ddt, 1H, $J$ = 17, 10, 7 Hz).

**4,6,8,10,12,14,16,18,20,22,24-Undecamethoxy-1-nonacosene (5)**: HRESIMS *m/z* 737.5728 ($C_{40}H_{80}O_{11}$, $[M + H]^+$, Δmmu of -4.51); $^1$H NMR (400 MHz, benzene-$d_6$) δ 0.91 (t, 3H, $J$ = 7.1 Hz), 1.30 (m, 4H), 1.44 (m, 2H), 1.57 (m, 2H), 1.68 (m, 2H), 1.81 (m,

8H), 2.03 (m, 10H), 2.30 (m, 2H), 3.16 (s, 3H), 3.21 (s, 3H), 3.22 (s, 3H), 3.24 (s, 3H), 3.25 (s, 3H), 3.27 (s, 6H), 3.27 (s, 3H), 3.28 (s, 9H), 3.37 (m, 2H), 3.64 (m, 9H), 5.07 (dd, 1H, $J$ = 10, 2 Hz), 5.10 (dd, 1H, $J$ = 17, 2 Hz), 5.90 (ddt, 1H, $J$ = 17, 10, 7 Hz).

**4,6,8,10,12,14,16,18,20,22,24,26-Dodecamethoxy-1-hentriacontene (6)**: HRESIMS *m/z* 795.6150 ($C_{43}H_{86}O_{12}$, $[M + H]^+$, Δmmu of -4.22); $^1$H NMR (400 MHz, benzene-$d_6$) δ 0.91 (t, 3H, $J$ = 7.1 Hz), 1.30 (m, 4H), 1.44 (m, 2H), 1.57 (m, 2H), 1.68 (m, 2H), 1.81 (m, 9H), 2.03 (m, 11H), 2.30 (m, 2H), 3.16 (s, 3H), 3.21 (s, 3H), 3.22 (s, 3H), 3.24 (s, 3H), 3.25 (s, 3H), 3.27 (s, 6H), 3.27 (s, 3H), 3.28 (s, 12H), 3.37 (m, 2H), 3.64 (m, 10H), 5.07 (dd, 1H, $J$ = 10, 2 Hz), 5.10 (dd, 1H, $J$ = 17, 2 Hz), 5.90 (ddt, 1H, $J$ = 17, 10, 7 Hz).

*2.3.4. Characterization of Polymethoxy-1-alkenes from C. raciborskii*

Purified compounds were characterized by NMR and mass spectrometry. $^1$H- and $^{13}$C/DEPT-135 NMR, as well as two-dimensional homonuclear (i.e., COSY) and heteronuclear (i.e., HMQC and HMBC) analyses, were done on a Bruker AVANCE 400 MHz instrument. Mass spectrometry was performed on a Thermo TSQ Quantum Access ESI/triple quadrupole instrument coupled to a Thermo Accela UHPLC; high-resolution mass spectrometry data was done on a Thermo LTQ ESI-Orbitrap.

**4,6,8,10,12,14,16,18-Octamethoxy-1-tricosene (2)**: HRESIMS *m/z* 563.4489 ($C_{31}H_{62}O_8$, $[M + H]^+$, Δmmu of -2.90); $^1$H NMR (400 MHz, benzene-$d_6$) 3.1643 (s, 3H), 3.2114 (s, 3H), 3.2185 (s, 3H), 3.2437 (s, 3H), 3.2525 (s, 3H), 3.2715 (s, 3H), 3.2750 (s, 3H), 3.2810 (s, 3H).

**4,6,8,10,12,14,16,18,20-Nonamethoxy-1-pentacosene (3)**: HRESIMS *m/z* 621.4900 ($C_{34}H_{68}O_9$, $[M+H]^+$, Δmmu of -3.64); $^1$H NMR (400MHz, benzene-$d_6$) δ 0.91 (t, 3H, *J* = 7.1 Hz), 1.30 (m, 4H), 1.42 (m, 2H), 1.56 (m, 2H), 1.67 (m, 2H), 1.81 (m, 6H), 2.03 (m, 8H), 2.30 (m, 2H), 3.1637 (s, 3H), 3.2101 (s, 3H), 3.2174 (s, 3H), 3.2427 (s, 3H), 3.2508 (s, 3H), 3.2705 (s, 3H), 3.2742 (s, 3H), and 3.2792 (s, 6H), 3.37 (m, 2H), 3.64 (m, 7H), 5.07 (dd, 1H, *J* = 10,2 Hz), 5.10 (dd, 1H, *J* = 17,2 Hz), 5.90 (ddt, 1H, *J* = 17,10,7 Hz); $^{13}$C NMR (100MHz, benzene-$d_6$) δ 14.6, 23.4, 25.4, 32.8, 34.3, 38.3, 38.5, 38.6, 38.9, 38.9 (3C), 39.0 (4C), 52.2, 56.3, 56.3 (3C), 56.4 (2C), 56.5, 75.9, 76.0 (2C), 76.1, 76.1, 77.9, 78.4, 117.3, 135.6.

**4,6,8,10,12,14,16,18,20,22-Decamethoxy-1-heptacosene (4)**: HRESIMS *m/z* 679.5312 ($C_{37}H_{74}O_{10}$, $[M+H]^+$, Δmmu of -4.27); $^1$H NMR (400MHz, benzene-$d_6$) δ 0.91 (t, 3H, *J* = 7.1 Hz), 1.30 (m, 4H), 1.42 (m, 2H), 1.55 (m, 2H), 1.67 (m, 2H), 1.81 (m, 7H), 2.02 (m, 9H), 2.30 (m, 2H), 3.16 (s, 3H), 3.21 (s, 3H), 3.22 (s, 3H), 3.24 (s, 3H), 3.25 (s, 3H), 3.27 (s, 3H), 3.27 (s, 3H), 3.28 (s, 9H), 3.37 (m, 2H), 3.65 (m, 8H), 5.07 (dd, 1H, *J* = 10,2 Hz), 5.10 (dd, 1H, *J* = 17,2 Hz), 5.90 (ddt, 1H, *J* = 17,10,7 Hz).

**4,6,8,10,12,14,16,18,20,22,24-Undecamethoxy-1-nonacosene (5)**: HRESIMS *m/z* 737.5733 ($C_{40}H_{80}O_{11}$, $[M+H]^+$, Δmmu of -4.08); $^1$H NMR (400MHz, benzene-$d_6$) δ 0.91 (t, 3H, *J* = 7.1 Hz), 1.30 (m, 4H), 1.44 (m, 2H), 1.58 (m, 2H), 1.68 (m, 2H), 1.81 (m, 8H), 2.04 (m, 10H), 2.30 (m, 2H), 3.16 (s, 3H), 3.21 (s, 3H), 3.22 (s, 3H), 3.24 (s, 3H), 3.25 (s,

3H), 3.27 (s, 6H), 3.28 (s, 12H), 3.37 (m, 2H), 3.65 (m, 9H), 5.07 (dd, 1H, *J* = 10,2 Hz), 5.10 (dd, 1H, *J* = 17,2 Hz), 5.90 (ddt, 1H, *J* = 17,10,7 Hz).

## 2.4. Conclusions

In the present study, the zebrafish embryo model was used to identify, isolate (via bioassay-guided fractionation) and characterize a homologous series (Figures 2.1 and 2.2) of isotactic PMAs, including one novel variant, as toxic components of the lipophilic fraction of the Lake Kinneret isolate of *A. ovalisporum* and the Australia isolate of *C. raciborskii*. To our knowledge, this is the first report of the PMAs as toxic or otherwise bioactive metabolites. It is, accordingly, suggested that these metabolites may not only explain previously observed developmental toxicity (Berry *et al.*, 2009) of lipophilic fractions from *A. ovalisporum* and *C. raciborskii*, but that these previously unrecognized (as toxic) components may contribute to the overall toxicity of these CYN-producing bloom species, and to the cyanobacteria perhaps more generally. Indeed, the prior isolation of these compounds (albeit as non-toxic metabolites) from other cyanobacterial species (Banker *et al.*, 2000; Mynderse and Moore, 1979; Mori *et al.*, 1991a and 1991b; Rao and Faulkner, 2002) may suggest that these toxic metabolites are relatively widespread, particularly within the cyanobacteria. As such, these findings suggest a need to further investigate these possibly widespread toxic metabolites of the cyanobacteria.

## References


1. Banker, R.; Carmeli, S.; Hadas, O.; Teltsch, B.; Porat, R.; Sukenik, A. Identification of cylindrospermopsin in *Aphanizomenon ovalisporum* (Cyanophceae) isolated from Lake Kinneret, Israel. *J. Phycol.* **1997**, *33*, 613–616.

2. Banker, R.; Teltsch, B.; Sukenik, A.; Carmeli, S. 7-Epicylindrospermopsin, a toxic minor metabolite of the cyanobacterium *Aphanizomenon ovalisporum* from Lake Kinneret, Israel. *J. Nat. Prod.* **2000**, *63*, 387–389.

3. Berry, J.; Gantar, M.; Gibbs, P.; Schmale, M. The zebrafish (*Danio rerio*) embryo as a model system for identification and characterization of developmental toxins from marine and freshwater microalgae. *Comp. Biochem. Physiol*. *C Pharmacol. Toxicol.* **2007**, *145*, 61–72.

4. Berry, J.; Gibbs, P.; Schmale, M.; Saker, M. Toxicity of cylindrospermopsin, and other apparent metabolites from *Cylindrospermopsis raciborskii* and *Aphanizomenon ovalisporum*, to the zebrafish (*Danio rerio*) embryo. *Toxicon* **2009**, *53*, 289–299.

5. Berry, J.P.; Gantar, M.; Gawley, R.E.; Wang, M.; Rein, K.S. Pharmacology and toxicology of pahayokolide A, a bioactive metabolite from a freshwater species of *Lyngbya* Isolated from the Florida everglades. *Comp. Biochem. Physiol. C Pharmacol. Toxicol.* **2004**, *139*, 231–238.

6. Brand, M.; Granato, M.; Nüsslein-Volhard, C. Keeping and Raising Zebrafish. In *Zebrafish*; Nüsslein-Volhard, C., Dahm, R., Eds.; Oxford University Press: Oxford, UK, **2002**; pp. 7–37.

7. Carmichael, W.W. A world overview—One-hundred-twenty-seven years of research on toxic cyanobacteria—Where do we go from here? *Adv. Exp. Med. Biol.* **2008**, *619*, 105–125.

8. Cox, P.A.; Banack, S.A.; Murch, S.J.; Rasmussen, U.; Tien, G.; Bidigare, R.R.; Metcalf, J.S.; Morrison, L.F.; Codd, G.A.; Bergman, B. Diverse taxa of cyanobacteria produce β-methylamino-L-alanine, a neurotoxic amino acid. *Proc. Natl. Acad. Sci. USA* **2005**, *102*, 5074–5078.

9. Ferrão-Filho, A.; Kozlowsky-Suzuki, B. Cyanotoxins: Bioaccumulation and effects on aquatic animals. *Mar. Drugs* **2011**, *9*, 2729–2772.

10. Gantar, M.; Berry, J.P.; Thomas, S.; Wang, M.; Perez, R.; Rein, K.S. Allelopathic activity among cyanobacteria and microalgae isolated from Florida freshwater habitats. *FEMS Microbiol. Ecol.* **2008**, *64*, 55–64.

11. Hill, A.J.; Teraoka, H.; Heideman, W.; Peterson, R.E. Zebrafish as a model vertebrate for investigating chemical toxicity. *Toxicol. Sci.* **2005**, *86*, 6–19.

12. Krüger, T.; Mönch, B.; Oppenhäuser, S.; Luckas, B. LC-MS/MS determination of the isomeric neurotoxins BMAA (β-*N*-methylamino-L-alanine) and DAB (2,4-diaminobutyric acid) in cyanobacteria and seeds of *Cycas revolute* and *Lathyrus latifolius*. *Toxicon* **2010**, *55*, 547–557.

13. Leão, P.; Pereira, A.R.; Liu, W.T.; Ng, J.; Pevzner, P.A.; Dorrestein, P.C.; König, G.M.; Vasconcelos, V.M.; Gerwick, W.H. Synergistic allelochemicals from a freshwater cyanobacterium. *Proc. Natl. Acad. Sci. USA* **2010**, *107*, 11183–11188.

14. MacMillan, J.B.; Ernst-Russell, M.A.; de Ropp, J.S.; Molinski, T.F. Lobocyclamides A–C, lipopeptides from a cryptic cyanobacterial mat containing *Lyngbya confervoides*. *J. Org. Chem*. **2002**, *67*, 8210–8215.

15. Mori, Y.; Kohchi, Y.; Noguchi, H.; Suzuki, M.; Carmeli, S.; Moore, R.E.; Patterson, G.M.L. Isotactic polymethoxy-1-alkenes from the terrestrial blue-green alga, *Scytonema ocellatum*: Structure and synthesis. *Tetrahedron* **1991**, *47*, 4889–4904.

16. Mori, Y.; Kohchi, Y.; Suzuki, M. Isotactic polymethoxy-1-alkenes from blue-green algae. Synthesis and absolute stereochemistry. *J. Org. Chem*. **1991**, *56*, 631–637.

17. Mynderse, J.S.; Moore, R.E. Isotactic polymethoxy-1-Alkenes from the blue-green alga *Tolypothrix conglutinata* var. *chlorata*. *Phytochemistry* **1979**, *18*, 1181–1183.

18. Rao, M.R.; Faulkner, D.J. Isotactic polymethoxydienes from the Philippines sponge *Myriastra clavosa*. *J. Nat. Prod.* **2002**, *65*, 1201–1203.

19. Staunton, J.; Weissman, K.J. Polyketide biosynthesis: A millenium review. *Nat. Prod. Rep.* **2001**, *18*, 380–416.

20. Teraoka, H.; Dong, W.; Hiraga, T. Zebrafish as a novel experimental model for developmental toxicology. *Congenit. Anom.* **2003**, *43*, 123–132.

21. Valério, E.; Chaves, S.; Tenreiro, R. Diversity and impact of prokaryotic toxins on aquatic environments: A review. *Toxins* **2010**, *2*, 2359–2410.

22. Wang, P.J.; Chien, M.S.; Wu, F.J.; Chou, H.N.; Lee, S.J. Inhibition of embryonic development by microcystin-LR in zebrafish, *Danio rerio*. *Toxicon* **2005**, *45*, 303–308.

# CHAPTER 3

## THE APPARENT BIOSYNTHETIC PATHWAY FOR POLYMETHOXY-1-ALKENES AND THEIR TAXONOMIC DISTRIBUTION IN DIFFERENT GENERA OF FRESHWATER CYANOBACTERIA

## 3.1. Introduction

It has been suggested that these PMAs are derived from the polyketide biosynthetic pathway on the basis of their linear polymethoxylated structure, specifically their pattern of 1,3-oxygenation, and their isolation with other toxins biosynthesized by this pathway (i.e., cylindrospermopsin; Banker *et al.*, 2000). It was also suggested that these compounds are produced by the bacteria (*A. ovalisporum*) only when it was producing CYN because PMAs could not be identified when the strain stopped producing the cyanotoxin (Banker *et al.*, 2000). This could indicate that PMAs are synthesized by similar mechanisms to those of CYN as a result of the loss of production of these two metabolites at the same time. According, this hypothesis was further tested to identify if the biosynthesis of the PMAs involved the PKS biosynthetic pathway. Additionally, these PMAs have been isolated from over three decades ago on the basis of their structure and have subsequently been found in various other strains terrestrial, marine, and freshwater cyanobacteria belonging to the order Nostocales (Mynderse and Moore, 1979; Mori *et al.*,1991a and 1991b; Banker *et al.*, 2000). It was therefore thought that these compounds may be widespread and so a culture collection of different genera of cyanobacteria was obtained to determine the prominence of these compounds.

### *3.1.1. Polyketide synthases biosynthetic pathway*

The linear polymethoxylated structure of the PMAs suggests a possible biosynthetic origin based on the polyketide synthase (PKS) pathway found conspicuously throughout the secondary metabolism of fungi, bacteria and microalgae (Staunton and Weissman, 2001). Indeed, this biosynthetic route - and specifically the sequential

condensation of acetate - for the PMAs has been previously suggested by other authors. Banker *et al.* (2000), for example, proposed such a biosynthetic origin as a result of both consideration of structure, and the observation that PMAs were not found among *A. ovalisporum* cultures that lost their ability to produce the PKS-derived CYN. Similarly, both Mynderse and Moore (1979) and Mori *et al.* (1991a and 1991b) identified PMAs from strains of *Tolypothrix* and *Scytonema*, respectively, known to produce the polyketide, tolytoxin. Given the abundance of PKS-derived secondary metabolites among cyanobacteria (examples Figure 3.1) and other microalgae, this biosynthetic origin may further support a widespread distribution of the PMAs.

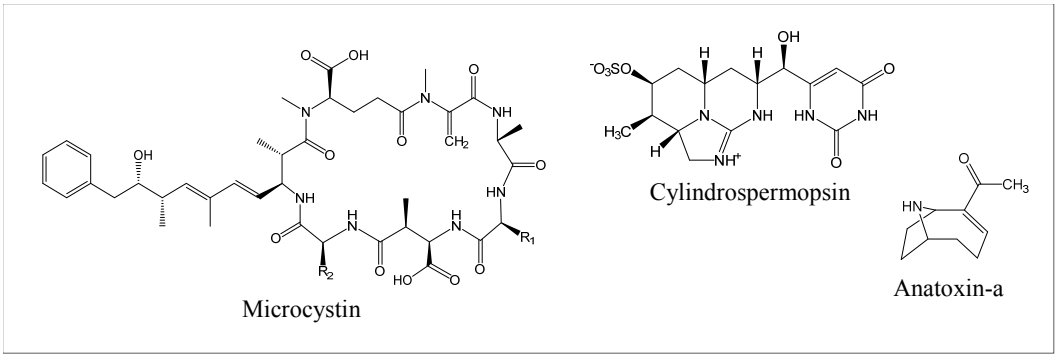


Figure 3. 1: Structure of compounds from freshwater cyanobacteria with biosynthesis involving the PKS biosynthetic pathway.

Polyketides are a diverse group of secondary metabolites that are commonly found in microorganisms (bacteria, fungi and microalgae) and are produced by a family of modular enzymes called polyketide synthases (PKSs). The carbon backbone of the polyketides is biosynthesized by way of Claisen Condensation of acyl coenzyme A (CoA), using acetate as the starter units, and further modified into bioactive metabolites (Snyder *et al.*, 2003).

Microorganisms that produce these readily uptake labeled substrates for the biosynthesis of metabolites (Staunton and Weissman, 2001) and as such feeding experiments with $^{13}$C-labeled acetate is commonly carried out to confirm biosynthesis via the PKS pathway. In the current study, we report the identification and purification of a series of PMAs (**2-5**) from a cultured strain of *C. raciborskii* (designated CAQS), originally isolated from an aquaculture pond in Australia (Saker and Eaglesham, 1999) and the suggested biosynthesis via the polyketide biosynthetic pathway.

### *3.1.2. Previously identified genera of PMA-producing cyanobacteria*

Polymethoxy-1-alkenes (**2-4**) were first isolated from a terrestrial tolytoxin-producing cyanobacterium, *Tolypothrix* because of its unusual structure (Mynderse & Moore, 1979). More than a decade later, these PMAs were isolated from another tolytoxin-producing cyanobacterium, *Scytonema burmanicum*, with two additional variants (n = 5 and n = 6) being found in *S. mirabile* (Mori *et al.*, 1991a). Additionally variations to these PMAs were identified in *S. ocellatum*, a cultured terrestrial tolytoxin-producing cyanobacterium (Mori *et al.*, 1991b). Another decade later, similar PMAs (**3-6**) were identified in a cultured cylindrospermopsin-producing strain of *A. ovalisporum*, isolated from Lake Kinneret, Israel. These PMAs were isolated according to their structure because there were no signs of bioactivity by the conventional cell-based assays. Recently, the zebrafish embryo was used in a bioassay-guided fraction for the isolation of six PMAs from *A. ovalisporum*, with a novel variant (**1**, n =7), showing that these compounds are indeed bioactive, thus contributing to the toxicity of these toxin-producing cyanobacterial strains.

## 3.2. Results & Discussion

### *3.2.1. Biosynthetic Origin of PMAs*

In order to investigate the possible biosynthetic origins of the **2-5**, and specifically the possible involvement of PKS pathways, cultures of *C. raciborskii* AQS were fed 1-$^{13}$C-labeled acetate (as a recognized "building blocks" of PKS-derived polyketides). Subsequently, **2-5** were purified (as for unlabeled cultures; see *Experimental Section 2.3.2*) from $^{13}$C-acetate-fed *C. raciborskii* cultures. Purified **2-5** were then analyzed for the incorporation of $^{13}$C by LC-MS and NMR spectroscopy (1D: Inverse-gated decoupled $^{13}$C).

**Mass spectrometric analysis of the $^{13}$C-labeled PMAs:** From partial purification of the PMAs from CAQS fed with $^{13}C_1$-labeled acetate, we identified all six PMAs (**1-6**) that were previously identified in *A. ovalisporum*, including minor uncharacterized PMAs, with only **2-5** purified in sufficient quantities. All the PMAs identified showed incorporation of $^{13}$C as determined by the sequence of additional peaks with a *m/z* 1 observed in the MS data, suggesting that these compounds are synthesized via the PKS pathway (Figure 3.2). PMA **3** was obtained in the highest quantity and was therefore used for further LC-MS and NMR analysis. Analysis by LC-MS of purified **3** (Figure 3.3) showed clear incorporation of $^{13}$C-heavy atom, and specifically a sequential ladder of masses starting from *m/z* 643 $[M+Na]^+$ to *m/z* 658, indicating that a possible fourteen $^{13}$C-atoms may have been incorporated (according to the number of additional *m/z* of +1

observed). All the other PMAs showed a sequential ladder of *m/z* of +1, again indicating the incorporation of the $^{13}C$ atoms into the molecules (Figure 3.2).

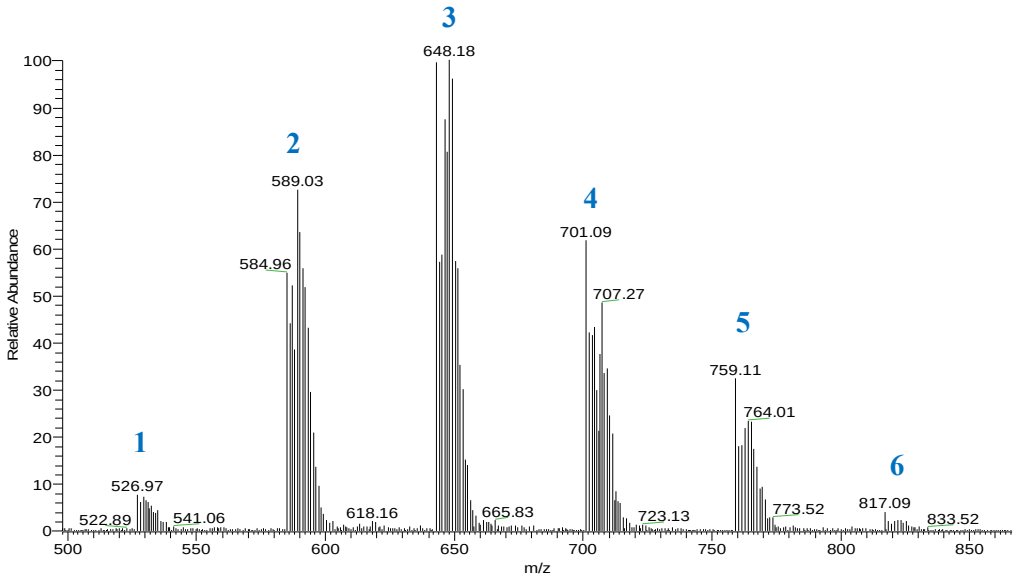


Figure 3. 2: LC-MS analysis of the isolated PMAs from CAQS showing the incorporation of the $^{13}C_1$-labeled acetate as shown from the additional *m/z* of +1.

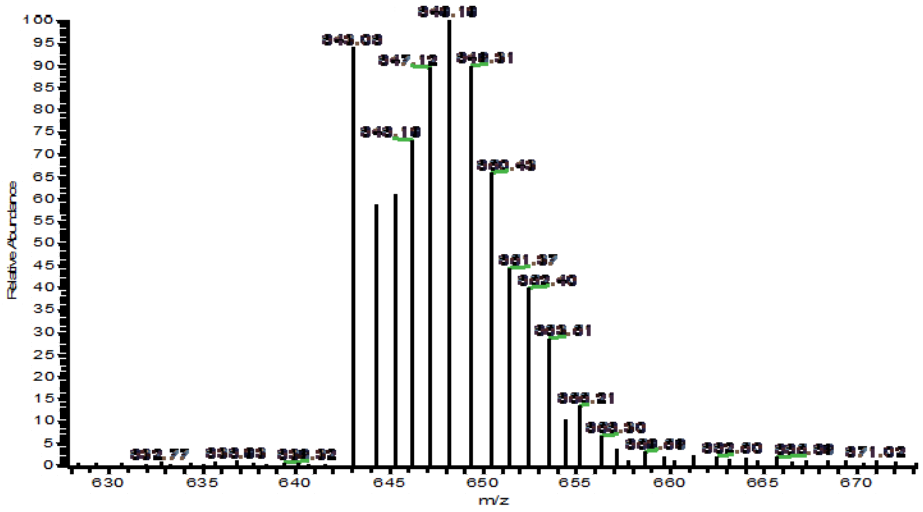


Figure 3. 3: LC-MS analysis of purified **3** from C-AQS after the feeding experiments with the labeled $^{13}C_1$-acetate.

The incorporation of $^{13}C$-label via exogenous acetate generally confirms that **2-5** were biosynthesized by the cultured organism. It also indicates that this incorporation from acetate, as biosynthetic building blocks, or alternatively by metabolic/catabolic products derived from acetate. The incorporation is also generally consistent with the PKS biosynthesis, however, to confirm that the pattern is by means of sequential condensation of the acetate building blocks (according to the PKS mechanisms), NMR studies were required.

**NMR Analysis of the $^{13}C$-Labeled PMAs:** The specific areas of $^{13}C$ incorporation were determined by NMR spectroscopy where an increase in the signals (relative to the unlabeled signals) of the corresponding chemical shifts indicated an incorporation of the carbon isotope. Isotopic enrichment was calculated using the method by Liu *et al.* (2012) by determining the integration of the carbon signals for both the natural abundance and enriched samples, and then calculating the percent of enrichment of the enriched sample compared to the natural abundance sample. Signals showing enrichment greater than 200% indicates regions of incorporation. The purified samples of PMA **3** (both enriched and natural abundance) were analyzed by NMR using the inverse-gated decoupled $^{13}C$ experiment in order to reduce the enhancement effects from the attached protons. Carbon signals were integrated for both samples, normalizing to a signal that is not expected to be enriched and calculated for percent enrichment.

Assignments of the chemical shifts and the corresponding percent enrichment for each signal is shown below in Table 3.1. Integration of the signals were normalized to C-

25 and the overlapping signals were divided by the corresponding number of carbons for the final % enrichment. Incorporation of the $^{13}$C-isotope was expected in the oxymethine carbons (C-6, 8, 10,…,20) according to the patterns observed with the PKS pathway. Enrichment was observed in the carbons assigned 1, 2, 22, 23, 24, and 25 which was not in agreement with what was expected. As a result of the overlap of the signals for the oxymethine carbons (C-6,8,…,18), methylene carbons (C-3,5,…,19), and the methoxy carbons (C26-34), determination of individual enrichments was not possible.

Table 3. 1: Assignments of the carbons from $^{13}$C-NMR and the percent enrichment of each signal. Integration of the signals was normalized to C-25.

| **Carbon assignments** | **$\delta_C$ (ppm)** | **Percent enrichment (%)** |
|---|---|---|
| 2 | 117.35 | **385.6** |
| 1 | 135.56 | **407.6** |
| 4 | 77.89 | 149.8 |
| 20 | 78.42 | 125.2 |
| 3,5,7,..,19 | 38.35-38.97 | 45.7 |
| 26-34 | 56.24-56.47 | 22.4 |
| 6,8,10,…,18 | 75.92-76.11 | 40.7 |
| 21 | 34.26 | 186.6 |
| 23 | 32.82 | **234.6** |
| 22 | 25.40 | **276.7** |
| 24 | 23.40 | **218.7** |
| 25 | 14.60 | **228.4** |

From the analysis of the NMR spectrum (Figure 3.4), splitting of the NMR signals was observed in all the individual carbon signals (C1, C2, C3, C4, C20, C21, C22, C23, C24, and C25) and partially in the overlapping signals of the oxymethine carbons (C6, C8,…, C18) observed at δ 75.9-76.1 as well as the overlapping methylene carbons (C5, C7,…,C19) observed at δ 38.9-39.0. As expected, there was no coupling observed for the

methoxy carbons due to the presence of the adjacent heteroatom. The couplings observed with the carbon signals indicate that there is incorporation of the $^{13}C$-isotope throughout the alkyl chain of the molecule and not just in alternating signals as hypothesized according to the PKS pathway. This ubiquitous incorporation of the $^{13}C$ atom suggests that the $^{13}C_1$-labeled acetate was possibly metabolized and utilized by a different biosynthetic pathway which uses the $^{13}C$ atoms to synthesize the PMAs. Further analysis is required to identify how these labeled carbon atoms are being incorporated into the molecule.

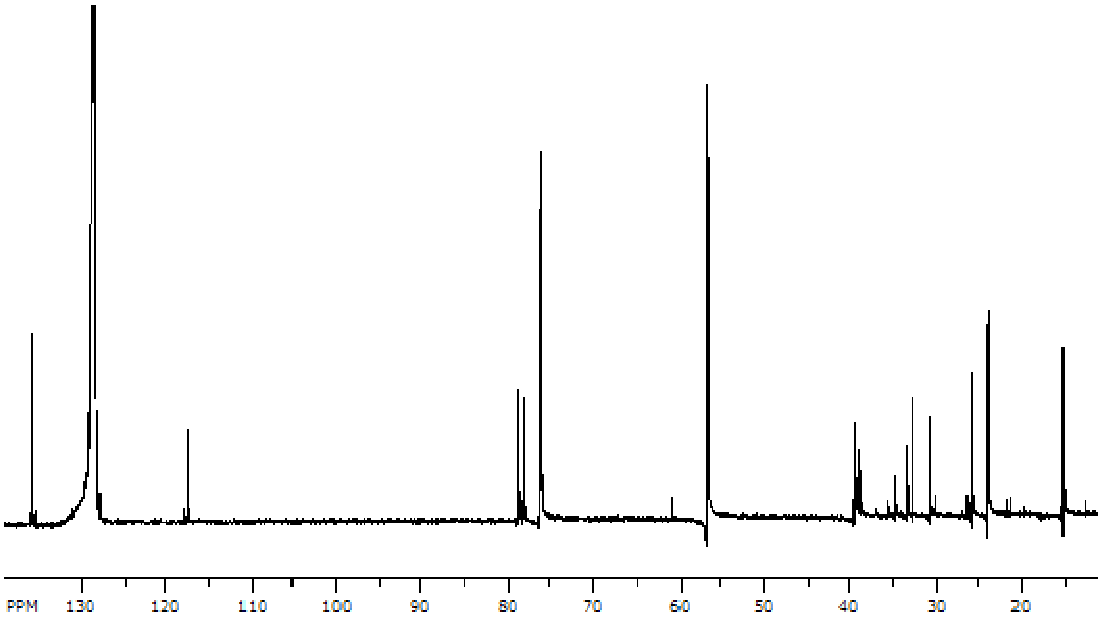


Figure 3. 4: Inverse-gated decoupled $^{13}C$-NMR spectrum of purified **3**.

The biosynthesis of PMAs by the PKS pathway was previously suggested by Banker *et al.* (2000) where it was observed that PMAs were not observed in strains of *Aphanizomenon* that no longer produced CYN (which is derived from the PKS

biosynthetic pathway). Likewise, PMAs were also previously isolated from strains of cyanobacteria that produce CYN (e.g., *A. ovalisporum*) or other PKS-derived toxins (e.g., tolytoxin; Mynderse and Moore, 1979 and Mori *et al.*, 1991a and 1991b). In the current study, PMAs were also identified from a CYN-producing strain of *C. raciborskii* (AQS), however, they were not observed in our non-CYN-producing strain of the same species (*C. raciborskii* 121-1; See Table 3.2). Further analysis of different strains of CYN-producing cyanobacteria will need to be analyzed to assess the co-occurrence of these two compounds.

*3.2.2. Taxonomic distribution of the PMAs*

In order to determine the distribution of PMAs, algal isolates (ninety-seven cyanobacteria and green algae) were analyzed for the presence of PMAs by LC-MS using a data-dependent scan, using the $[M+Na]^+$ as the target ion for each of the PMAs (Table 3.2). All three fractions (40% ethyl acetate in hexane, 100% ethyl acetate and 100% methanol) were screened for the presence of the PMAs with the PMAs being found in the 40% ethyl acetate in hexane fraction, including fractions from APH and CAQS which were used as controls to confirm that the methods for fractionation and MS analysis were successful in identifying the PMAs. PMAs were identified in the 40% ethyl acetate fraction.

From the data-dependent screening of the isolates, PMAs were observed in eight isolates which included both cyanobacteria and green algae. Cyanobacterial isolates identified to produce PMAs are *Anabaena* 66-2 (PMA **3**), *Microcystis* 81-11 (PMA **3**), *Nostoc* 23-2 (PMAs **2**-**5**), and *Pseudanabaena* 108-1 (PMAs **2**-**3**), all of which belong to

the order Nostocales with the exception of *Microcystis* which belongs to the order Chroococcales. Green algae isolates in which PMAs were identified are *Pediastrum* 104-6 (PMA **2**), *Scenedesmus* 3-4 (PMAs **2**-**5**), *Scenedesmus* 79-1 and 80-15 (PMAs **2**-**3**). Previously, PMAs were isolated from cyanobacterial strains belonging to the order Nostocales (Mynderse and Moore, 1979; Mori *et al.*, 1991a and 1991b; Banker *et al.*, 2000), however from this current screening, the PMAs seemed to be more widespread being found in *Microcystis* (Order Chroococcales) and green algae, a different organism than cyanobacteria.

Table 3. 2: Screening of cyanobacterial and green algal extracts for the presence of PMAs analyzed by LC-MS in data-dependent scan mode. PMAs were determined based on retention times and *m/z* of the $[M+Na]^+$ ions.

| ***Cyanobacterial Isolates*** | **Polymethoxy-1-alkenes** | | | | | | ***Cyanobacterial Isolates*** | **Polymethoxy-1-alkenes** | | | | | |
|---|---|---|---|---|---|---|---|---|---|---|---|---|---|
| | **1** | **2** | **3** | **4** | **5** | **6** | | **1** | **2** | **3** | **4** | **5** | **6** |
| ***Aphanizomenon*** | X | X | X | X | X | X | *Microcystis* 95-11 | | | | | | |
| ***Cylindrospermopsis* AQS** | X | X | X | X | X | X | *Microcystis* 95-12 | | | | | | |
| | | | | | | | *Microcystis* 95-13 | | | | | | |
| *Arthronema* 63a-5 | | | | | | | *Microcystis* 95-4 | | | | | | |
| *Amatoidea*/*Calothrix* 70-1 | | | | | | | *Microcystis* 99-1 | | | | | | |
| *Anabaena* 48-2 | | | | | | | *Nostoc* 15-7b | | | | | | |
| *Anabaena* 66-2 | | | X | | | | *Nostoc* 23-2 | | X | X | X | X | |
| *Anabaena* S12 | | | | | | | *Nostoc* 23-2a-1 | | | | | | |
| **Ankistrodesmus* 45-2 | | | | | | | *Nostoc* 64-15 | | | | | | |
| *Aphanothece* 103-7 | | | | | | | *Nostoc* EV-1 | | | | | | |
| *Aphanothece* 104-9 | | | | | | | *Nostoc* S2 | | | | | | |
| *Arthronema* 37-8-1 | | | | | | | *Oscillatoria* 101-1A8 | | | | | | |
| *Arthronema* 63-1 | | | | | | | *Oscillatoria* 21-9-3 | | | | | | |
| *Arthronema* 95-2a | | | | | | | **Pediastrum* 104-6 | | | X | | | |
| *Calothrix* 13-3 | | | | | | | *Phormidium* 49-1 | | | | | | |
| *Calothrix* 30-3 | | | | | | | *Phormidium* 62-2 | | | | | | |
| *Calothrix* 3-26 | | | | | | | *Phormidium* 64-13 | | | | | | |
| *Calothrix* 3-27 | | | | | | | *Phormidium* 69-9 | | | | | | |
| *Calothrix* 33-2 | | | | | | | *Plectonema* 33-7 | | | | | | |
| *Calothrix* 67-1 | | | | | | | *Pseudanabaena* 108-1 | | X | X | | | |
| **Coelastrum* 104-10 | | | | | | | *Pseudanabaena* 81-4 | | | | | | |

| ***Cyanobacterial Isolates*** | **Polymethoxy-1-alkenes** | | | | | | ***Cyanobacterial Isolates*** | **Polymethoxy-1-alkenes** | | | | | |
|---|---|---|---|---|---|---|---|---|---|---|---|---|---|
| | **1** | **2** | **3** | **4** | **5** | **6** | | **1** | **2** | **3** | **4** | **5** | **6** |
| *Cyanosarcina* 33-3 | | | | | | | *Pseudanabaena* 95-13a | | | | | | |
| ***Cylindrospermopsis* 121-1** | | | | | | | *Pseudoanabaena* 69-7 | | | | | | |
| *Dictiospherium* 107-2 | | | | | | | *Pseudoanabaena* 73-2 | | | | | | |
| *Fischerella* 114-12 | | | | | | | *Pseudocapsa* 64-17 | | | | | | |
| *Fischerella* 114-4 | | | | | | | **Scenedesmus* 3-4 | | X | X | X | X | |
| *Fischerella* 52-1 | | | | | | | **Scenedesmus* 79-1 | | X | X | | | |
| *Fischerella* 52-1 | | | | | | | **Scenedesmus* 80-15 | | X | X | | | |
| *Gleocapsa* 30-1-5 | | | | | | | *Scytonema* 26-1 | | | | | | |
| *Gleocapsa* 37-8 | | | | | | | *Scytonema* 26-1 | | | | | | |
| **Kirchneriella* 104-2 | | | | | | | *Spirulina* 21-0 | | | | | | |
| *Leptolyngbya* 102c-1 | | | | | | | *Synechococcus* 103-5 | | | | | | |
| *Leptolyngbya* 30-1-2 | | | | | | | *Synechococcus* 21-10a | | | | | | |
| *Leptolyngbya* 69-2 | | | | | | | *Synechococcus* 21-11 | | | | | | |
| *Leptolyngbya* 69-5 | | | | | | | *Synechococcus* 84-2a | | | | | | |
| *Leptolyngbya* 71-2 | | | | | | | *Synechococcus* 22-1 | | | | | | |
| *Limnothrix* 16-1 | | | | | | | *Synechococcus* 47-1 | | | | | | |
| *Limnothrix* 21-2-2 | | | | | | | *Synechococcus* 47-1 | | | | | | |
| *Limnothrix* 39-1 | | | | | | | *Synechococcus* 71-3 | | | | | | |
| *Limnothrix* 48-1 | | | | | | | *Synechococcus* 74-1 | | | | | | |
| *Limnothrix* 60-1 | | | | | | | *Synechocystis* 104-3 | | | | | | |
| *Lyngbya* 105-2 | | | | | | | *Synechocystis* 108-7 | | | | | | |
| *Lyngbya* 15-2 | | | | | | | *Synechocystis* 63a-2 | | | | | | |
| *Lyngbya* 29-3 | | | | | | | *Synechocystis* 79-3 | | | | | | |
| *Microcystis* 22-6 | | | | | | | *Synechocystis* 84-1 | | | | | | |

| ***Cyanobacterial Isolates*** | **Polymethoxy-1-alkenes** | | | | | | ***Cyanobacterial Isolates*** | **Polymethoxy-1-alkenes** | | | | | |
|---|---|---|---|---|---|---|---|---|---|---|---|---|---|
| | **1** | **2** | **3** | **4** | **5** | **6** | | **1** | **2** | **3** | **4** | **5** | **6** |
| *Microcystis* 36-1 | | | | | | | *Tolypothrix* 30-1-4 | | | | | | |
| *Microcystis* 75-1 | | | | | | | *Tolypothrix* 30-1-40 | | | | | | |
| *Microcystis* 81-11 | | | X | | | | *Tolypothrix* 38-6 | | | | | | |
| *Microcystis* 84-2 | | | | | | | *Tolypothrix* 64-11 | | | | | | |

*Note*: Isolates with an asterisk (*) are green algae and the isolates in bold are those from which PMAs have been purified.

## 3.3. Methods

### *3.3.1. 1-$^{13}$C-labeled acetate feeding experiments*

The polymethoxy-1-alkenes have slight resemblance to polyketides synthesized by the polyketide-synthase mechanism. As such, this hypothesis was evaluated by doing a feeding experiment with 1-$^{13}$C-labeled acetate and evaluated for incorporation of $^{13}$C in the molecules. Cyanobacterial cultures (APH and CAQS) were grown in 3L flasks in BG11 medium under cool-white fluorescent light (intensity 30μEm$^{-2}$sec$^{-1}$) with constant aeration (Gantar *et al.*, 2008). For feeding experiments, an actively growing culture of CAQS was sub-cultured (see Section *2.3.1. Culturing of Cyanobacteria*), and on days 2, 9, 16 and 23 supplemented with 500 mg of 1-$^{13}$C-labeled acetate; cultured material was harvested on day 25.

### *3.3.2. Purification of 1-$^{13}$C-labeled PMAs and Chemical Characterization*

Purification of the PMAs was carried out as before using the silica-gel column, with the 100% ethyl acetate fraction containing the labeled PMAs. Two HPLC purifications were performed to purify the PMAs; first with an increasing gradient of acetonitrile in water followed by an isocratic elution of 65% acetonitrile with each PMA being individually collected for chemical characterization. Mass spectral data was obtained by LC-MS using a HESI source. To determine the percentage enrichment of $^{13}$C in the PMAs, NMR experiments (specifically inverse-gated decoupled $^{13}$C) were carried out and compared to those of the unlabeled PMAs.

*3.3.3. Preparation of cyanobacterial extracts for PMA screening*

Ninety-seven algal isolates were obtained from a culture collection (obtained from Dr. Miroslav Gantar, FIU) and prepared based on the isolation of the PMAs. Isolates were extracted twice in chloroform, using the freeze-thaw method to break open the cells. The samples were filtered and the extracts (supernatant) were dried down and re-suspended in 1mL of chloroform. Extracts were fractionated using solid-phase extraction (SPE) cartridge (Supelclean LC-Si SPE Tubes, bed weight 100mg, volume 1mL) and three fractions were collected; 40% ethyl acetate in hexane, 100% ethyl acetate, and 100% methanol, with LC-MS analysis being done on all three fractions.

*3.3.4. Mass spectrometric analysis of the occurrence of PMAs*

All 3 fractions of the cyanobacterial isolates from the SPE were analyzed for the presence of PMAs by LC-MS on a reversed-phase column (Phenomenex Kinetex 2.6 µm C18 100 Å LC Column 100 × 4.6 mm). The fractions were analyzed using an acetonitrile gradient starting with 50% acetonitrile in water for 5mins with an increasing gradient up 100% acetonitrile over 15mins and kept at 100% acetonitrile for 5mins for a total run time of 25mins. A data-dependent MS analysis was done using electrospray ionization (ESI), and the retention times and masses were evaluated for the presence of PMAs using APH and CAQS as controls.

**3.4. Conclusion**

Analysis of the results from the feeding experiments testing the hypothesis that the biosynthesis of the PMAs occurs via the PKS biosynthetic pathway were inconclusive,

however there is some suggestion of a possibly different mechanism for the biosynthesis. The MS analysis indicates that there is incorporation of the $^{13}C$-labeled acetate, suggesting a PKS biosynthetic route, however NMR analysis showed that incorporation was seen throughout the entire molecule which is not consistent with the pattern of a PKS biosynthetic route. It can be however be concluded that these compounds were synthesized by the cultured organism. Further analysis is required to identify how the labeled acetate is being incorporated into the compounds.

PMAs were previously thought to be produced by cyanobacteria in the order of Nostocales. Results have shown that not only are they produced by many different genera of cyanobacteria (terrestrial, marine, and freshwater), they are also produced by green algae. This indicates that these molecules are widely produced in different environments, as well as from different organisms. These compounds may therefore contribute to the toxicity of cyanoHABs and other symbiotic organisms in various environments.

**References**


1. Banker, R.; Teltsch, B.; Sukenik, A.; Carmeli, S. 7-Epicylindrospermopsin, a toxic minor metabolite of the cyanobacterium *Aphanizomenon ovalisporum* from Lake Kinneret, Israel. *J. Nat. Prod.* **2000**, *63*, 387–389.

2. Gantar, M.; Berry, J.P.; Thomas, S.; Wang, M.; Perez, R.; Rein, K.S. Allelopathic activity among cyanobacteria and microalgae isolated from Florida freshwater habitats. *FEMS Microbiol. Ecol.* **2008**, *64*, 55–64.

3. Liu, L.; Bearden, D. W.; Rodriguez, J. C.; Rein, K. S. Biosynthesis of Athmu, a α,γ-hydroxy-β-amino acid of pahayokolides A–B. *Tetrahedron Lett.* **2012***, 53*, 6758-6760.

4. Mori, Y.; Kohchi, Y.; Noguchi, H.; Suzuki, M.; Carmeli, S.; Moore, R.E.; Patterson, G.M.L. Isotactic polymethoxy-1-alkenes from the terrestrial blue-green alga, *Scytonema ocellatum*: Structure and synthesis. *Tetrahedron* **1991**, *47*, 4889–4904.

5. Mori, Y.; Kohchi, Y.; Suzuki, M. Isotactic polymethoxy-1-alkenes from blue-green algae. Synthesis and absolute stereochemistry. *J. Org. Chem*. **1991**, *56*, 631–637.

6. Mynderse, J.S.; Moore, R.E. Isotactic polymethoxy-1-Alkenes from the blue-green alga *Tolypothrix conglutinata* var. *chlorata*. *Phytochemistry* **1979**, *18*, 1181–1183.

7. Saker, M. L.; Eaglesham, G. K. The accumulation of cylindrospermopsin from the cyanobacterium Cylindrospermopsis raciborskii in tissues of the Redclaw crayfish Cherax quadricarinatus. *Toxicon* **1999***, 37*, 1065-1077.

8. Snyder, R.; Gibbs, P.; Palacios, A.; Abiy, L.; Dickey, R.; Lopez, J.; Rein, K. Polyketide synthase genes from marine dinoflagellates. *Marine Biotechnology* **2003***, 5*, 1-12.

9. Staunton, J.; Weissman, K. J. Polyketide biosynthesis: a millennium review. *Nat. Prod. Rep.* **2001***, 18*, 380-416.

# CHAPTER 4*

## ASSESSMENT OF THE TOXICOLOGICAL EFFECTS OF POLYMETHOXY-1-ALKENES FROM *APHANIZOMENON OVALISPORUM* USING THE ZEBRAFISH EMBRYO BIOASSAY

*A portion of the work described in this chapter has been published in the journal, *Marine Drugs* (Jaja-Chimedza *et al.*, 2012).

## 4.1. Introduction

In several previous studies (Berry *et al.*, 2004; Berry *et al.*, 2007; Berry *et al.*, 2009; Walton *et al.*, in preparation), we have utilized the zebrafish (*Danio rerio*) embryo, as a model of vertebrate development, and specifically a toxicological (i.e. bioassay) system, to investigate "developmental toxicity" (i.e. inhibition or impairment of developmental pathways) of cyanobacterial secondary metabolites. The zebrafish embryo has become an increasingly important vertebrate model owing to a number of practical advantages including: a high fecundity capable of producing hundreds of eggs with a single breeding; rapid embryonic development with most internal organs being fully differentiated by 96 hours post fertilization (hpf); as well as a nearly transparent outer chorion allowing for development to be easily monitored using a light microscope (Berry *et al.*, 2007). As such, this model system is finding utility in fields ranging from genetics to toxicology/pharmacology to biotechnology (Teraoka *et al.*, 2003; Hill *et al.*, 2005). In prior studies (Berry *et al.*, 2004; Berry *et al.*, 2007; Berry *et al.*, 2009), the zebrafish embryo assay has been specifically applied to identification (i.e screening), purification (i.e. bioassay-guided fractionation) and characterization of developmental toxins from cyanobacteria.

As part of this on-going research, Berry *et al.* (2009) previously evaluated the hepatotoxin, cylindrospermopsin (CYN), as well as extracts from unialgal cultures of several CYN producing and non-producing strains of the widespread toxigenic cyanobacterial species, *Cylindrospermopsis raciborskii* and *Aphanizomenon ovalisporum*. Although CYN was found to be toxic, apparent impermeability of the embryonic chorion and/or cellular membranes, with respect to the water-soluble toxin,

necessitated microinjection of the pure compound for toxicity to be observed. In fact, a similar apparent impermeability – and requirement for microinjection – was, likewise, observed for the equally water-soluble microcystins (Wang *et al.*, 2005). Moreover, toxicity of microinjected CYN was generally only associated with a dose-dependent increase in mortality of embryos, but no clear or reproducible developmental dysfunction (Berry *et al.*, 2009). In contrast, however, concurrent evaluation of crude, non-polar (i.e. chloroform) extracts from strains of both *C. raciborskii* and *A. ovalisporum* identified developmental toxicity, clearly unrelated to the presence of CYN, and specifically associated with apparent lipophilic metabolites from extracts of all of the isolates evaluated (Berry *et al.*, 2009).

Toward understanding the possible contribution of these apparent lipophilic metabolites to the toxigenicity of these cyanobacterial species, the present study used the zebrafish embryo bioassay to guide purification for subsequent chemical and toxicological characterization of the previously identified (Berry *et al.*, 2009) developmental toxin(s) from one of these isolates. Indeed, in the present study, bioassay-guided fractionation, as previously described, led to the isolation, and chemical characterization of these previously identified polymethoxy-1-alkenes (PMAs), i.e. **4**-**6**, as well as three additional members (**1**-**3**) of the apparent homologous series (Figure 2.1), as lipophilic developmental toxins from the Lake Kinneret strain of *A. ovalisporum*. Although three of the six PMAs reported here have been isolated previously from this strain (Banker *et al.*, 2000) - as well as at least two other genera (i.e. *Scytonema*, *Tolypothrix*) of the cyanobacterial order Nostocales (Mynderse and Moore, 1979; Mori *et al.*, 1991a and 1991b) – in studies spanning more than three decades, they have not

previously been associated with toxicity. We report here on their developmental toxicity in the zebrafish embryo model, and specifically the apparent synergistic activity of congeners in the series.

## 4.2. Results & Discussion

Crude extracts containing PMAs and purified PMAs (**1**-**5**) from both strains of PMA-producing cyanobacteria were tested using the zebrafish embryos to have a better understanding of its toxicological effects. Additional bioactivity was evaluated using other bioasssays include mosquito larvicidal bioassay, cytotoxicity assay and antibacterial assay.

### *4.2.1. Zebrafish Embryo Bioassay*

Although previously isolated from *A. ovalisporum* (Banker *et al.*, 2000), and several other cyanobacterial species (Mynderse and Moore, 1979; Mori *et al.*, 1991a and 1991b), PMAs have not been previously associated with toxicity or other bioactivity. Indeed, Mynderse and Moore (1979) first isolated the isotactic PMAs, including **2**, **3** and **4**, as components of "non-toxic mixture," while looking for the cytotoxic polyketide, tolytoxin A. As such, the present study is the first report of the biological activity of the PMAs. It should, however, be noted that a parallel series of polymethoxydienes isolated from the marine sponge, *Myriastra clavosa*, were found to be moderately cytotoxic to a human colon cancer cell-line, and suggested in fact, based on chemical similarity, to be derived (via diet and metabolic transformation) from cyanobacteria (Rao and Faulkner, 2002).

**Individual PMAs**: In the current study, five of the six PMAs (**1**-**5**) were obtained in sufficient (i.e., accurately weighable) quantities, and subsequently evaluated for developmental toxicity in the zebrafish embryo model. Zebrafish embryos, exposed (five embryos per concentration) to a representative concentration range (10, 25, 50 and 100 μg $mL^{-1}$) of **1**-**5**, were observed up to five days post-fertilization (dpf) for mortality and apparent developmental dysfunction. It should be noted that solubility, and consequently the absolute dissolved concentration, of PMAs in aqueous assay medium remains uncertain; however, the assumption of relatively low water-solubility of these lipophilic compounds would suggest that prepared exposure concentrations may, in fact, overestimate actual dissolved exposure concentrations.

Notably, toxicity of PMAs in the zebrafish embryo assay seemed to correlate with chain length and/or associated degree of methoxylation of the variants. With regards to embryo mortality (Table 4.1), no effect was observed at the lowest exposure concentrations (10 and 25 μg $mL^{-1}$) for any of the variants tested. In a typical experiment, however, 100% mortality at 5 dpf was observed for embryos exposed to both 50 and 100 μg $mL^{-1}$ of the three smallest congeners (**1**-**3**), whereas relatively little (i.e., 20%-40%) or no mortality for the same doses were observed for embryos exposed to the two increasingly larger congeners (i.e., **4** and **5**, respectively) tested. For comparison, mortality in untreated controls was very low (i.e., approximately 1.7%, n = 60 embryos). Similarly, there was an apparently parallel, congener-dependent effect on hatching rates (Table 4.1). Again, little or no effect on hatching (i.e., 80%-100% hatching rate at 4 dpf; n = 5 eggs) was observed for lowest exposure concentrations (10 and 25 μg $mL^{-1}$) of any

of the PMAs tested relative to the untreated controls (98% hatching, n = 60 eggs). However, the hatching of embryos was inhibited by PMAs in a dose- and congener-dependent manner at the two highest exposure concentrations (50 and 100 μg $mL^{-1}$). Specifically, hatching (4 dpf) was completely inhibited in embryos exposed to 100 μg $mL^{-1}$ of congeners **1**-**3**, but only partially inhibited for embryos exposed to **4**, and not appreciably affected in embryos exposed to the largest variant tested (**5**). Supporting a dose and congener dependent effect, at 50 μg $mL^{-1}$ hatching was completely inhibited by only the two smallest congeners (**1** and **2**), and decreasingly affected by the larger **3**-**5**. These observations were further supported by a preliminary evaluation of **3**-**5**, which were initially purified in sufficient quantities to test. This preliminary exposure study showed a similar pattern to that reported in Table 4.1 for these congeners, with **3** causing 100% mortality as well as gross development defects at the highest concentrations tested (50 and 100 μg $mL^{-1}$), while **4** caused only low mortality (20%) at the highest concentration (100 μg $mL^{-1}$) and none at lower concentrations, and **5** did not cause mortality at any exposure level at 5 dpf. Although little or no mortality was observed for embryos exposed to **4** at these highest concentrations, all surviving embryos were characterized by developmental dysfunction and deformity (as discussed further below); in contrast, no distinguishable effects on development were observed for embryos exposed to any concentration of **5**. Thus, while the limited availability of purified material precluded conducting a full-scale quantitative toxicological characterization of the PMAs, the consistency of the trends observed strongly supports a dose and congener related toxicity effect on these embryos.

Table 4. 1: Mortality and Hatching Rates for Zebrafish Embryos Exposed to PMAs (**1**-**5**) from *A. ovalisporum* (Lake Kinneret, Israel). Mortality was recorded at five days post-fertilization (dpf) for five embryos per concentration. Hatching rates were recorded at 4 dpf.

| | **% Mortality (5 dpf)** [b] | | | | **Hatching Rate (4 dpf)** [b] | | | |
|---|---|---|---|---|---|---|---|---|
| **PMA** | | | | | | | | |
| **[a]Conc.:** | **10** | **25** | **50** | **100** | **10** | **25** | **50** | **100** |
| **1** | 20% | 0% | **100%** | **100%** | 100% | 100% | **0%** | **0%** |
| **2** | 0% | 0% | **100%** | **100%** | 100% | 80% | **0%** | **0%** |
| **3** | 0% | 0% | **100%** | **100%** | 100% | 80% | **40%** | **0%** |
| **4** | 0% | 0% | **40%** | **20%** | 100% | 100% | **60%** | **60%** |
| **5** | 0% | 0% | **0%** | **0%** | 100% | 100% | **80%** | **80%** |

[a] Concentration of PMAs tested at 10, 25, 50 and 100 μg $mL^{-1}$; [b] In treated wells n = 5 and in untreated controls, mortality was approximately 1.7%, while hatching rate was 98% (n = 60 embryos).

In addition to the effects on mortality and hatching rate, there was also an apparent correlation between both exposure dose and structural variation of the PMAs (i.e., degree of methoxylation, chain length) and observed morphological developmental effects (Figure 4.1). At the highest concentration tested (100 μg $mL^{-1}$), embryos exposed to the smallest congener (**1**) exhibited several indications of severely impaired development (Figure 4.1E), including near lack of pigmentation, impaired organogenesis (e.g., reduced eye formation), deformity of the yolk sac and other gross abnormalities. Although developmental effects were less profound for congeners **2** and **3** at the same exposure concentration (100 μg $mL^{-1}$), embryos exposed to both of these larger variants were also characterized (Figure 4.1F,G, respectively) by similar defects as well as the formation of edemas (along with reduced hatching rates; see above). Developmental dysfunction was uniformly observed (i.e., 100% of embryos), although the severity of this dysfunction varied, and in each case, was followed by embryo mortality within 5-6 dpf. In contrast, embryos exposed to the highest dosage of congener **4** showed relatively

limited developmental effects (e.g., slightly curved body axes; Figure 4.1H) and those exposed to **5** were indistinguishable (data not shown) from untreated controls (Figure 4.1I). Development was also inhibited and abnormal in all embryos exposed to a lower concentration (50 μg $mL^{-1}$) of **1**-**3**, but there was no clear correlation of prevalence or severity of defects with congener size. (Figure 4.1A-C). However, similar to the effects observed at the higher concentrations, there were clearly minimal effects of congener **4** (Figure 4.1D) and no detectable effects associated with **5**. One particularly notable effect observed was an apparent pooling of blood between the anterior surface of the yolk and the heart in embryos exposed to **1**-**3** (indicated by arrows in Figure 4.1); this was most obvious in embryos exposed to the lower concentration (50 μg $mL^{-1}$) of all three of these congeners and the higher concentration (100 μg $mL^{-1}$) of the largest of these variants (**3**). This effect was not observed in the more severely deformed embryos exposed to the highest concentration of **1** and **2**, where it was likely obscured by the numerous severe developmental defects present in these fish. As for the assessment of mortality and hatching rate (see above; Table 4.1), data from a single experiment are presented, due to limitations of the purified PMAs. However, additional studies with a subset of these congeners, including both evaluation of initially purified amounts of **3**-**5** (as discussed above), and the subsequent evaluation of **3** and **4** with respect to apparent interactive effects (Figure 4.2; discussed below), likewise generally confirm the observed congener-dependent trend of delayed and/or dysfunctional development.

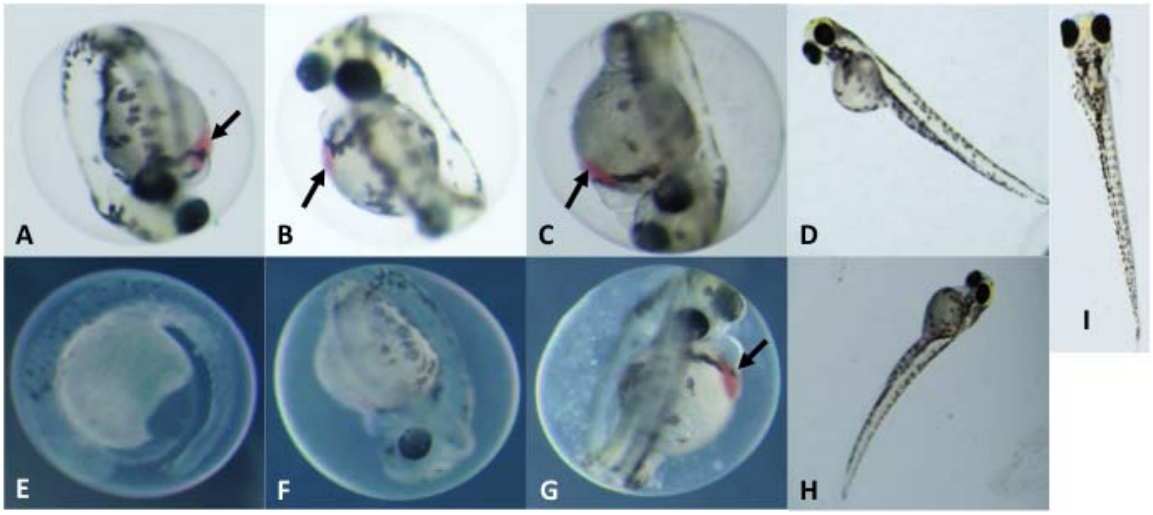


Figure 4. 1: Developmental Toxicity of PMAs (**1**-**4**) Isolated from *A. ovalisporum* (Lake Kinneret, Israel). Photomicrographs of embryos at 4 dpf. Shown are embryos exposed to 1-4 at 50 μg $mL^{-1}$ (A-D, respectively) and 100 μg $mL^{-1}$ (E-H, respectively). Untreated control embryo at 4 dpf (I) shown for comparison. Arrows indicate areas where blood is pooled adjacent to the heart. Images in A-C and E-G, are not to scale with D, H and I.

**Synergistic Effects**: Based on the qualitatively more pronounced developmental toxicity observed during bioassay-guided fractionation compared to that of individual congeners, we evaluated pair-wise combinations of **3** and **4** - as two of the most abundant variants (i.e., purified in the largest quantity) with the latter showing only relatively limited toxicity - in order to assess possible synergistic and/or additive effects of the PMAs. Interestingly, a clear interactive effect of the congeners, in terms of embryos toxicity, was observed for embryos exposed to a combination of two variants when compared to either **3** or **4**, individually. Embryos exposed to 50 and 100 μg $mL^{-1}$ of each compound were characterized by the typically moderate developmental dysfunction observed for these variants (Figure 4.1 and 4.2A-C). However, when exposed to equivalent total concentrations comprised of equal amounts congeners **3** and **4** (i.e., 25 μg $mL^{-1}$ and 50 μg $mL^{-1}$, respectively, of **3** and **4**), there was a clearly more pronounced

inhibition of development (Figure 4.2D,E). All embryos exposed to both combined concentrations were characterized by a severe inhibition of organogenesis and overall differentiation and development of the embryo that was not observed for embryos exposed to any of the congeners individually at an equivalent concentration. This observation is consistent with a synergistic effect of these variants and may explain increased toxicity of PMA mixtures (when compared to individual variants). Synergistic interactions of biologically active cyanobacterial metabolites have been previously reported. Recently, for example, Leão *et al.* (2010) documented similar synergistic effects with regards to algicidal activity of the cyclic peptide congeners, portoamides A and B, isolated as apparent allelochemicals from a freshwater strain of *Oscillatoria*. Likewise, a similarly synergistic effect of lobocyclamides A and B, isolated from a marine cyanobacterial species, Lyngbya confervoides, was previously reported (MacMillan *et al.*, 2002), specifically in relation to antifungal activity of these lipopeptides.

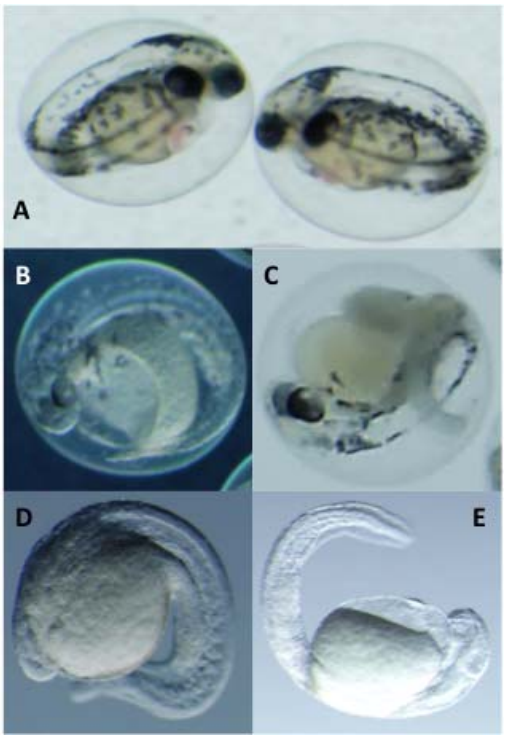


Figure 4. 2: Apparent synergistic interactions in the developmental toxicity of **3** and **4**. Shown are embryos exposed to 50 µg $mL^{-1}$ of **3** (A), and 100 µg $mL^{-1}$ of **3** (B) and 4 (C), compared to an equivalent combined total concentration (i.e., 25 and 50 µg $mL^{-1}$ of each) of the two variants (D and E, respectively). Embryos shown at 4 dpf.

The identification of toxicity associated with the PMAs, combined with the previous isolation of related variants from other distantly related marine, freshwater and terrestrial cyanobacterial genera (Mynderse and Moore, 1979; Mori *et al.*, 1991a and 1991b), as well as the cyanobacterially derived polymethoxydienes found in marine sponges (Rao and Faulkner, 2002), suggests that PMAs may represent a relatively widespread toxic metabolite from the blue-green algae. Moreover, preliminary evaluation by LC-MS, and subsequent purification and identification (by MS and $^{1}$H-NMR), confirmed the presence of **1-6** in the extracellular medium of the *A. ovalisporum* cultures (data not shown), and suggests that these lipophilic metabolites may, to some degree, be released - either actively by excretion, or passively via senescence of algal cells - into the

surrounding aqueous environment. Accordingly, it is proposed that the presence of these lipophilic metabolites may not only contribute to previously observed toxicity associated with lipophilic fractions of toxigenic cyanobacteria (Berry *et al.*, 2009), but to the observed toxicity of the bloom-forming cyanobacteria more generally.

### *4.2.2. Mosquito Larvicidal Bioassay*

Mosquito larvae (*Aedes aegyptii*) were used to test for larvicidal activity of the PMAs, using both crude extracts and purified compounds. Chloroform extracts of APH and CAQS, and SPE fractions (40% ethyl acetate, 100% ethyl acetate, and 100% methanol) were tested at different doses and bioactivity was observed over a period of 8 days. For the chloroform extracts, bioactivity was observed in doses of 10 and 50µL, with no bioactivity being observed at 100µL. At 10µL, 25% mortality was observed by day 3 and 50% mortality was observed by day 5 until the end of the bioassay. At 50µL, 25% mortality was observed at day 5 and for the rest of the bioassay. The only SPE fraction that showed bioactivity was 100% ethyl acetate at 100µL where 25% mortality was observed from day 4 onwards. There was 3% mortality observed for the controls and the mortality occurred at day 6.

For the purified PMAs, bioactivity was only observed with PMA **4** at 100µg/mL in both bioassays using the new and the old eggs. For the new eggs, no mortality was observed up to 8 days, however the larvae were slow moving and there was slightly slow development. At 5 days, the larvae were still at the 2$^{nd}$ instar stage and remained there until day 7 after which further development slowly continued with the larvae being noticeably smaller than the controls. There were no mortalities in the controls (solvent

and water) and development was normal. For the old eggs, 25% mortality was observed from day 2 to day 8. At day 3, all larvae were at the 1st instar stage and by day 5 only one larva was at the 2nd instar stage. By day 6, all larvae were at the 2nd instar stage with one larva being very early. This slow development continued throughout the rest of the bioassay with only one larva reaching 3rd instar by the end of the bioassay. There were no mortalities observed in the controls and development proceeded as normal.

In both new and old eggs, PMA **4** only showed slight bioactivity at the highest concentration tested. None of the other PMAs showed any bioactivity suggesting that the mosquito larvae are not very susceptible to these compounds. Though there was slow development observed in the larvae exposed to PMA 4, there were no apparent developmental abnormalities. This observed slow development was slightly more pronounced in the old eggs than the new eggs, which is to be expected since the new eggs tend to be more robust than the old eggs.

Table 4. 2: PMA exposures to mosquito larvicides, showing results at day 8 of the bioassay.

| | **% Mortality (Instar)** [b] New Eggs (2 weeks) | | | | **% Mortality (Instar)** [b] Old Eggs (2 mnths) | | | |
|---|---|---|---|---|---|---|---|---|
| **PMA** | | | | | | | | |
| **[a]Conc.:** | **10** | **25** | **50** | **100** | **10** | **25** | **50** | **100** |
| **1** | 0 (3) | 0 (3) | 0 (3) | ND | 0 (3) | 0 (3) | 0 (3) | ND |
| **2** | 0 (3) | 0 (3) | 0 (3) | ND | 0 (3) | 0 (3) | 0 (3) | ND |
| **3** | 0 (3) | 0 (3) | 0 (3) | ND | 0 (3) | 0 (3) | 0 (3) | ND |
| **4** | 0 (3) | 0 (3) | 0 (3) | 0 (2) | 0 (3) | 0 (3) | 0 (3) | 0 (2) |
| **5** | 0 (3) | 0 (3) | 0 (3) | ND | 0 (3) | 0 (3) | 0 (3) | ND |

Note: Control larvae were at late stage 3rd instar upon termination of the bioassay.

*4.2.3. Cytotoxicity Bioassay*

Crude extracts containing PMAs were analyzed using a cell based bioassay to test for cytotoxicity against 3 different cell lines; PC-3, SKMEL-5, and HEPG-2. Chloroform extracts of APH, CAQS, and CMEX were used and the hexane extract of MC 81-11. Cells were dried down and resuspended in 25µL of DMSO for a total concentration of approximately 2% DMSO (maximum amount that the cells can withstand). No bioactivity was observed in the cells using any of the cyanobacterial isolates as indicated by the pink color from the alamar blue solution. The PMAs originally isolated showed no bioactivity against cell lines (Mynderse and Moore, 1979) which was also similar to what was observed for these cyanobacterial extracts containing crude mixtures of PMAs.

*4.2.4. Antibacterial Bioassay*

Five bacterial strains, including Gram-negative (*E. coli*) and Gram-positive, were used to identify any potential antibacterial activity with the crude cyanobacterial extracts known to contain the PMAs. Chloroform extracts were used for APH, CAQS, and CMEX, and the hexane extract of MC 81-11 against the five strains of bacteria as shown in the Table 4.2. Slight bioactivity was observed in the extracts from CAQS, CMEX, and MC 81-11 against the bacteria *B. megaterium* and in the CAQS extract against *E. coli*, however there was no other bioactivity observed against the other bacterial strains. No bioactivity was observed for the APH against any of the bacterial strains. Since no significant bioactivity was observed with any of the cyanobacterial isolates no further fractionation was performed and no further analysis was carried out.

Table 4. 3: Antibacterial activity of extracts of the cyanobacterial isolates using 5 different strains of bacteria.

| **Cyanobacterial** | **Bacterial Strain** | | | | |
|---|---|---|---|---|---|
| **Isolate** | ***B. megaterium*** | ***B. subtilis*** | ***E. coli*** | ***M. luteus*** | ***S. aureus*** |
| APH | - | - | - | - | - |
| CAQS | + | - | + | - | - |
| CMEX | + | - | - | - | - |
| MC 81-11 | + | - | - | - | - |

## 4.3. Methods

### *4.3.1. Zebrafish Maintenance and Breeding*

The zebrafish (*Danio rerio*) embryo was used as a model of developmental toxicity for both bioassay-guided fractionation and subsequent toxicological characterization. The maintenance and breeding of adult zebrafish, and the embryo toxicity bioassays, were carried out as previously described by Berry *et al.* (2004 and 2007) and according to protocols approved by the FIU Institutional Animal Care and Use Committee (IACUC). The zebrafish lines used for this experiment were obtained from Dr. Patrick Gibbs (University of Miami Rosenstiel School of Marine and Atmospheric Science –RSMAS; P4 line) and Petco Animal Supplies Inc. Adult zebrafish (males and females) were maintained in tanks with dechlorinated tap water (treated with Amquel) at 26 ± 0.5$^{o}$C on a diet of fish flakes and brine shrimp. The zebrafish were subjected to a light/dark cycle of 14h/10h with mating and spawning occurring at the beginning of the light cycle.

For breeding, about 10-20 male and female zebrafish were placed above a mesh enclosure in a 10-L tank within 15 minutes of the onset of the light cycle. Upon successful breeding, the fertilized eggs would fall through the mesh and settle at the

bottom of the tank where they could be collected. After the eggs were collected, they were rinsed fish water and subsequently placed in a Petri dish with E3 medium containing methylene blue (5mM NaCl, 0.17mM KCl, 0.33mM $CaCl_2$, and 0.33mM $MgSO_4$: Brand *et al.,* 2002). Unfertilized and poor quality embryos were removed from the dish and the remaining embryos were subsequently used (usually within 2-3 hpf) for developmental toxicological studies.

*4.3.2. Zebrafish Embryo Bioassay (Exposure Studies)*

Toxicity was evaluated in solvent-resistant, polypropylene 24-well plates (Evergreen Scientific, Los Angeles, CA) with five embryos per well in E3 medium (Brand *et al.*, 2002). Extracts and fractions were typically evaluated at a high- (100 μL) and low- (10 μL) exposure concentration, and vehicle (corresponding solvent) and "untreated" controls were also included in each assay. The solvent was evaporated from the assay plates, prior to adding medium (E3) and embryos, and accordingly there was no observed effect of the solvent (relative to the untreated controls). The embryos were observed up to 5 days post fertilization (dpf) for bioactivity. In addition to percent hatching and mortality, developmental toxicity was recorded by photomicrography using an Olympus SZX7 stereomicroscope equipped with an Olympus DP72 digital camera.

**Exposures with Individual PMAs:** Purified PMAs were evaluated at concentrations of 2, 5, 10, 25, 50 and 100 μg $mL^{-1}$ (in acetonitrile). Vehicle (acetonitrile-only) and "untreated" controls were also included with each exposure.

**Synergism Experiments:** During purification of the PMAs, there was some evidence to suggest that there was a synergistic relationship with the different PMAs which led to the development of a synergistic experiment to analyze this possibility. Only PMAs **3** and **4** were obtained in sufficient quantities to do additional exposures and therefore were initially used as a preliminary assessment of synergism at individual concentrations of 10, 25 and 50 μg $mL^{-1}$ for a total concentration of 20, 50 and 100 μg $mL^{-1}$ (for a total of 3 treatments).

*4.3.3. Mosquito Larvicidal Bioassay*

The mosquito larvicidal bioassay was performed by Jerry Berry using the following protocol. Crude extracts and purified compounds were placed in 24-well polypropylene plates and the solvent was allowed to evaporate. The plates were then filled with newly hatched mosquito larvae ($1^{st}$ instar stage) in water using 4 larvae per well, for a total of 1mL. Solvent controls were prepared in the same manner as the cyanobacterial samples. Larvae were fed daily with 30μL of a 0.1% yeast powder solution, and assessed for up to 8 days for mortality, current instar stage, and developmental effects.

Crude chloroform extracts of CAQS were tested at doses of 10, 50 and 100μL and SPE fractions (40% hexane in ethyl acetate, 100% ethyl acetate, and 100% methanol) using new eggs (approximately 2 weeks old). Purified PMAs (**3**-**6**) from CAQS were used for the mosquito larvicidal bioassay at concentrations of 10, 25, and 50μg/mL for all PMAs and up to 100μg/mL for PMA **4** only because it was the most abundant. Purified samples were tested using both new (2 weeks) and old (2 months) eggs, representing the wet and dry seasons respectively.

*4.3.4. Cytotoxicity Bioassay*

The cytotoxicity bioassay was carried out using two different cancer cell lines obtained from American Type Culture Collection (ATCC; Virginia, USA); prostate cancer (PC-3), skin melanoma (SKMEL-5), and hepatoma (HEPG-6) cell lines. Cells were sub-cultured using RPMI medium (for PC-3 and SKMEL-5) and Eagle's medium (for HEPG-6) in 96-well plates for bioassay. Exposures were carried out once the cells were confluent. Prepared chloroform extracts containing a mixture of PMAs were tested for cytotoxic activity at dosages of 0.25, 0.5, 1, and 2µL, using dimethylsulfoxide (DMSO) as the solvent. Cells were incubated overnight after which the medium was removed and replaced with 10% alamar blue in RPMI or Eagle's medium for 4 hours to assess for mortality. For dead cells, the medium will remain blue, and for live cells, the medium will turns red/pink due to metabolism by the cells.

*4.3.5. Antibacterial Bioassay*

The antibacterial bioassay was carried out with five bacterial strains provided by Miroslav Gantar (FIU, Department of Biological Sciences); *Escherichia coli*, *Staphylococcus aureus*, *Bacillus megaterium*, *Bacillus subtilis*, and *Micrococcus luteus*. Liquid cultures of the bacteria were prepared using nutrient broth for the bioassay. Bioassays were done using the disc-diffusion method, using 6mm discs. Chloroform extracts of APH and CAQS were applied to the discs (30µL) and the solvent was allowed to evaporate before placing on the agar plate. Negative controls (solvent only) and positive controls (neomycin at 0.1 and 0.5mg/mL) were also carried out. Liquid cultures (approximately 1mL) were placed on the agar plates and dispersed for full coverage.

Discs containing the samples and the controls were then placed on the plates which were left to incubate overnight, and subsequently observed for inhibition of growth.

### 4.4. Conclusion

In the present study, the zebrafish embryo model was used to evaluate the toxicological effects of a homologous series (Figure 2.1) of isotactic PMAs which are toxic components of the lipophilic fraction of the Lake Kinneret isolate of *A. ovalisporum*. Although, toxicological evaluation of these compounds was somewhat limited by availability of purified amounts of the toxins - particularly given the relatively low solubility/activity, and high exposure concentrations required, for the individual congeners - our initial studies suggest both a dose-dependent toxicity relationship (Figure 4.2) and a relationship between toxicity in the zebrafish embryo model and structural variations (i.e. chain length, degree of methoxylation) of the congeners. Moreover, evaluation of the interactive effects indicates a possible synergism between variants with enhanced developmental toxicity (Figure 4.3) observed for pair-wise combinations of the PMAs (e.g. **3** and **4**).

This is the first report of the PMAs as toxic or otherwise bioactive metabolites. It is, accordingly, suggested that these metabolites may not only explain previously observed developmental toxicity (Berry *et al.*, 2009) of lipophilic fractions from *A. ovalisporum*, but that these previously unrecognized (as toxic) components may contribute to the overall toxicity of this CYN-producing bloom species, and the cyanobacteria perhaps more generally. Indeed, the prior isolation of these compounds (albeit as non-toxic metabolites) from other cyanobacterial species (Mynderse and

Moore, 1979; Mori *et al.*, 1991a and 1991b; Banker *et al.*, 2000; Rao and Faulkner, 2002), and current identification of these compounds in additional strains of cyanobacteria and also isolates of green algae suggests that these toxic metabolites are relatively widespread, and not only within the cyanobacteria. As such, these compounds contribute to the toxicity of cyanoHABs as well as green algal blooms.

**References**


1. Banker, R.; Teltsch, B.; Sukenik, A.; Carmeli, S. 7-Epicylindrospermopsin, a toxic minor metabolite of the cyanobacterium *Aphanizomenon ovalisporum* from Lake Kinneret, Israel. *J. Nat. Prod.* **2000**, *63*, 387–389.

2. Berry, J.; Gantar, M.; Gibbs, P.; Schmale, M. The zebrafish (Danio rerio) embryo as a model system for identification and characterization of developmental toxins from marine and freshwater microalgae. Comp. Biochem. Physiol. C Pharmacol. Toxicol. 2007, 145, 61–72.

3. Berry, J.; Gibbs, P.; Schmale, M.; Saker, M. Toxicity of cylindrospermopsin, and other apparent metabolites from Cylindrospermopsis raciborskii and Aphanizomenon ovalisporum, to the zebrafish (Danio rerio) embryo. Toxicon 2009, 53, 289–299.

4. Berry, J.P.; Gantar, M.; Gawley, R.E.; Wang, M.; Rein, K.S. Pharmacology and toxicology of pahayokolide A, a bioactive metabolite from a freshwater species of Lyngbya Isolated from the Florida everglades. Comp. Biochem. Physiol. C Pharmacol. Toxicol. 2004, 139, 231–238.

5. Brand, M.; Granato, M.; Nüsslein-Volhard, C. Keeping and Raising Zebrafish. In *Zebrafish*; Nüsslein-Volhard, C., Dahm, R., Eds.; Oxford University Press: Oxford, UK, 2002; pp. 7–37.

6. Hill, A. J.; Teraoka, H.; Heideman, W.; Peterson, R. E. Zebrafish as a model vertebrate for investigating chemical toxicity.*Toxicol. Sci.* **2005***, 86*, 6-19.

7. MacMillan, J. B.; Molinski, T. F. Lobocyclamide B from Lyngbya confervoides. Configuration and Asymmetric Synthesis of β-Hydroxy-α-amino Acids by (-)-Sparteine-Mediated Aldol Addition. *Org. Lett.* **2002***, 4*, 1883-1886.

8. Mori, Y.; Kohchi, Y.; Noguchi, H.; Suzuki, M.; Carmeli, S.; Moore, R.E.; Patterson, G.M.L. Isotactic polymethoxy-1-alkenes from the terrestrial blue-green alga, *Scytonema ocellatum*: Structure and synthesis. *Tetrahedron* **1991**, *47*, 4889–4904.

9. Mori, Y.; Kohchi, Y.; Suzuki, M. Isotactic polymethoxy-1-alkenes from blue-green algae. Synthesis and absolute stereochemistry. *J. Org. Chem*. **1991**, *56*, 631–637.

10. Mynderse, J.S.; Moore, R.E. Isotactic polymethoxy-1-Alkenes from the blue-green alga *Tolypothrix conglutinata* var. *chlorata*. *Phytochemistry* **1979**, *18*, 1181–1183.

11. Rao, M.R.; Faulkner, D.J. Isotactic polymethoxydienes from the Philippines sponge *Myriastra clavosa*. *J. Nat. Prod.* **2002**, *65*, 1201–1203.

12. Teraoka, H.; Dong, W.; Hiraga, T. Zebrafish as a novel experimental model for developmental toxicology. Congenit. Anom. 2003, 43, 123–132.

13. Wang, P.J.; Chien, M.S.; Wu, F.J.; Chou, H.N.; Lee, S.J. Inhibition of embryonic development by microcystin-LR in zebrafish, *Danio rerio*. *Toxicon* **2005**, *45*, 303–308.

# CHAPTER 5

BIOACTIVE CAROTENOIDS FROM *CYLINDROSPERMOPSIS RACIBORSKII* AQS INHIBIT VERTEBRATE DEVELOPMENT IN ZEBRAFISH (*DANIO RERIO*) EMBRYOS

## 5.1. Introduction

Carotenoids are pigmented organic compounds which are found in many plants and other photosynthetic microorganisms such as algae, fungi, and also cyanobacteria. Carotenoids are generally thought to have two major roles in photosynthetic organisms; light harvesting for photosynthesis (via the transfer to chlorophyll) and prevention of photooxidative damage (Paerl, 1984; Hirschberg and Chamovitz, 1994). They can be commonly found in the membranes, making up an integral part of the complex structure of the membrane.

Many of the carotenoids are typically composed of a C-40 hydrocarbon backbone (eight isoprenoid units), biosynthesized via the tail-to-tail attachment of two C-20 geranylgeranyl diphosphate molecules. Extension of this C-40 backbone can occur, forming C-45 and C-50 carotenoids and the backbone can also be shortened, forming apocarotenoids of various lengths. The hydrocarbon backbone can also be modified by 1) cyclization of one of both ends of the molecule, 2) changes in the level of hydrogenation, and 3) incorporation of oxygen into functional groups (reviewed by Britton, 1995). As such, carotenoids can be divided into two classes; carotenes (which contain only hydrogen and carbon) and xanthophylls (which contain hydrogen, carbon, and oxygen).

One of the most characteristic structural features of carotenoids is the long series of conjugated double bonds along the polyene chain which gives rise to their light-absorbing properties and hence their corresponding colors, which ranges from yellow to red. Each double bond within the hydrocarbon chain of the carotenoid molecule can exist in the *cis* or *trans* configuration, with the *cis* configuration being less thermodynamically stable

due to steric hindrance between the methyl groups and the hydrogen atoms. In nature, most carotenoids typically occur in the all-*trans* configuration (Britton, 1995).

Carotenoids, when isolated, are very unstable molecules that readily undergo oxidation and isomerization when exposed to oxygen, heat, light, or acids after extraction. It has been observed that carotenoids tend to undergo isomerization in extracts containing chlorophyll and also when stored in acetone and exposed to light. In vivo, carotenoids are much more stable than when isolated because they are stabilized by proteins and other molecules. However if they come in contact with oxidizing species or free radicals, they are still susceptible to oxidative damage in vivo, but to a considerably lesser degree. Accordingly, great care must be taken during the extraction and isolation of these compounds to prevent their decomposition. The most favorable conditions usually involve working in dimly lit environments and keeping the samples dry and under inert conditions.

### *5.1.1. Carotenoids from Cyanobacteria*

Cyanobacteria are one of the oldest known photosynthetic organisms and are therefore known to contain many pigments including chlorophyll, carotenoids, and other accessory pigments which are involved in photosynthesis. In cyanobacteria, carotenoids are found as major pigments in the thylakoid membrane, cytoplasmic membrane, and outer membrane. They are commonly found as complexes with proteins. In the thylakoids, they are bound to important membrane proteins that are a part of the reaction center involved in photosynthesis, where they are involved in photoprotection (Vermaas *et al.*, 2008). In a *Synechocystis* sp. strain of cyanobacteria (PCC 6714), it was found that

the carotenoids are found in the outer membrane of the cell wall with the more polar carotenoids such as myxoxanthophyll, other carotenoid-glycosides and zeaxanthin are major components of the cell wall, while the more non-polar carotenoids such as β-carotene and echinenone are the minor components (Jurgens and Weckesser, 1985). For carotenoid-glycosides (specifically myxoxanthophyll), it was determined that one molecule of carotenoid spans the one monolayer of outer membrane with the sugar moiety acting as the polar head (Hirschberg and Chamovitz, 1994).

The carotenoids produced by cyanobacteria are thought to be the same as those produced in plants with the exception of some xanthophylls that are unique to cyanobacteria such as 2-hydroxy-derivatives, ketocarotenoids, and glycosidic carotenoids. Ketocarotenoids and glycosidic carotenoids are thought to be unique in nature, especially within photosynthetic organisms (Britton *et al.*, 2004). Figure 5.1 shows carotenoids that are commonly found in cyanobacteria include β-carotene, zeaxanthin, echinone, canthaxanthin, and myxoxanthophyll, with echinenone being found only in cyanobacteria (Hirschberg and Chamovitz, 1994). Table 5.1 below lists the different carotenoids that are found in cyanobacteria and the genera in which they have been found.

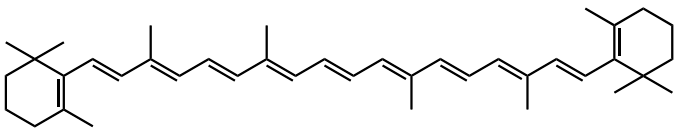

β-carotene

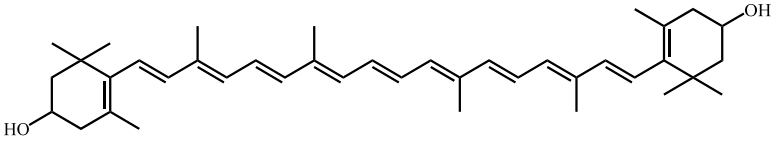


Zeaxanthin

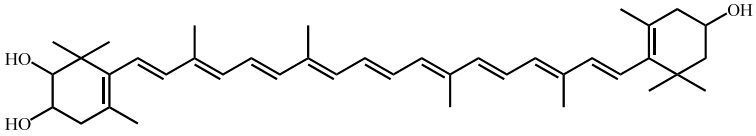


Caloxanthin

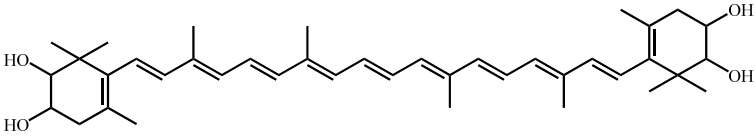


Nostoxanthin

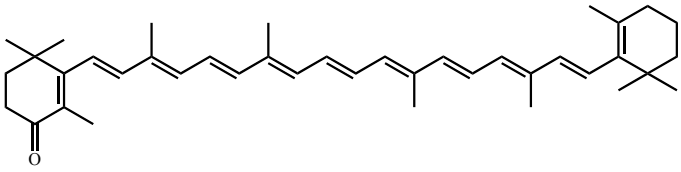


Echinenone

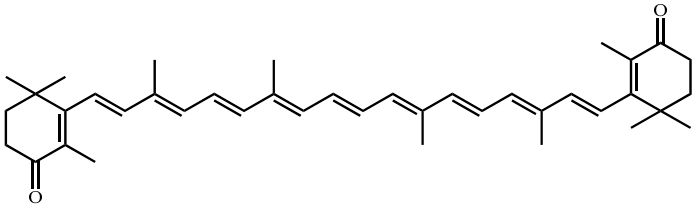


Canthaxanthin

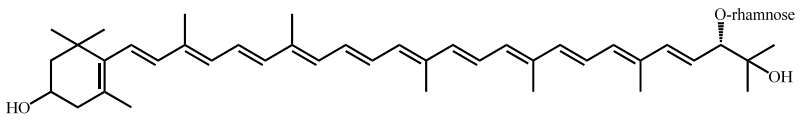


Myxoxanthophyll

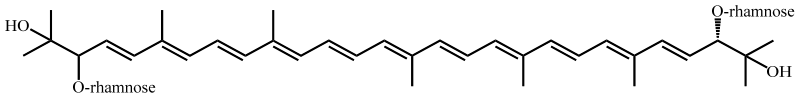


Oscillaxanthin

Figure 5. 1: Chemical structures of some carotenoids commonly found in cyanobacteria.

There is a wide variation in the composition of carotenoids found in cyanobacteria which may be due to the occurrence of the specific genes and pathways involved in the biosynthesis of the carotenoids. It is well know that the composition of carotenoids within the cyanobacteria is dependent on the growth conditions which includes growth stage, light intensity, source and concentration of nitrogen in the cultures. It is also dependent on the strain type within a given species (Takaichi and Mochimaru, 2007).

Table 5. 1: Commonly occurring carotenoids in cyanobacteria with their maximum absorption ($\lambda_{max}$) and spectral fine structure (%III/II)

| **Carotenoids** | **Cyanobacterial Genera** | **$\lambda_{max}$/nm (solvent[a])** | **# of CDB** | **%III/II (S[a])** |
|---|---|---|---|---|
| γ-carotene | *Chlorogloea, Oscillatoria* | 439, 461, 491 (A) | 11 | 40 (H), 35 (E) |
| β-carotene | *Anabaena, Aphanizomenon, Aphanothece, Arthrospira, Calothrix, Chlorogloea, Coccochloris, Cylindrospermum, Mastigocladus, Merimopedia, Microcoleus, Microcystis, Nostoc, Oscillatoria, Phormidium, Spirulina, Synechococcus, Tolypothrix* | 429, 452, 478 (A) | 11 | 25 (M) |
| Astaxanthin | *Anabaena, Aphanizomenon, Calothrix, Cylindrospermum, Nostoc, Oscillatoria, Phormidium, Synechococcus, Tolypothrix* | 480 (A) | 13 | single spectrum |
| Caloxanthin | *Aphanothece, Arthrospira, Calothrix, Chlorogloea, Nostoc, Phormidium, Synechococcus* | 426, 449, 475 (E) | 11 | 32 (M) |
| Canthaxanthin | *Anabaena, Aphanizomenon, Calothrix, Chlorogloea, Merimopedia, Microcystis, Nostoc, Oscillatoria, Phormidium, Spirulina, Synechococcus, Tolypothrix* | 474 (E) | 13 | single spectrum |
| β-cryptoxanthin | *Anabaena, Aphanothece, Arthrospira, Chlorogloea, Mastigocladus, Merimopedia, Microcystis, Oscillatoria, Phormidium, Spirulina, Synechococcus* | 428, 450, 478 (E) | 10 | 25 (H) |
| Echinenone | *Anabaena, Aphanizomenon, Aphanothece, Arthrospira, Calothrix, Chlorogloea, Coccochloris, Cylindrospermum, Mastigocladus, Merimopedia, Microcoleus, Microcystis, Nostoc, Oscillatoria, Phormidium, Spirulina, Synechococcus, Tolypothrix* | 460 (A) | 12 | single spectrum |
| Nostoxanthin | *Aphanothece, Calothrix, Chlorogloea, Phormidium, Nostoc, Synechococcus* | 428, 450, 478 (E) | 11 | 31 (M) |
| Oscillaxanthin | *Arthrospira, Chlorogloea, Microcystis, Oscillatoria* | 464, 491, 525 (M) | 13 | 40 (M) |

| | | | | |
|---|---|---|---|---|
| Zeaxanthin | *Anabaena, Aphanizomenon, Aphanothece, Arthrospira, Calothrix, Chlorogloea, Coccochloris, Cylindrospermum, Mastigocladus, Merimopedia, Microcystis, Nostoc, Oscillatoria, Phormidium, Spirulina, Synechococcus, Tolypothrix* | 424, 449, 476 (P) | 11 | 25 (P) |
| Myxol 2'-glycoside (Myxoxanthophyll) | *Anabaena, Aphanizomenon, Aphanothece, Arthrospira, Calothrix, Chlorogloea, Coccochloris, Cylindrospermum, Mastigocladus, Merimopedia, Microcoleus, Microcystis, Nostoc, Oscillatoria, Phormidium, Spirulina, Synechococcus, Tolypothrix* | 450, 478, 510 (A)<br>446, 472, 502, (M) | 12 | 55(M), 57(A) |
| Aphanizophyll<br>4-Keto-myxol-2' methylpentoside | *Aphanizomenon, Microcystis, Oscillatoria, Anabaena*<br>*Anabaena, Oscillatoria, Synechococcus* | 450, 476, 507 (A) | 12 | 57 (A) |

[a]Solvents: P- petroleum ether, H-hexane, E-ethyl acetate, A-acetone, M-methanol

## 5.2. Results and Discussion

### *5.2.1. Isolation of the Carotenoids*

The zebrafish embryo bioassay was used to guide the purification of two bioactive compounds from the methanol fraction of C-AQS, both of which were pigments. The 10% methanol fraction obtained from the silica-gel column was subjected to RP-18 SPE (Extract-Clean$^{TM}$ SPE C18-HC 10000 mg/75mL) with the bioactive fraction eluting in 95% methanol in water with the resulting fraction have a red color. Further purification was done on the HPLC with a PDA detector (Prominence SPD M20A; scanning the wavelengths from 200-700 nm) using an isocratic solvent system of 65% acetonitrile in water, where the peaks were individually collected and tested on the zebrafish embryos. The two peaks determined to be bioactive were observed at retention times of 6.68mins (peak **1**, which was red) and 8.59 mins (peak **2**, which was orange) (Figure 5.2) and were shown to cause inhibition of development in the zebrafish embryos. Other peaks were identified in the fraction which seemed to be related to the bioactive peaks based on the UV-vis spectrum; however no bioactivity (using the zebrafish embryos) was observed with these peaks. Further analysis indicated that these peaks were the *cis* carotenoids corresponding to the *trans* carotenoids isolated.

The bioactive peaks identified were individually collected and dried (under vacuum) for chemical characterization. During the drying process, heat was applied to a portion compound **1**, which resulted in a loss of color to the sample, however the remaining portion was dried without heat and these samples were kept separate. Carotenoids are known to be very unstable and readily undergo decomposition when

exposed to oxygen, heat, light, or acids after extraction. The typical indication for the decomposition of the carotenoids is bleaching (loss of color). As such, it is thought that the sample that was gently heated during the drying process underwent decomposition as a result of its loss of color. It is therefore imperative to take the necessary precautions during extraction and analysis of carotenoids to prevent the transformation of these compounds.

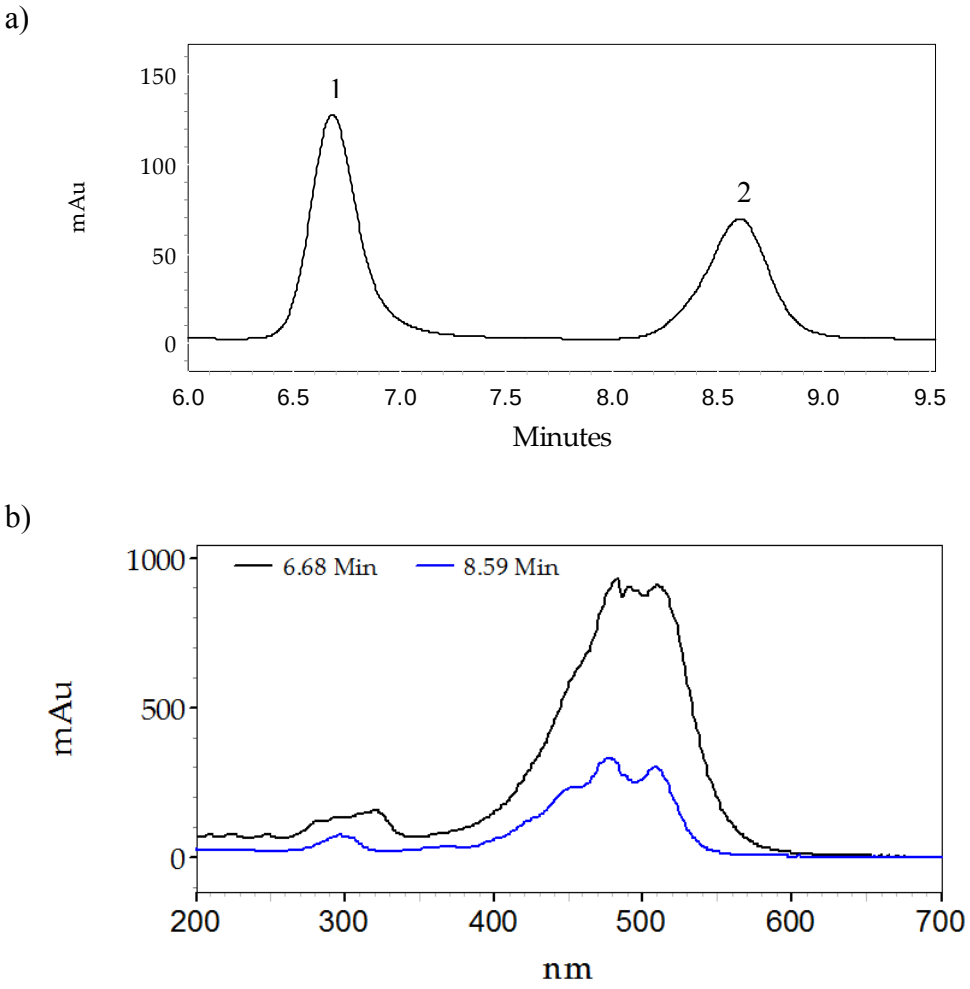


Figure 5. 2: a) HPLC Chromatogram of the bioactive fraction from the SPE cartridge showing the two bioactive peaks at retention times of 6.68 mins (**1**) and 8.59 mins (**2**) and b) UV-Vis spectra of the bioactive peaks from the chromatogram.

*5.2.2. Chemical Characterization of the Carotenoids from C. raciborskii AQS*

The first steps in the identification of carotenoids usually involves the chromatographic behavior and the UV-visible spectra which are distinctive for the carotenoids present. The chromatographic behavior gives information about the polarity of the carotenoids and the UV-vis absorption spectra gives important information about the maximum absorption ($\lambda_{max}$) and the spectral fine structure. The UV-vis spectra for many carotenoids usually shows three distinct peaks with maximum absorptions ($\lambda_{max}$) between 420-520 nm which can be shifted depending on the number of conjugated double bonds and conjugated cyclization within the structure. Substituents such as hydroxyl groups, methoxy groups, non-conjugated rings, and non-conjugated carbonyl groups have little or no effect on the $\lambda_{max}$. This three-peak spectrum is highly indicative of a carotenoid and can be used to assist in the determination of the number of conjugated double bonds within the structure. The spectral fine structure (usually expressed as %III/II) is an indication of the shape of the spectra which is also characteristic of the chromophore and can be affected by the cyclization within the structure. The spectral fine structure reaches its maximum when the number of conjugated double bonds (N) is eight and decreases as it moves away from eight within the non-conjugated β-ring structure (Takaichi and Shimada, 1992). The %III/II is calculated by diving the height of the longest wavelength peak by the height of the middle wavelength peak (taking the minimum between the two as the baseline) and multiplying by 100.

For peak **1**, the $\lambda_{max}$ which was observed in 65% acetonitrile in water, was 321, 449sh, 480, and 509 nm which, in conjunction with the color of the compound (red), indicates the possibility of the compound being a carotenoid. The three-peak spectrum

observed was %III/II was determined to be 12% (Appnedix 5.1A), however this was difficult to determine because the trough between the two peaks was very shallow. This is usually indicative of a carotenoid with conjugated carbonyl group and in some case only shows a single peak and the $\lambda_{max}$ is usually hard to determine (Takaichi and Shimada, 1992). For peak **2**, the $\lambda_{max}$ which was also observed in 65% acetonitrile in water, was 295, 368, 450, 478, and 509 nm which, again with the color of the compound, also suggested that the compound is a carotenoid. The three-peak spectrum for this compound was 450, 478, and 509 nm from which the %III/II was determined to be 58% as shown in Figure 5.3. Based on the %III/II and the $\lambda_{max}$ observed, these compounds were suggested to be carotenoids, more specifically as derivatives of γ–carotene, which are well-known to be produced by cyanobacteria (Hirschberg and Chamovitz, 1994).

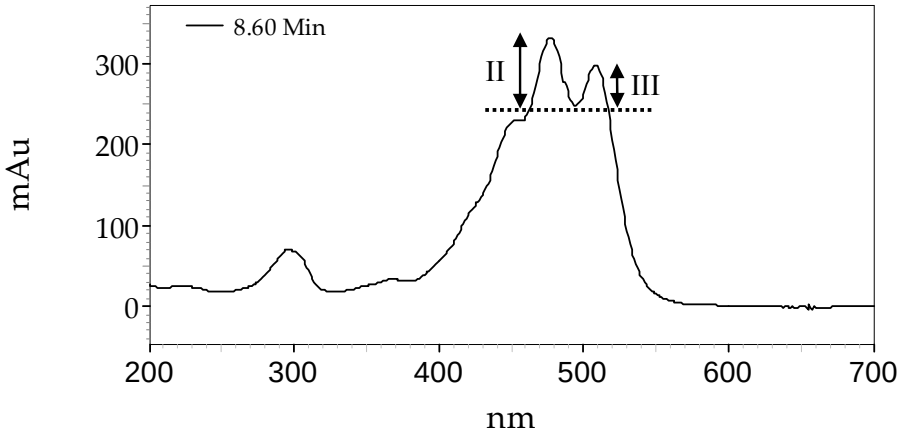


Figure 5. 3: Determination of the spectral fine structure (%III/II) for peak **2**.

Mass spectrometric analysis (Figure 5.4) of the bioactive peak at retention time of 6.68 mins (**1**) from the HPLC showed *m/z* of 744.4 determined to be $M^+$ peak and a *m/z*

of 767.4 for the $[M+Na]^+$ peaks. High resolution analysis gave an accurate mass of *m/z* 744.4548 corresponding to a molecular formula of $C_{46}H_{64}O_8$ and having a ring and double bond equivalent of 15 which correlates with the observed UV-Vis spectra. A fragment peak was also identified at *m/z* of 581.4 giving a loss of *m/z* 163. The fragment at *m/z* 581.4 could correspond to a myxol, which is a γ-carotene derivative, suggesting that the loss of *m/z* 163 corresponds to a methylpentoside indicating that the suggested carotenoid (*m/z* 744) is a myxol derivative with a glycosidic functional group. Fragmentation of both the molecular ion peak and the fragmentation peak at *m/z* 581 (Appendix 5.1B) shows a sequential ladder loss of *m/z* 14 in the region with *m/z* below 300, which corresponds to the loss of methyl groups associated with carotenoids.

a)

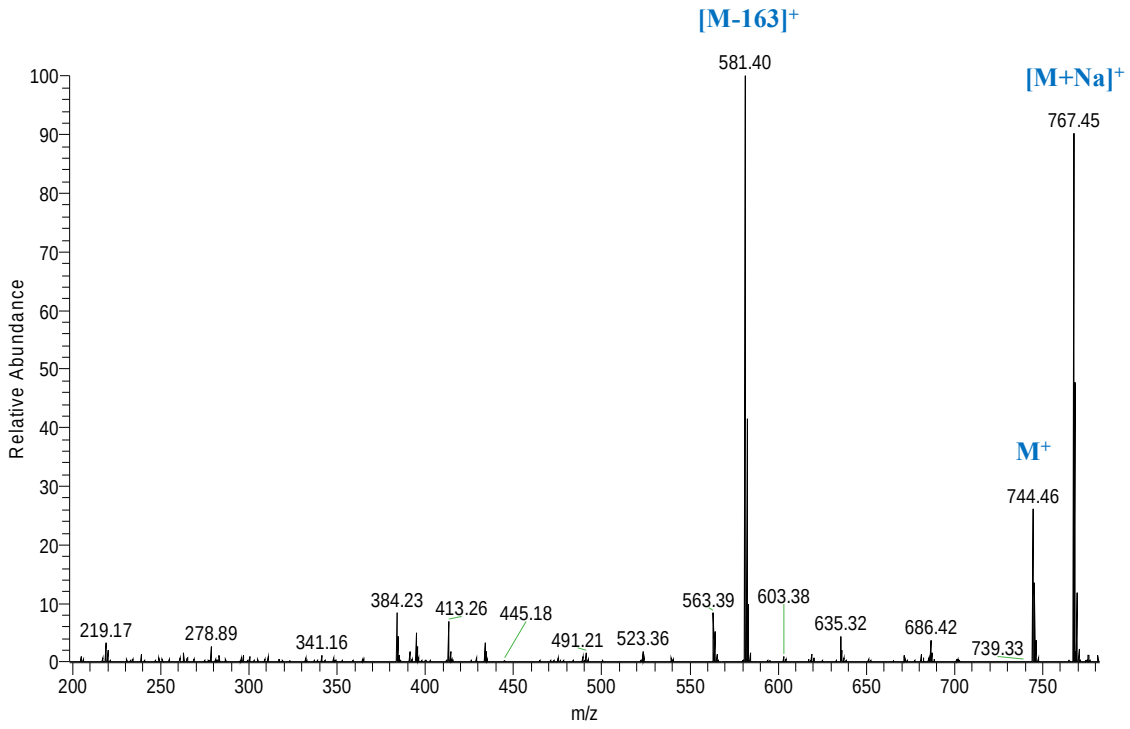


b)

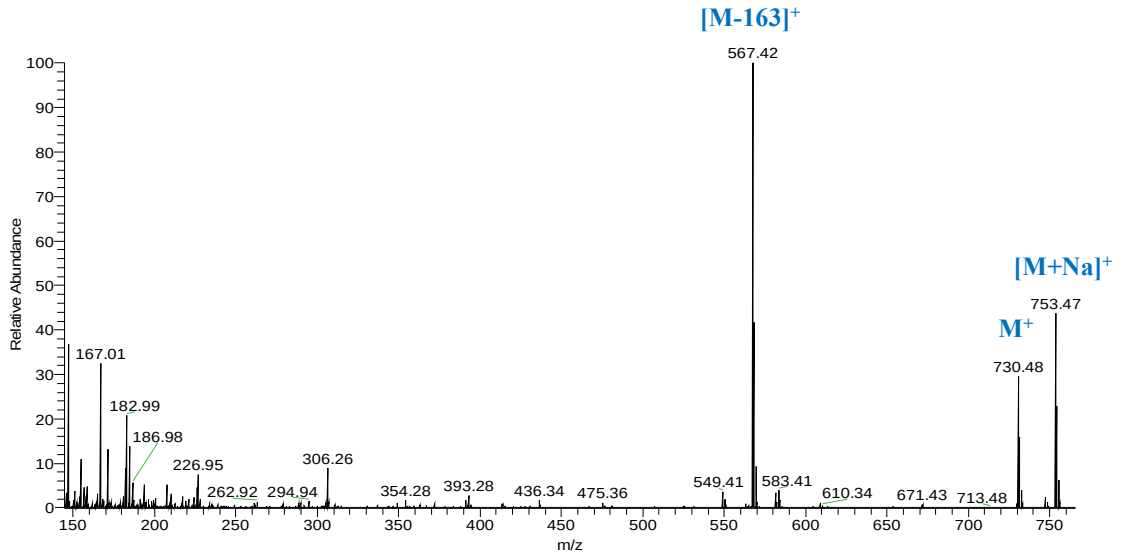


Figure 5. 4: ESIMS data of the purified bioactive compounds from in *C. raciborskii* showing the molecular ion peaks and fragmentation peaks: a) Peak 1 with $M^+$ peak of *m/z* 744.46 and fragmentation peak of *m/z* 581.40 $[M-163]^+$ and b) Peak 2 with $M^+$ peak of *m/z* 730.48 and fragmentation peak of *m/z* 567.42 $[M-163]^+$.

The second bioactive peak (**2**) that was isolated ($t_R$ 8.59 mins) and analyzed using the LC-MS (low resolution), showed a *m/z* of 730.5 for the $M^+$ peak and a *m/z* of 753.5 for the $[M+Na]^+$ peak. Analysis using the HRESIMS gave a molecular ion peak of *m/z* 730.4801 corresponding to a molecular formula of $C_{46}H_{66}O_7$ with a ring and double bond equivalent of 14. A fragmentation peak was identified with a *m/z* 567.4 $[M-163]^+$ which again possibly corresponds to the presence of a methylpentoside. Fragmentation of both the molecular ion peak and the fragment peak at *m/z* 567.4 showed a similar sequential loss of *m/z* 14 (data not shown) to that of **1**, which in conjunction with the UV-Vis analysis, suggests that these compounds are carotenoids.

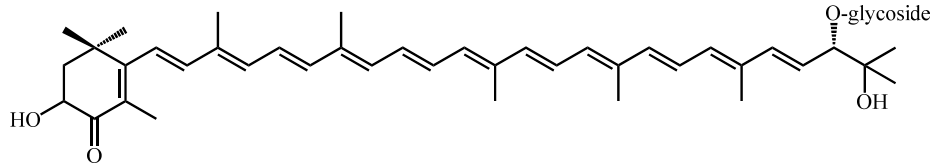


Peak **1** (*m/z* 744)

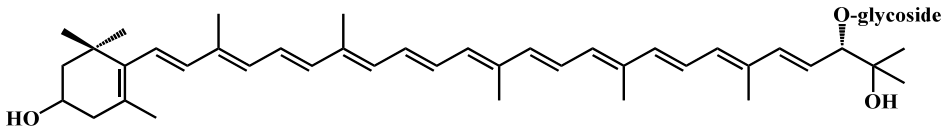


Peak **2** (*m/z* 730)

Figure 5. 5: Structure of 4-ketomyxol 2'-glycoside and myxol 2'-glycoside: the proposed compounds for peaks **1** and **2** respectively.

Both compounds are thought to have a glycosidic functional group and based on the MS fragmentation (loss of *m/z* 163) and previously identified glycosidic carotenoids, suggest that the glycosidic group could be a methyl pentoside. The glycosidic group of previously identified carotenoids with a methyl pentoside have been characterized as a rhamnose or fucose, depending on the species from which they were identified (Takaichi

*et al.*, 2005). Determination of the glycosidic group for the currently isolated carotenoids was not achieved due to the insufficient amounts of sample obtained and the constant degradation of the compounds.

### *5.2.3. Bioactivity of the Carotenoids (Zebrafish Embryo Bioassay)*

The zebrafish embryo bioassay was used to purify the bioactive compounds from *C. raciborskii*, where a similar bioactivity was observed in the crude extract and each subsequent bioactive fraction (Figure 5.6). Embryos were observed at 4dpf at which stage normal untreated embryos should have hatched and the development of the body parts and body axis is almost complete. Embryos exposed to extracts and fractions were observed to not have development of the body axis as well as no distribution of the color, with most of the color remaining in the head of the embryos. The embryos also did not appear to have differentiation of the various body parts including the eyes, gills, and fins. There was no hatching of the embryos up to 5dpf exposed to all treatments. There was also no mortality observed as indicated by coagulated embryos however it was difficult to ascertain a heartbeat due to the lack of complete development of the organs, especially the heart.

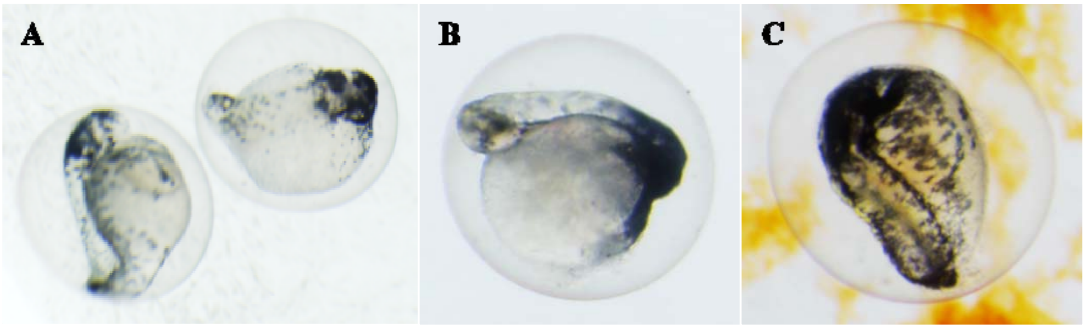


Figure 5. 6: Bioactivity of the extracts and fractions from *C. raciborskii* throughout the fractionation process, showing the inhibition of development in the zebrafish embryos at 4dpf. A) $CHCl_3$ extract at 10µL, B) 10% MeOH fraction from glass column, C) 95% MeOH from RP-18 SPE cartridge.

The purified compounds were tested on the zebrafish embryos to confirm their bioactivity. Compound **1** was tested at a range of concentrations; 1, 5, 10, 20 and 50 µg/mL with bioactivity observed only at 20 and 50 µg/mL (Figure 5.7A and B). Embryos at the lower concentration (20µg/mL) showed partial development of the body parts such as the eyes, however the body axis was slightly shortened and curved and there was pericardial edema. At 5dpf, hatching of the embryos (n=5) was at 40% and there was 20% mortality observed. At the higher concentration (50µg/mL) the embryos showed closer resemblance to the crude fractions with little or no differentiation of the eyes and a shortened body axis. There was no hatching observed (0% hatching) up to 5dpf and also no mortality observed. From the observations of the development of the embryos, it can be seen that the higher concentrations showed greater inhibition of development of the embryo and their hatching but there were no substantial effects on mortality up to 5dpf. Embryos were not observed beyond this stage. For compound **2**, the concentration tested on the zebrafish embryos was unknown because it was tested directly from the HPLC, however similar effects were observed as that of compound **1** at 5dpf (Figure 5.7C).

The presumed decomposed sample of compound **1** was also tested on the zebrafish embryos to determine if there was still bioactivity, however the tests were done at unknown concentrations (10 and 100µL). No deformities were observed at the lower dosage (10µL) but at the higher dosage (100µL), the embryos showed slight deformities including bent tails and pericardial edema (Figure 5.7D). Additionally, there seemed to be no effect on the hatching of the embryos at both dosages, with 100% hatching observed at 5dpf.

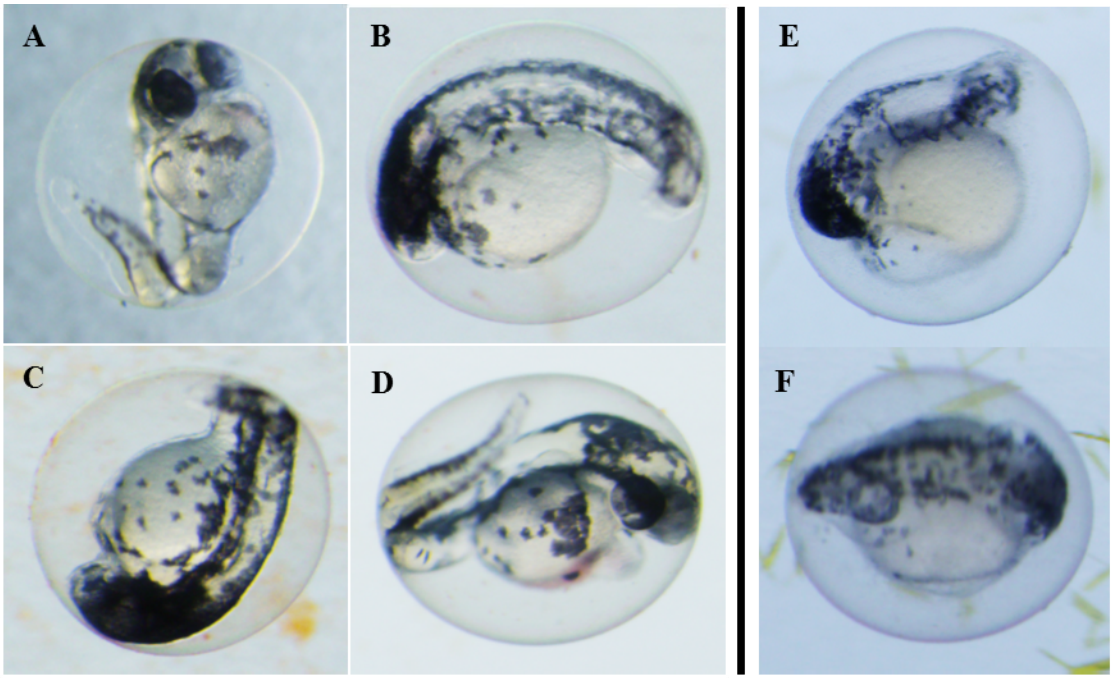


Figure 5. 7: Bioactivity of the purified carotenoids from *C. raciborskii* showing the inhibition of development in the zebrafish embryos at 3dpf. A) Peak **1** at 20µg/mL, B) Peak **1** at 50µg/mL, C) Peak **2** (unknown concentration), D) Peak **1** (loss of color; unknown concentration), E) Retinoic acid at 10nM, and F) Retinoic acid at 100nM.

Carotenoids undergo oxidative cleavage of the double bonds within the conjugated system (See Figure 5.8) to form a class of aldehydes known as apocarotenals, including

retinol, retinal, retinoic acid, and derivatives of each, such as 4-ketoretinoids. The most well-known apocarotenal is retinal, a 20-C aldehyde which is formed from the cleavage of the C15-C15' double bond (Trautmann *et al.*, 2013). Retinal is then converted to retinoic acid in vertebrates by the enzyme retinal dehydrogenases. Retinoic acid acts as a signaling molecule (morphogen) that produces specific cellular response based on the concentration. These previously mentioned retinoids have been shown to cause teratogenic effects in various organisms, including zebrafish embryos (Hermann, 1995), mice (Nau, 1990), *Xenopus* larvae (Durston *et al.*, 1989), and chicken embryo (Thaller and Eichele, 1987). Zebrafish embryos were exposed to different concentrations of retinoic acid and its analogues at 5 hours post fertilization (5hpf) after which they observed various malformations including edema, brain deformities, and shortened and bent tails (Herrmann, 1995 and Figure 5.7E and F). These malformations were similar to those observed in the embryos exposed to the isolated carotenoids from CAQS (See Figure 5.7).

It can therefore be proposed that the effects observed in the zebrafish embryos after exposure to the glycosidic carotenoids could be due to the biotransformation into apocarotenals or the corresponding retinoids, which have previously been shown to cause malformations in fish and amphibians, and not necessarily the intact carotenoid. Provitamin A carotenoids such as *β*-carotene have been extensively studied and shown to undergo oxidative cleavage into retinoic acid and retinal. Non-provitamin A carotenoids can also undergo oxidative cleavage into their corresponding retinoids and also other metabolites, most of which are currently unknown (Nagao, 2004). Some of these metabolites can be further metabolized under oxidative stress for elimination while the

retinoid metabolites can interact with the same receptors as retinoic acid (Nagao, 2004; Maden, 2002). Retinoids, including retinoic acid, are known to interact with retinoic acid receptors (RAR) and retinoid X receptors (RXR) which then homodimerizes, binding to the RA-response element (RARE) and subsequently activating the transcription of RA target genes (Maden, 2002). Exposure of organisms to exogenous retinoids is known to cause various malformations in vertebrates. The biotransformation of carotenoids could lead to the increase in the amount of retinoids, which could be the cause of the inhibition of development in the zebrafish embryos upon exposure to the carotenoids. A proposed mechanism of action of the carotenoids in the zebrafish embryos is therefore via their biotransformation into retinoids, causing an increase in the retinoids, which are known teratogens.

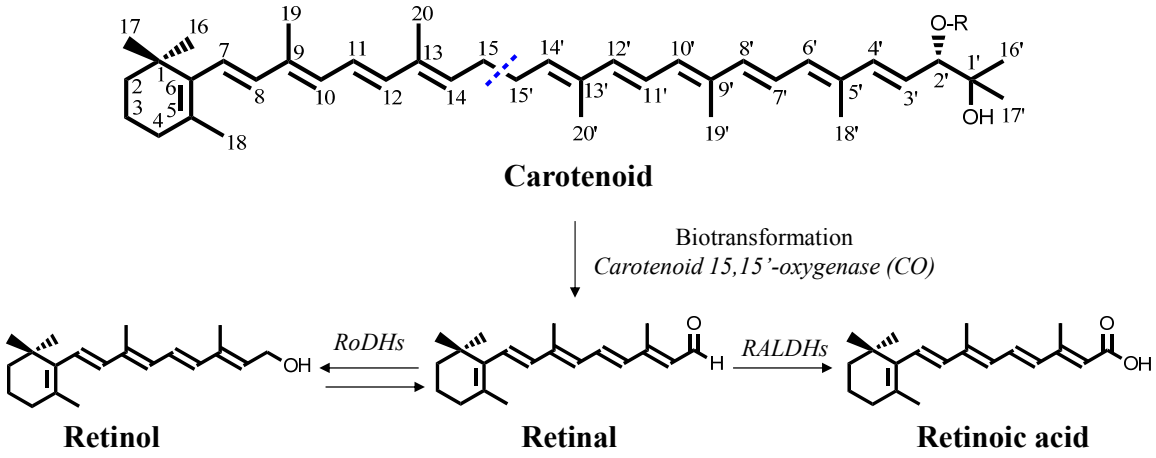


Figure 5. 8: Reaction showing the biotransformation of carotenoids to retinoids by the cleavage of the 15-15' bond through the action of a carotenoid 15,15'-oxygenase to form retinal followed by the conversion to retinol or retinoic acid by retinol dehydrogenases (RoDHs) or retinaldehyde dehydrogenases (RALDHs) respectively.

Furthermore, high incidences of malformations were observed in amphibians, predominantly aquatic, from which various factors associated with these deformations have been proposed (Gardiner *et al.*, 2003). One such proposed factor is the occurrence of teratogenic retinoids produced by cyanobacterial blooms, specifically a *Microcystis* bloom in Lake Taihu, China (Wu *et al.*, 2012 and 2013). Wu *et al.* (2012 and 2013) identified high amounts of retinoids, namely retinoic acid, retinal, and 4-oxo-retinoic acid, in the cyanobacterial species found in these lakes. A hypothesis can therefore be made that carotenoids can undergo oxidative cleavage to form retinoids which can contribute to the teratogenic effects associated with these blooms of cyanobacteria.

## 5.3. Methods

### *5.3.1. Bioassay-Guided Fractionation of the Bioactive Compound*

A bioassay-guided fraction using the zebrafish embryo as the bioassay was implemented for the isolation and purification of the bioactive compound from the strain of *C. raciborskii*, C-AQS. The freeze-dried biomass was extracted twice in chloroform in a ratio of 10:1 (mg:mL) after which the filtered extract was fractionated by normal-phase flash-chromatography on a silica-gel glass column (Silica Gel 60Å, Commercial 40–63 μm). A stepwise gradient was used of ethyl acetate in hexane and then 10% methanol in ethyl acetate. The zebrafish embryo bioassay was used to identify the bioactive fraction (10% methanol in ethyl acetate), which was then further fractionated on a reverse-phase solid phase extraction (RP-18, SPE) cartridge also with a stepwise gradient of methanol in water. The bioactive fraction was observed to be the 95% methanol in water which was further separated by reverse-phase HPLC (Phenomenex Luna 5 μm C5 100 Å LC

Column 100 × 4.6 mm; isocratic 65:35 acetonitrile/water) with a PDA detector (Prominence SPD M20A), wavelength range from 200-700nm). The zebrafish embryo bioassay was then used to identify the two bioactive peaks at retention times of 6.68 and 8.59 minutes.

*5.3.2. Characterization of bioactive compounds from C. raciborskii AQS*

The purified compound was chemically characterized by UV-Vis analysis, and mass spectrometry (low- and high-resolution). Analyses by mass spectrometry included low-resolution analysis on a Thermo TSQ Quantum Access ESI/triple quadrupole instrument coupled to a Thermo Accela UHPLC and high-resolution analyses on a Thermo Orbitrap. Chemical characterization by NMR included one-dimensional experiments ($^1$H) and two-dimensional experiments (homonuclear: COSY) on a Bruker AVANCE 400 MHz instrument.

**4-ketomyxol 2'-glycoside (1)**: HRESIMS *m/z* 744.4548 ($C_{46}H_{64}O_8$, $[M]^+$, Δmmu of -2.24); RDB 15; UV/Vis 321, 449sh, 480, and 509 nm; %III/II 12

**Myxol 2'-glycoside (2)**: HRESIMS *m/z* 730.4801 ($C_{46}H_{66}O_7$, $[M]^+$, Δmmu of -2.24); RDB 14; UV/Vis 295, 368, 450, 478, and 509 nm; %III/II 58.

*5.3.3. Zebrafish Embryo Bioassay (Exposure Studies)*

The zebrafish (*Danio rerio*) embryo was used as a model of developmental toxicity for both bioassay-guided fractionation and toxicity studies. Maintenance and

breeding of adult zebrafish, and the toxicology studies with the embryos, were carried out as previously described by Berry *et al.* (2007 and 2009) and according to the protocols that were approved by the FIU Institutional Animal Care and Use Committee (IACUC). All the toxicity studies were done in solvent-resistant, polypropylene 24-well plates (Evergreen Scientific, Los Angeles, CA). Exposures were carried out using five embryos per well in E3 medium (Brand *et al.*, 2002). Extracts and fractions were typically evaluated at a high- (100 µL) and low- (10 µL) exposure concentration; purified compound **1** only was evaluated at 2, 5, 10, 20, and 50 µg/mL concentrations (in methanol). Retinoic acid (obtained for Sigma Aldrich) was also tested at 10 and 100 nM and the bioactivity was compared to that of the carotenoids. Solvent and "untreated" controls were included in each assay; the solvent was evaporated from assay plates, prior to adding medium and embryos, and accordingly there were no observed effects of the solvent (relative to the untreated controls). The embryos were observed up to 5 days post fertilization (dpf) for bioactivity which included mortality, inhibition of hatching, and inhibition of development. In addition to percent hatching and mortality, developmental toxicity was recorded by photomicrography using an Olympus SZX7 stereomicroscope equipped with an Olympus DP72 digital camera.

### 5.4. Conclusion

The zebrafish embryos were used in the bioassay-guided isolation of two bioactive glycosidic carotenoids. The occurrence of carotenoids in cyanobacteria has been well documented and there is good evidence to suggest that they play a role in photosynthesis

and also in the prevention of photooxidative damage. These identified glycosidic carotenoids have been previously identified in other genera of cyanobacteria, including *Cylindrospermopsis*. The sugar moiety of these carotenoids in *Anabaena* sp. and *Nostoc punctiforme* was identified as fucose and not rhamnose (Takaichi *et al.*, 2005), which could be the same for these carotenoids identified from CAQS, however this remains to be determined.

The bioactivities previously observed with these glycosidic carotenoids have been related to photoprotection and antioxidant activity (Heydarizadeh *et al.*, 2013). There have not been any previous reports which shows these carotenoids to be toxic, however from this study, it can be seen that these accessory pigments inhibit the development in zebrafish embryos which was used as a model for vertebrate development. It could be suggested that the cause of this bioactivity could be due to the decomposition of the carotenoids into the corresponding retinoids which have been shown to be teratogenic in zebrafish embryos and also amphibians. Further analysis is required to test this hypothesis.

**References**


1. Berry, J. P.; Gantar, M.; Gibbs, P. D. L.; Schmale, M. C. The zebrafish (*Danio rerio*) embryo as a model system for identification and characterization of developmental toxins from marine and freshwater microalgae. *Comparative Biochemistry and Physiology Part C: Toxicology & Pharmacology* **2007***, 145*, 61-72.
2. Berry, J. P.; Gibbs, P. D. L.; Schmale, M. C.; Saker, M. L. Toxicity of cylindrospermopsin, and other apparent metabolites from Cylindrospermopsis raciborskii and Aphanizomenon ovalisporum, to the zebrafish (Danio rerio) embryo. *Toxicon* **2009***, 53*, 289-299.

3. Brand, M.; Granato, M.; Nüsslein-Volhard, C. Keeping and Raising Zebrafish. In Zebrafish; Nüsslein-Volhard, C., Dahm, R., Eds.; Oxford University Press: Oxford, UK, **2002**; pp. 7–37.

4. Britton, G. Structure and properties of carotenoids in relation to function. *The FASEB Journal* **1995***, 9*, 1551-1558.

5. Britton, G.; Liaaen-Jensen, S.; Pfander, H. *Carotenoids: handbook;* Springer: 2004

6. Durston, A. J.; Timmermanns, J. P. M.; Hage, W. J.; Hendriks, H. F. J.; de Vries, N. J.; Heideveld, M.; Nieuwkoop, P. D. Retinoic acid causes an anterior posterior transformation in the developing nervous system. *Nature* **1989**, 340, 140-144.

7. Gardiner, D.; Ndayibagira, A.; Grün, F.; Blumberg, B. Deformed frogs and environmental retinoids. *Pure and applied chemistry* **2003***, 75*, 2263-2273.

8. Herrmann, K. Teratogenic effects of retinoic acid and related substances on the early development of the zebrafish (*Brachydanio rerio*) as assessed by a novel scoring system. *Toxicology in vitro* **1995***, 9*, 267-283.

9. Heydarizadeh, P.; Poirier, I.; Loizeau, D.; Ulmann, L.; Mimouni, V.; Schoefs, B.; Bertrand, M. Plastids of marine phytoplankton produce bioactive pigments and lipids. *Marine drugs* **2013***, 11*, 3425-3471.

10. Hirschberg, J.; Chamovitz, D. In *Carotenoids in cyanobacteria;* The molecular biology of cyanobacteria; Springer: **1994**; pp 559-579.

11. Jurgens, U. J.; Weckesser, J. Carotenoid-containing outer membrane of Synechocystis sp. strain PCC6714. *J. Bacteriol.***1985***, 164*, 384-389.

12. Maden, M. Retinoid signalling in the development of the central nervous system. *Nature Reviews Neuroscience* **2002**, *3*, 843-853

13. Nau, H. Correlation of transplacental and maternal pharmacokinetics of retinoids during organogenesis with teratogenicity. *Methods in Enzymology* **1990**, 190(B), 437-448.

14. Paerl, H. W. Cyanobacterial carotenoids: their roles in maintaining optimal photosynthetic production among aquatic bloom forming genera. *Oecologia* **1984***, 61*, 143-149.

15. Takaichi, S.; Mochimaru, M. Carotenoids and carotenogenesis in cyanobacteria: unique ketocarotenoids and carotenoid glycosides. *Cellular and molecular life sciences* **2007***, 64*, 2607-2619.

16. Takaichi, S.; Mochimaru, M.; Maoka, T.; Katoh, H. Myxol and 4-ketomyxol 2′-fucosides, not rhamnosides, from *Anabaena* sp. PCC 7120 and *Nostoc punctiforme* PCC 73102, and proposal for the biosynthetic pathway of carotenoids. *Plant and cell physiology* **2005***, 46*, 497-504.

17. Takaichi, S.; Shimada, K. Characterization of carotenoids in photosynthetic bacteria. *Meth. Enzymol.* **1992***, 213*, 374-385.

18. Thaller, C.; Eichele, G. Identification and spatial distribution of retinoids in the developing chick embryo. *Nature* **1987**, 327, 625-628.

19. Trautmann, D.; Beyer, P.; Al-Babili, S. The ORF slr0091 of Synechocystis sp. PCC6803 encodes a high-light induced aldehyde dehydrogenase converting apocarotenals and alkanals. *FEBS Journal* **2013***, 280*, 3685-3696.

20. Vermaas, W. F. J.; Timlin, J. A.; Jones, H. D. T.; Sinclair, M. B.; Nieman, L. T.; Hamad, S. W.; Melgaard, D. K.; Haaland, D. M. In vivo hyperspectral confocal fluorescence imaging to determine pigment localization and distribution in cyanobacterial cells. *Proceedings of the National Academy of Sciences* **2008***, 105*, 4050-4055.

21. Wu, X.; Jiang, J.; Hu, J. Determination and Occurrence of Retinoids in a Eutrophic Lake (Taihu Lake, China): Cyanobacteria Blooms Produce Teratogenic Retinal. *Environ. Sci. Technol.* **2013***, 47*, 807-814.

22. Wu, X.; Jiang, J.; Wan, Y.; Giesy, J. P.; Hu, J. Cyanobacteria blooms produce teratogenic retinoic acids. *Proceedings of the National Academy of Sciences* **2012***, 109*, 9477-9482.

# CHAPTER 6

IDENTIFICATION OF LIPOPHILIC BIOACTIVE FRACTIONS IN THE OTHER TOXIGENIC STRAINS OF FRESHWATER CYANOBACTERIA USING THE ZEBRAFISH EMBRYO BIOASSAY

## 6.1. Introduction

Cyanobacterial toxins were identified from 2 of the 4 isolates, proposed in this project, namely APH and CAQS, however only partial purification was obtained with the other two isolates, *C. raciborskii 121-1* (denoted CMEX) and *M. aeruginosa* (denoted MC 81-11). This chapter will therefore focus on the identification and partial purification of the bioactive compounds/fractions identified from these two isolates.

*M. aeruginosa* 81-11 is a great lakes isolate that is known to produce microcystin. *C. raciborskii* 121-1 (Mexico) was isolated from the Lake Catemaco, located in Vera Cruz, Mexico where they have been seen to form large blooms year round. The toxins CYN and paralytic shellfish toxins (PSTs), known to be produced by the genus *Cylindrospermopsis*, have been shown to be present in this lake (Berry and Lind, 2010). This lake represents one of the most productive fisheries in Mexico (Komarkova and Tavera, 2003) and other studies have shown that there is bioaccumulation of these toxins in tegogolo snails and finfish (Berry *et al.*, 2012). With the importance of this fishery and the prevalence of blooms of *Cylindrospermopsis*, this ecosystem provides a good opportunity to study the effects of these known cyanobacterial toxins and unidentified toxins on these aquatic species as well as the subsequent effects on human health.

Even though there were no bioactive compounds isolated from CMEX and MC 81-11, multiple fractions from these lipophilic extracts showed bioactivity with there being some indication to the nature of the compounds in a couple of these fractions. In addition to the compounds that have been identified, there still remains many toxic metabolites from these cyanoHABs that are unrelated to the known water-soluble toxins that contribute to the toxicity of these species.

## 6.2. Results & Discussion

### *6.2.1. Bioactive Fractions from C. raciborskii 121-1 (Mexico)*

The extract was fractionated on a silica-gel glass column using a combination of hexane, acetone, and methanol as the eluting solvents. A few sets of bioactive fractions were observed from the silica-gel column eluting in 10, 15, 35% acetone in hexane, 100% acetone, and 100% methanol. The methanol fraction was subsequently analyzed because of the observations from the zebrafish bioassay as well as the pigmentation of the fraction.

The chromatogram of the 100% MeOH fraction (Figure 6.1) using the same method as with CAQS, showed the bioactive peak (which was the main peak) to have a retention time of 4.56 mins, indicating that this compound is slightly more polar than those from CAQS. The UV-vis for the bioactive peak (denoted as **3**) showed $\lambda_{max}$ of 451, 476, and 507nm with the %III/II of 56. A small sample was analyzed by Dr. Bill Louda (Florida Atlantic University; Louda, 2008) with the sample eluting at 11.32 mins. The $\lambda_{max}$ of the peak was 450, 476, and 508nm with the %III/II of 56. The sample was also spiked with different standards of carotenoids (myxoxanthophyll and aphanizophyll; obtained from DHI; Denmark) with the aphanizophyll standard eluting at the same retention time as the main peak in the sample and having the same UV-vis spectrum (Appendix A6.2). This data along with the UV-vis spectrum indicates that the main peak is likely to be aphanizophyll (4-hydroxymyxol 2'-glycoside).

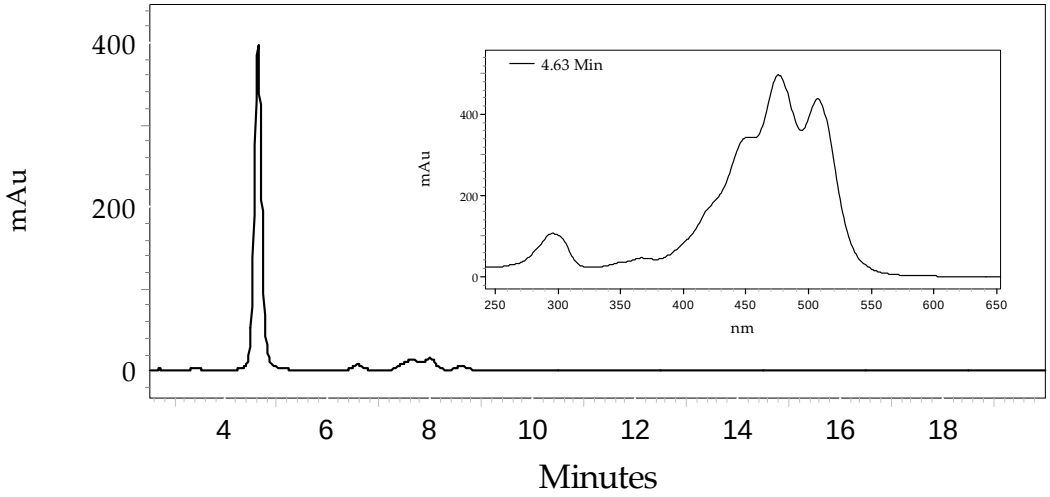


Figure 6. 1: HPLC Chromatogram of the bioactive fraction indicating the bioactive peak at 4.56mins with the UV-vis spectrum.

Analysis of the fraction by HR-ESI-MS gave a molecular ion peak of *m/z* 746.4762 corresponding to a molecular formula of $C_{46}H_{66}O_8$ with a ring and double bond equivalent of 14 (Figure 6.2) . Another peak at *m/z* 769.5 corresponding to $[M+Na]^+$,was observed as well as a fragment ion at *m/z* 583.4 giving a loss of 163, which is thought to be a glycosidic moiety such as a methylpentose as seen in the carotenoids from CAQS. MS/MS analysis of the molecular ion gave a series of losses of *m/z* 14 was observed in the region below *m/z* 200 which again is indicative of the presence of a long alkyl chain (Appendix A6.1B).

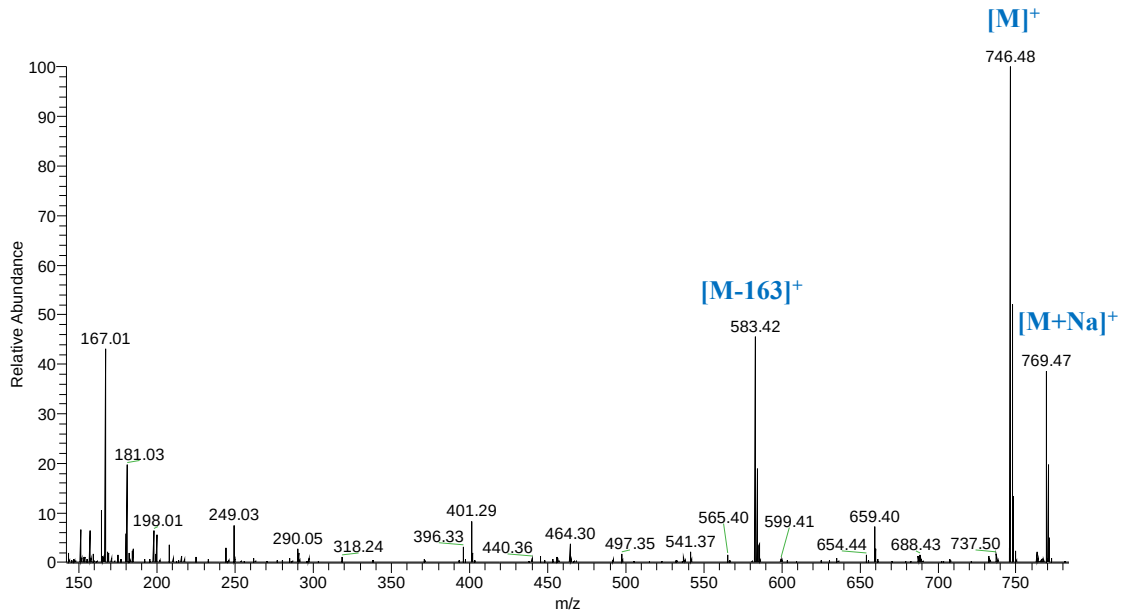


Figure 6. 2: HRESIMS of the bioactive peak with *m/z* 746.4762 corresponding to $M^+$, 769.4654 for $[M+Na]^+$, and the fragment ion at *m/z* 583.4152 $[M-163]^+$, indicative of a loss of a methyl glycoside.

Based on the data, the suggested structure of the compound is aphanizophyll (Figure 6.3) which was originally identified in the cyanobacteria, *Aphanizomenon flos-aquae*. This carotenoid have been previously identified in other strains of cyanobacteria; *M. aeruginosa*, *Oscillatoria tenui*, *Anabaena aerulosa oscillarotiaoides*, *Thermosynechococcus elongatus*, and *C. raciborskii*, however it has not been associated with bioactivity (Stransky and Hager, 1970; Iwai *et al.*, 2008; Mehnert *et al.*, 2012). Aphanizophyll was originally also called 4-hydroxymyxoxanthophyll (Hertzberg and Liaaen-Jensen, 1971) but with later changes of myxoxanthophyll to myxol 2'-glycoside (due to the different glycoside moieties present), it is now termed as 4-hydroxymyxol-2'-glycoside. Further characterization by NMR is required to confirm the identity of this compound and to determine the sugar moiety.

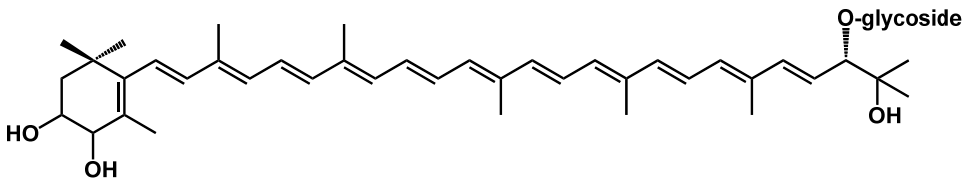


Figure 6. 3: Structure of 4-hydroxymyxol glycoside (aphanizophyll) identified from the methanol fractions of CMEX.

Due to the instability of carotenoids, especially during the extraction process (as mentioned in Chapter 5), purification of the compound for further structural elucidation was not accomplished. However, the above data strongly suggests that the bioactive compound associated with this isolate of *C. raciborskii* is indeed 4-hydroxymyxol glycoside.

### *6.2.2. Bioactive Fractions from M. aeruginosa*

A solvent partitioning in hexane, acetone, and then chloroform showed the hexane fraction as the only bioactive fraction and therefore hexane was used for all subsequent extractions of the biomass. The hexane fraction was then tested at different doses from which a clear dose-dependent relationship was observed (Figure 6.4) with 100% mortality being observed at the highest dose (200µL) and inhibition of development at sub-lethal doses down to 50µL. There was also a dose-dependent relationship observed for the hatching of the embryos with 0% hatching at and above 100µL, 60% hatching at 50µL and 100% hatching in the controls. The hexane extract was subsequently fractionated by two different methods to obtain the bioactive compound/s.

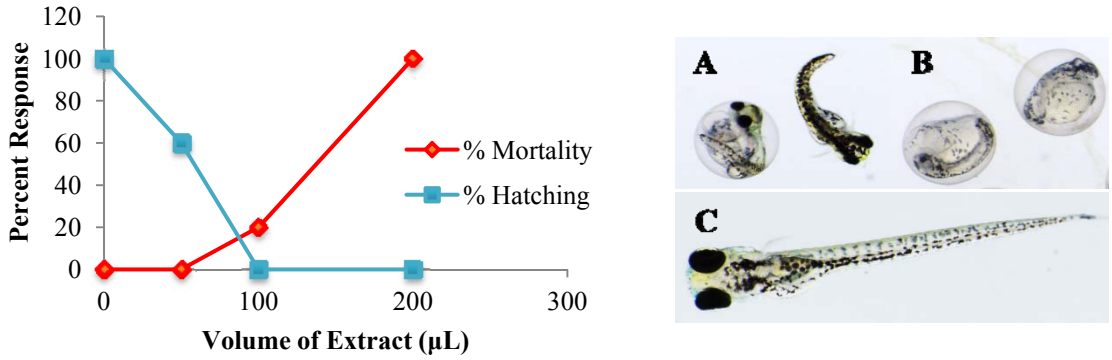


Figure 6. 4: Graph showing the percent mortality and hatching of zebrafish embryos exposed to different doses of MC 81-11 at 4dpf showing a clear dose-dependent relationship. The bioactivity observed at 4dpf with the hexane extract of MC 81-11 at 50µL (A), 100µL (B), and an untreated control (C).

**Fractionation Method 1:** The hexane extract was fractionated on a silica-gel column with increasing amounts of ethyl acetate in hexane (5, 10, 15, 20, 25, 30, 35, 40, and 50% ethyl acetate in hexane, and 100% ethyl acetate). With this solvent system, there was a lot of streaking observed throughout the column and large sets of adjacent fractions showed bioactivity suggesting that great separation of the compounds was not obtained. The main set of bioactive fractions were collected from 15-30% ethyl acetate in hexane and was pooled together for further separation on a prep-TLC. Five bands were observed on the TLC with the first three bands showing bioactivity. These three bands were subsequently run on the HPLC with fractions collected directly into the 24-well plate for the bioassay with the bioactive regions shown in Figure 6.5. From the results of the HPLC, there seems to still be overlapping of the bioactive peaks, with the same bioactive region being observed in bands 1 and 2 (28-30mins) and also bands 2 and 3 (24-26mins).

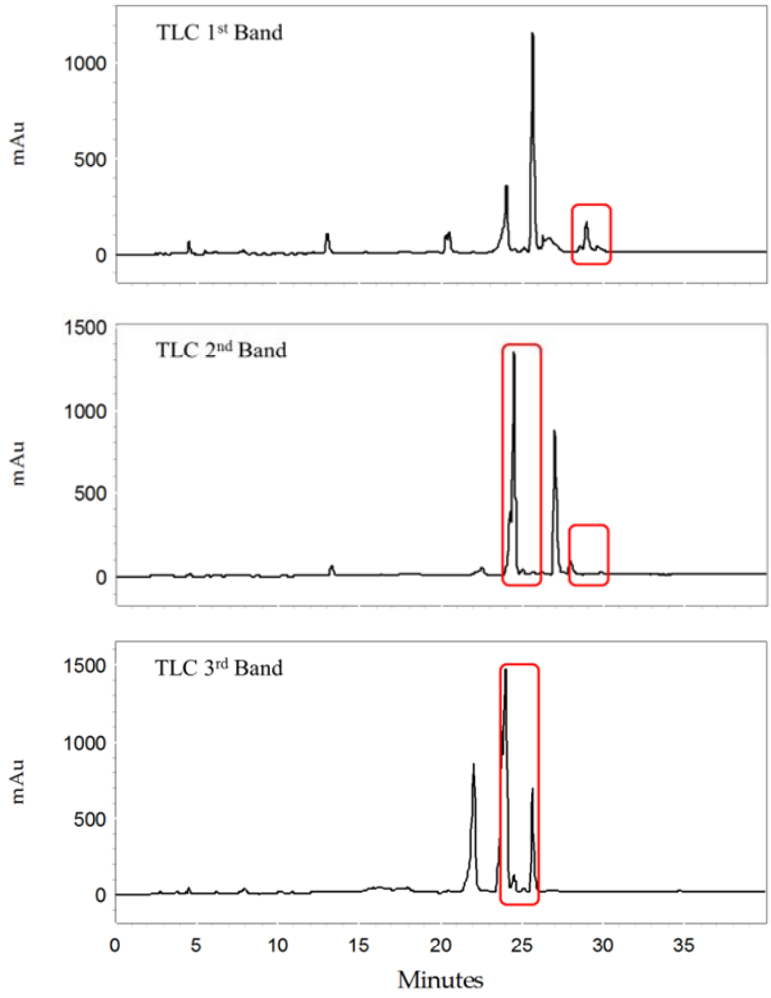


Figure 6. 5: HPLC Chromatogram of the bioactive regions collected from the TLC. Peaks were collected at every 2 minutes in 24-well plates and tested for bioactivity. Bioactive peaks showed no distinct UV spectra.

Mass spectral analysis was carried out to identify if the same masses were in the different bioactive fractions which would suggested the possibility of the same bioactive compound/s in the different bands. Table 6.3 shows the peaks with the same *m/z* and the corresponding retention times. For TLC bands 1 and 2 with the bioactive fraction at 28-30mins, there were no definitive peaks observed which showed similar masses between the two bands. For TLC bands 2 and 3 with the bioactive fraction at 24-26mins there

were 3 peaks observed in both fractions which showed the similar masses with similar fragmentation patterns, however the retention times were slightly different. The three peaks observed had decreasing masses of *m/z* of 44 with increasing retention times suggesting that these compounds may be related.

Table 6. 1: LCMS analysis of the bioactive fraction 24-26mins isolated from the HPLC showing the similar *m/z* peaks observed and the corresponding retention times.

| | | **Retention time /mins** | ***m/z*** | | | | |
|---|---|---|---|---|---|---|---|
| **Bioactive region 24-26mins** | *2nd band* | 15.37 | 493.09 | 476.91 | 471.98* | 454.91 | 300.83 |
| | | 16.23 | | 432.98 | 427.98* | 410.95 | 256.79 |
| | | 17.07 | | 388.90* | 383.96 | 366.93 | 212.84 |
| | *3rd band* | 17.59 | 492.93 | 476.96* | 471.99 | 454.89 | 300.79 |
| | | 18.45 | 448.92 | 432.93* | 427.99 | 410.95 | 256.80 |
| | | 19.42 | 404.87 | 388.91* | 383.95 | 366.93 | 212.85 |

*base peak

**Fractionation Method 2:** The hexane extract was fractionated on a silica-gel column with increasing amounts of acetone in hexane (5, 10, 15, 20, 30, 40, and 50% acetone in hexane, and 100% acetone) followed by a methanol flush. There were 11 fractions obtained from the silica-gel column of which three showed bioactivity in the zebrafish embryos; 5% acetone in hexane, the second fraction from 10% acetone in hexane, and 100% acetone. The 5% acetone in hexane fraction was run through another silica gel column using hexane and ethyl acetate as the eluting solvents with two bands observed using 5% ethyl acetate in hexane with the first band being bioactive. Further purification was attempted with TLC and HPLC however there was not enough sample remaining for subsequent bioassay-guided purification.

Another column was repeated to collect more of the bioactive fraction eluting in 5 and 10% acetone in hexane. Further fractionation using the HPLC was carried out on both fractions where fractions were collected every 2mins and subsequently tested on the zebrafish embryos.

For the 5% acetone fraction, no bioactivity was observed within any of the fractions. This could be due to the lipophilic nature of the compound and the bioactive compounds were retained on the column with the method used. As such another column was used and retested on the zebrafish embryos to identify any bioactive fractions. Figure 6.6 shows the chromatogram of the 5% acetone fraction indicating the two bioactive regions (based on the zebrafish bioassay) and two different wavelengths at which these compounds were observed.

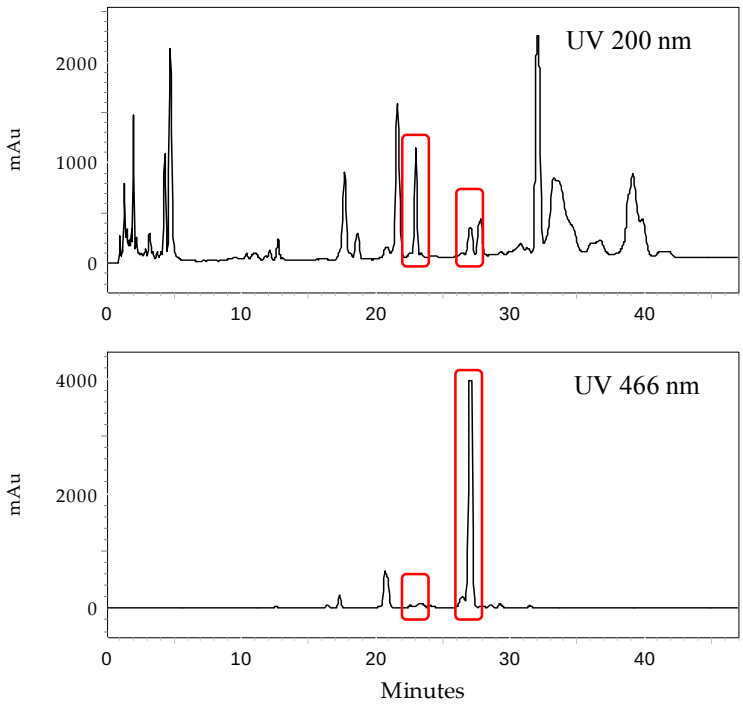


Figure 6. 6: HPLC Chromatogram of the 5% acetone in hexane fraction indicating the bioactive regions (22-24mins and 26-28mins), observed at two different wavelengths.

For the 10% acetone fraction, bioactivity was observed within 20-22mins and 24-26mins (Figure 6.7), where all the embryos showed 100% mortality at 1dpf.

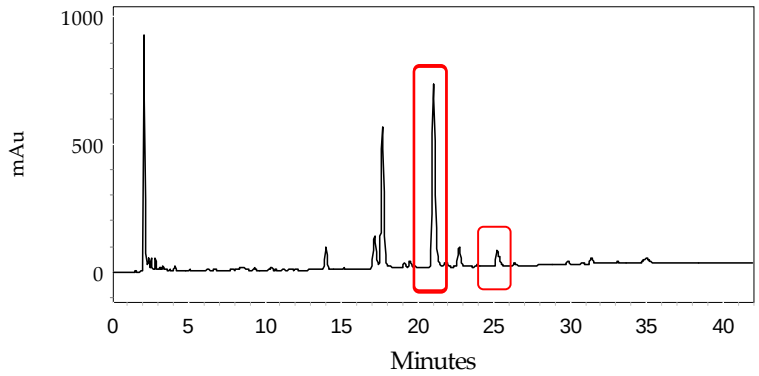


Figure 6. 7: HPLC Chromatogram of the 2nd band in the 10% acetone in hexane bioactive fractions at 20-22mins and 24-26mins.

## 6.3.Methods

### *6.3.1. Bioactive fractions from C. raciborskii (Mexico)*

Freeze-dried biomass was weighed and extracted in chloroform and sonicated. The extract was run through a silica-gel glass column using hexane, acetone, and methanol as the eluting solvents using the following solvent system; 10, 15, 20, 25, 30, 35, 40, and 50% acetone in hexane, 100% acetone, and 100% methanol. The methanol fraction had pigments similar to those observed in CAQS and was therefore analyzed for the presence of carotenoids using HPLC-PDA and HRESIMS.

Analysis of the pigments was carried out by William Louda (FAU) according to the method by Louda (2008). Separation was done using reverse-phase HPLC using a Waters NovaPak 4µ C18 column (3.9 x 150mm) coupled to a photodiode array detector (PDA)

for identification of the pigments. The HPLC solvent system implemented involved three solvent systems over a 48-minute period as shown in Table 6.4.

Table 6. 2: HPLC-PDA method used to separate and identify the carotenoids present in the methanol fraction of CMEX.

| Time (minutes) | Solvent "A" | Solvent "B" | Solvent "C" |
|---|---|---|---|
| 0 | 60 | 40 | 0 |
| 5 | 60 | 40 | 0 |
| 10 | 0 | 100 | 0 |
| 40 | 0 | 30 | 70 |
| 45 | 0 | 30 | 70 |
| 46 | 0 | 0 | 100 |
| 47 | 0 | 100 | 0 |
| 48 | 60 | 40 | 0 |

Solvents: A – 0.5M ammonium acetate in methanol/water (85:15, v/v), B – acetonitrile/water (90:10, v/v), C – ethyl acetate.

**4-hydroxymyxol glycoside (aphanizophyll)**: HRESIMS *m/z* 746.4762 ($C_{46}H_{66}O_8$, $[M]^+$, Δmmu of 0.850) with a ring and double bond equivalent of 14.0.

### *6.3.2. Purification of Bioactive Compounds from M. aeruginosa*

**Fractionation Method 1:** The biomass was extracted in chloroform. The extract was dried down and solvent partitioned in hexane, acetone, and chloroform. The only bioactive fraction was hexane; therefore further extractions were done with hexane. The hexane extract was fractionated on a silica-gel glass column with increasing percentages of ethyl acetate in hexane (0, 5, 10, 15, 20, 25, 30, 40, 50, 100% ethyl acetate). Bioactivity was observed in fractions within the solvent systems 10-30% ethyl acetate in hexane. These fractions were then pooled together and a preparative-TLC was done with the solvent system of 15% ethyl acetate, 3.75% isopropanol, 81.25% hexane (8.1:1.5:0.4 - Hexane:Ethyl acetate:Isopropanol). From the preparative-TLC, 8 different regions were

collected; 6 distinct bands plus the top and bottom of the TLC plate. Bioactivity was observed in bands 1-3 (100% mortality) and 5-6 (all embryos deformed) of the zebrafish embryos within 24hpf and as such the first 3 bands were collected and ran through the HPLC [Method: Phenomenex Luna 5u C-18 Analytical Column: Acetonitrile and water gradient starting with 50% acetonitrile for 5mins then increase to 100% over 20mins, kept at 100% acetonitrile for 15mins, then back to 50% acetonitrile over 5mins for a total of 40mins]. Fractions were collected from the HPLC at 2 minute increments and the bioactive bands observed were analyzed on the LCMS in an attempt to identify masses within the fractions.

**Fractionation Method 2:** This hexane extract was then fractionated using a silica-gel glass column with increasing amounts of acetone in hexane (0(1), 5(1), 10(2), 15(1), 20(2), 30(1), 50(1), 100% (1) acetone) then flushed with 100% (1) methanol for a total of 11 fractions. The 5% acetone in hexane bioactive fraction was solvent partitioned in methanol and then hexane, with the methanol fraction showing bioactivity. The methanol fraction was further subjected to a lipophilic-sephadex (LH-20) column, using methanol as the mobile phase solvent where no further separation was observed. Additional purification attempts were carried out to identify the bioactive compound/s using TLC and HPLC-UV, however no further bioactivity was observed with the subsequent fractionation steps, more likely as a result of insufficient sample. Additional biomass was obtained, extracted in hexane, and fractionated as before using the same column with hexane and acetone as the eluting solvents. The two bioactive fractions were then run on

the HPLC and fractions collected every two minutes in 24-well polypropylene plates to test on the zebrafish embryos.

## 6.4. Conclusion

The zebrafish embryo model was used as a bioassay to identify bioactive compounds within the lipophilic extracts of known toxigenic cyanoHAB species. Two sets of bioactive compounds were identified from two of these species (APH and CAQS) however there were additional isolates (CMEX and MC 81-11) in which bioactivity was observed, however only bioactive fractions containing more than one compounds were determined. Progress however was made towards the determination of the bioactive metabolite/s from both of these isolates. The isolate CMEX was shown to produce the carotenoid, aphanizophyll, a known carotenoid produced by cyanobacteria. This carotenoid as with others is associated with photoprotection however crude extracts containing aphanizophyll caused developmental malformations in zebrafish embryos. The lake in which this isolate of cyanobacteria is found is well known for its fisheries and the occurrence of these toxic metabolites may greatly affect the production of some fish species. MC 81-11 has also shown various fractions which are bioactive, causing mortality as well as inhibition of development in the zebrafish embryos. Further purification is needed to identify the bioactive compounds from these fractions.

## References

1. Berry, J. P.; Lind, O. First evidence of “paralytic shellfish toxins” and cylindrospermopsin in a Mexican freshwater system, Lago Catemaco, and apparent

bioaccumulation of the toxins in “tegogolo” snails (Pomacea patula catemacensis).*Toxicon* **2010***, 55*, 930-938.

2. Berry, J.; Jaja-Chimedza, A.; Dávalos-Lind, L.; Lind, O. Apparent bioaccumulation of cylindrospermopsin and paralytic shellfish toxins by finfish in Lake Catemaco (Veracruz, Mexico). *Food Additives & Contaminants: Part A* **2012***, 29*, 314-321.

3. Hertzberg, S.; Liaaen-Jensen, S. The constitution of aphanizophyll. *Phytochemistry* **1971***, 10*, 3251-3252.

4. Iwai, M.; Maoka, T.; Ikeuchi, M.; Takaichi, S. 2,2'-ß-Hydroxylase (CrtG) is Involved in Carotenogenesis of Both Nostoxanthin and 2-Hydroxymyxol 2'-Fucoside in Thermosynechococcus elongatus Strain BP-1. *Plant and Cell Physiology* **2008***, 49*, 1678-1687.

5. Komárková, J.; Tavera, R. Steady state of phytoplankton assemblage in the tropical Lake Catemaco (Mexico). *Phytoplankton and Equilibrium Concept: The Ecology of Steady-State Assemblages*; Springer: **2003**; pp 187-196.

6. Louda, J. W. HPLC-Based Chemotaxonomy of Florida Bay Phytoplankton: Difficulties in Coastal Environments. *J. Liq. Chromatogr. Rel. Technol.* **2007***, 31*, 295-323.

7. Mehnert, G.; Rücker, J.; Nicklisch, A.; Leunert, F.; Wiedner, C. Effects of thermal acclimation and photoacclimation on lipophilic pigments in an invasive and a native cyanobacterium of temperate regions. *Eur. J. Phycol.* **2012***, 47*, 182-192.

8. Stransky, H.; Hager, A. The carotenoid pattern and the occurrence of the light-induced xanthophyll cycle in various classes of algae. VI. Chemosystematic study. *Arch. Mikrobiol.* **1970***, 73*, 315-323.

# CHAPTER 7

CONCLUSION

### 7.1. Occurrence of Bioactive Lipophilic Secondary Metabolites

Cyanobacteria are known to produce a wide array of secondary metabolites, which when negatively associated with health effects, are termed toxins. It is still unclear the purpose of these cyanobacterial toxins, however it is known that there are additional bioactive compounds, different from the known cyanotoxins, within the lipophilic extracts of these cyanobacterial HABs that contribute to the toxicity of the strains. Within this project, we have identified and purified two sets of bioactive compounds, which although previously identified, have not been associated with negative health effects. Through the use of the zebrafish embryo assay as a model for vertebrate development, we were able to identify these compounds as bioactive lipophilic secondary metabolites and gain a better understanding of the bioactivity associated with these compounds.

PMAs have been identified over three decades ago and were identified based on their structure. There was no bioactivity observed with the PMAs according to traditional bioassays (such as the cytotoxicity assay) with this being the first reported bioactivity associated with these compounds. Identified from these strains were six variants of the PMAs, differing from each other by the number of methoxy groups present, with the methoxy groups ranging from seven to twelve. As previously mentioned, these compounds were previously identified in other genera of cyanobacteria suggesting that they may be widespread in nature. Analysis of a culture collection provided by Miroslav Gantar (FIU, Department of Biological Sciences), indicated that these metabolites are relatively widespread and can be found in a number of genera of cyanobacteria belonging to different orders, as well as different genera of green algae. The structure of the PMAs suggests that the biosynthesis may involve the PKS biosynthetic pathway and based on

the feeding experiments done with $^{13}C$-labeled acetate, this hypothesis seems to hold true. However, NMR analysis indicates that the pattern of incorporation does not follow that of a PKS biosynthetic route and suggests that the biosynthesis may occur via a different pathway. Evaluation of the bioactivity using the zebrafish embryos indicated a possible structure dependence on the bioactivity with the bioactivity decreasing with the increasing size of the molecules. This difference in bioactivity could also be related to the solubility of the compounds since the medium for the bioassay is water and the PMAs are lipophilic.

Carotenoids were the second set of compounds identified to inhibit the development in zebrafish embryos. Characterization by NMR was difficult due to the insufficient quantities obtained for each of the compounds as a results of their instability, however other tools were used to identify the nature of these compounds. Carotenoids are known to be primary metabolites, preventing against photooxidation and aiding in photosynthesis. Additionally, they have been largely used as antioxidants in humans and other animals. However, the glycosidic carotenoids identified from the two strains of *C. raciborskii* inhibits development of the zebrafish embryos, which is the first report of negative effects associated with these compounds. A possible mechanism of bioactivity could be the decomposition of the carotenoids to retinoids which have been shown to cause malformations in zebrafish embryos, amphibians, and chicks. Further biological characterization of these compounds are necessary to identify their mode of action.

Table 7. 1: Cyanobacteria and green algae chloroform extracts that were used in the screening against the zebrafish embryos, indicating the ones that showed bioactivity by inhibiting their development and were also shown to produce PMAs, carotenoids, or both.

| Isolates | PMAs | Carotenoids |
|---|---|---|
| **Cyanobacteria** | | |
| **Aphanothece* 103-7 | | |
| **Aphanizomenon* APH | X | |
| *C. raciborskii* 121-1 | | X |
| *C. raciborskii* AQS | X | X |
| **Microcystis* 81-11 | X | |
| *Pseudanabaena* 108-1 | X | |
| **Green Algae** | | |
| *Chlamydomonas* 80-1 | | |
| *Kirchneriella* 104-7 | | |
| *Scenedesmus* 79-1 | X | |
| *Scenedesmus* 80-15 | X | |

*Previously identified genera to produce myxoxanthophyll and other currently identified bioactive carotenoids.

Table 7.1 shows the cyanobacterial and green algal isolates that were shown to inhibit development in zebrafish embryos. From the screening of the PMAs, four of the cyanobacterial isolates and two of the green algal isolates produced one or more of the PMAs identified within this study. Bioactive glycosidic carotenoids were identified in two of the cyanobacterial isolates in this study while three of the other genera, namely Aphanothece, Aphanizomenon, and Microcystis are known to also produce glycosidic carotenoids, specifically myxol 2'-glycoside and 4-ketomyxol 2'-glycoside. The bioactivity associated with the lipophilic extracts of these isolates could be related to the presence of these bioactive compounds, namely PMAs, carotenoids, or both. There are also other compounds, other than the ones identified in this project, within these isolates that are responsible for the bioactivity observed which gives rise to the toxicity of the strain.

In addition to the identified bioactive compounds within this project, there still remains a whole suite of toxic secondary metabolites from these cyanoHABs that are unrelated to the known water-soluble toxins that may contribute to the toxicity of these HAB species. This may pose a great health risk to animals and humans due to the frequent occurrence of these cyanoHAB species and the possible bioaccumulation of these compounds in the food chain.

### 7.2. Zebrafish Embryos as a Model for Vertebrate Development

The zebrafish embryo was used in this project as a model for vertebrate development in the identification, purification, and characterization of lipophilic secondary metabolites from freshwater isolates of cyanobacterial HABs. The lipophilic extracts of these HAB species were previously identified to show that they contained bioactive compounds that inhibit the development in zebrafish embryos. Further evaluation of these extracts using the zebrafish embryo bioassay to guide the fractionation led to the purification of the previously mentioned bioactive compounds. Due to the advantages of this model, it allowed for the rapid and high-throughput analysis in bioassay-guided purifications of bioactive metabolites from various sources, including cyanobacteria.

The zebrafish embryo has also been well used as a toxicological model in evaluating the effects of the known cyanotoxins on the development. We were also able to use them in the analysis of the chemically characterized lipophilic metabolites isolated from the cyanobacteria to further understand their effects on vertebrate development. The zebrafish embryo model has therefore proven to be a well-suited model for the

identification of bioactive compounds as well as the study of known and unknown cyanobacterial toxins.

### 7.3. Future Directions

Cyanobacterial HABs are a continuous problem in today's environment due to the effects of climate change and the eutrophication of the water sources which are conducive for the growth and persistence of these blooms. As such, continued research is required in the identification of the novel metabolites produced by these blooms that will contribute to their toxicity as well as a better understanding for the known metabolites produced during these blooms events. This project was able to identify a new set of previously identified compounds not associated with bioactivity (PMAs), as well as a set of bioactive compounds that have only be associated with its beneficial effects (carotenoids). However, we know that there is still a suite of compounds that have not been identified as indicated from the bioactive fractions from the other cyanobacterial strains (*C. raciborskii* 121-1 and *M. aeruginosa*) both of which are highly recognized as HABs. Final purification and subsequently chemical characterization is required to identify these not yet identified compounds from the aforementioned cyanoHABs, especially due to the fact that these genera are recurrent HAB blooms in freshwater sources around the world. The Mexico strain of *C. raciborskii* is in constant bloom and therefore provides us with a great opportunity for the study of metabolites from this species and the impact the blooms have on the environment, including the aquatic life, and human and animal health.

These cyanoHABs produce a wide variety of compounds with different effects on organisms. It is understood how some of these compounds affect the organisms but these compounds are not produced individually. As such, it would be interesting to analyze the combined effects of these compounds produced by each isolate on the toxicity of organisms to assess the possibility of a synergistic effect or maybe even a protective effect of one or more of these compounds. This would help to understand the overall toxic effects associated with these blooms and not just the effects from the individual components, which would allow for better management of water sources during the times of these blooms.

Carotenoids are known for the beneficial impacts in cyanobacteria and in other organisms however, we now know that these molecules also have negative impacts, inhibiting the development of zebrafish embryos and possible other vertebrate species. It would therefore be important to be able to identify the different carotenoids produced by the different cyanobacterial species both in culture and in nature, and the bioactivity, if any, associated with them. Further investigation is required for the understanding of the mechanism of action of these carotenoids and to test the hypothesis of the biotransformation of the carotenoids into retinoids, specifically identifying which types of retinoids are formed from the different carotenoids. Also, it is known that different carotenoids are produced at different temperatures and with the changes in the climate, knowledge of the toxicity of the carotenoids produced at different temperatures will also help to understand the toxicity of these blooms.

# APPENDICES

## A2.1. PMAs Isolated from *A. ovalisporum*

*A2.1.1. PMA **1** $^1$H-NMR in $C_6D_6$*

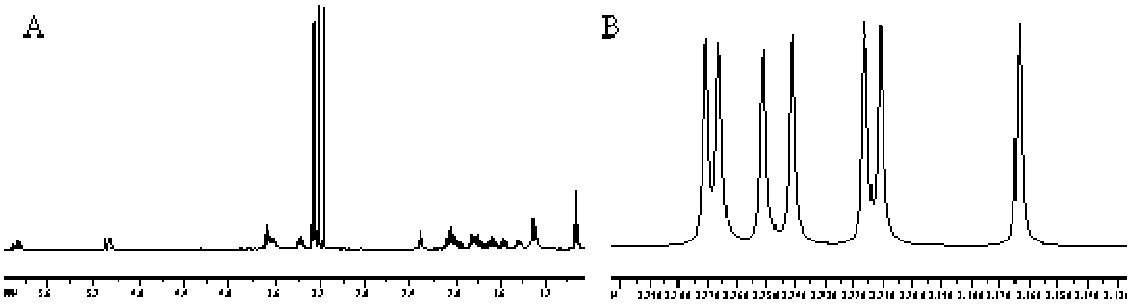


*A2.1.2. PMA **2** $^1$H-NMR in $C_6D_6$*

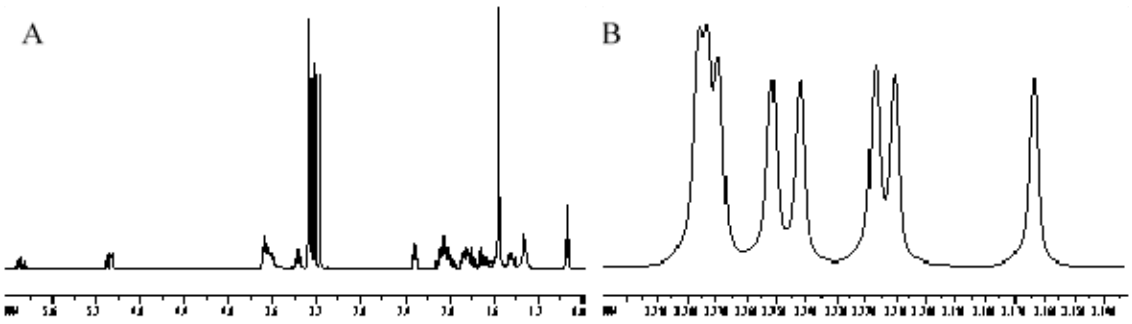


*A2.1.3 - PMA **3** $^1$H-NMR in $C_6D_6$*

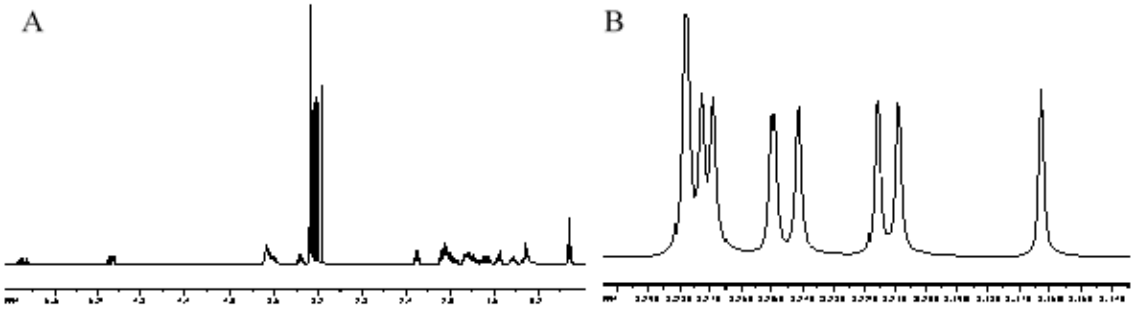

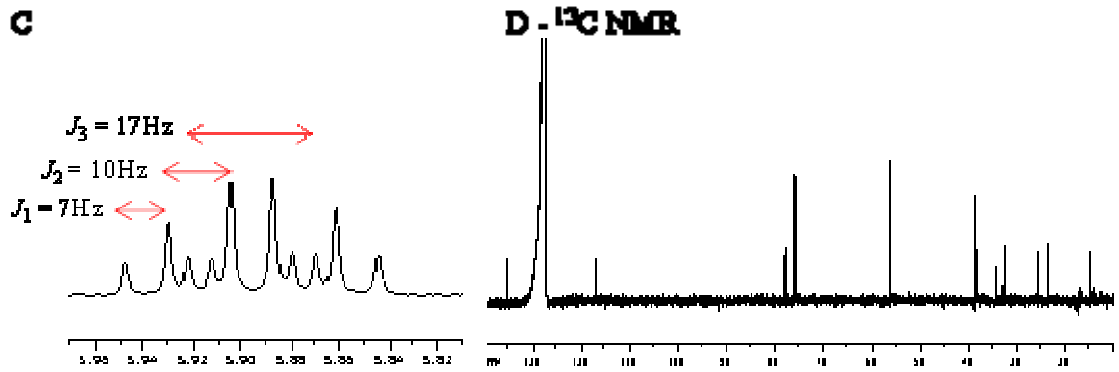


*A2.1.4. PMA **4** $^{1}$H-NMR in $C_6D_6$*

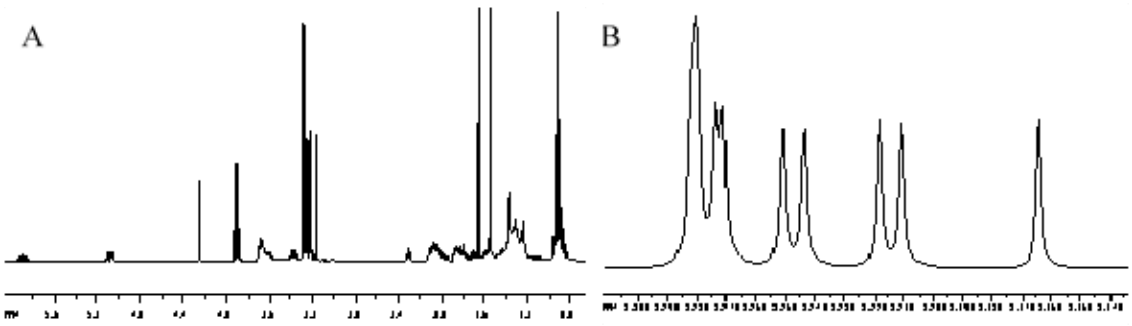


*A2.1.5. PMA **5** $^{1}$H-NMR in $C_6D_6$*

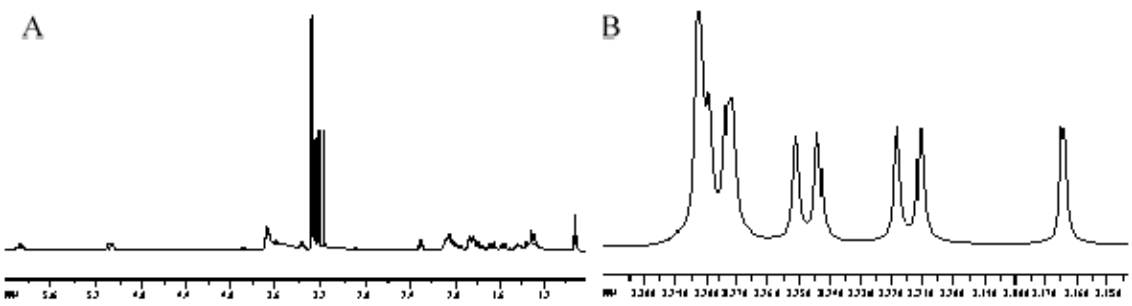

*A2.1.6. PMA* ***6*** *$^{1}$H-NMR in $C_6D_6$*

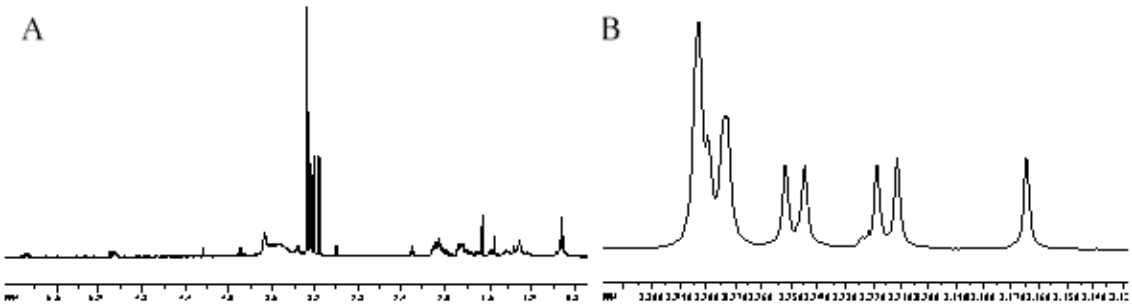


*A2.1.7. Blank (NMR tube for PMA 4)*

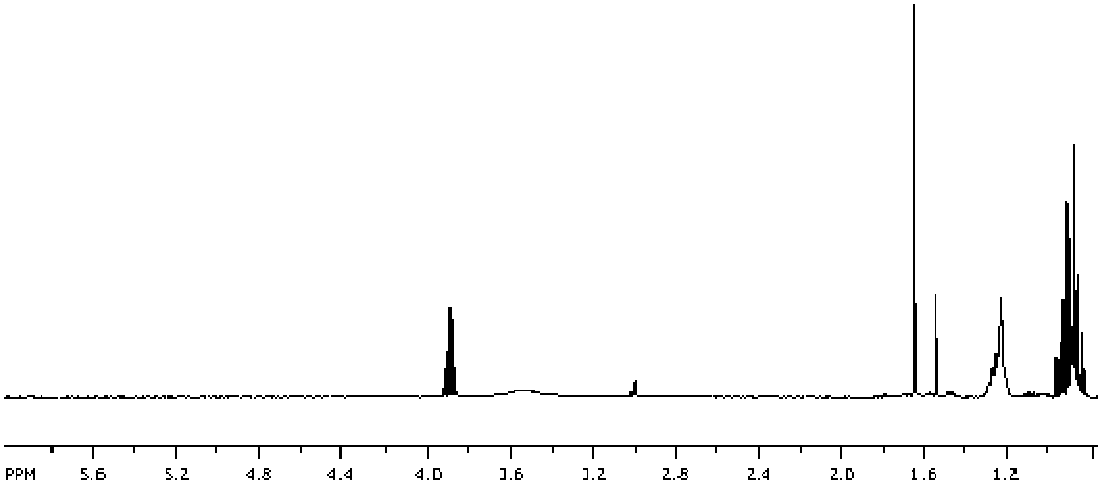


*Note*: Benzene blank with the same tube used for PMA 4 indicating the presence of impurities associated with the NMR tube.

**A2.2. PMAs Isolated from *C. raciborskii***

*A2.2.1. PMA **2** $^1$H-NMR in $C_6D_6$*

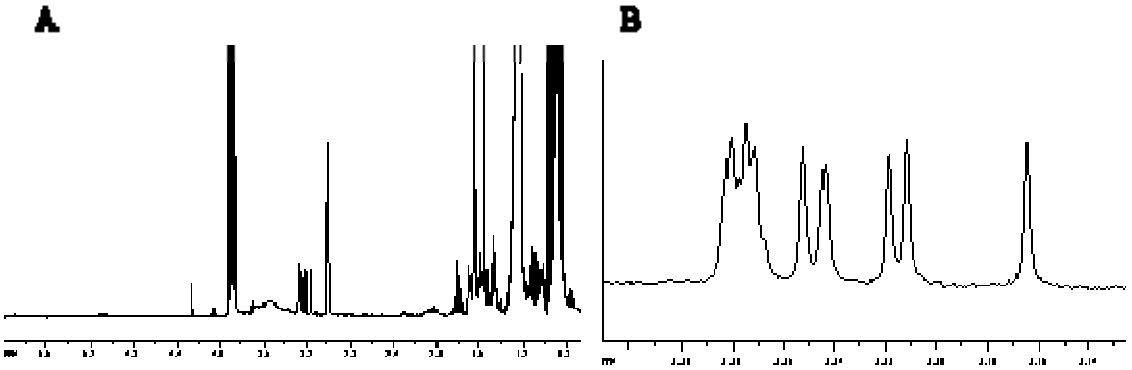


*A2.2.2. PMA **3** $^1$H-NMR in $C_6D_6$*

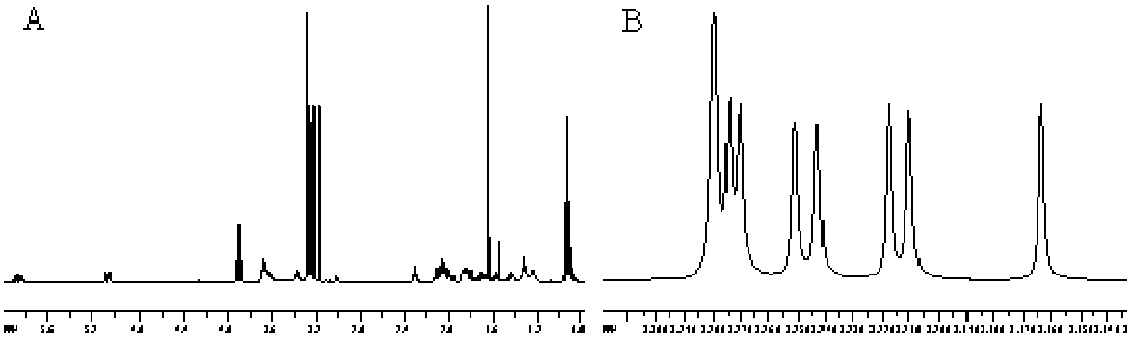


C – DEPT-135

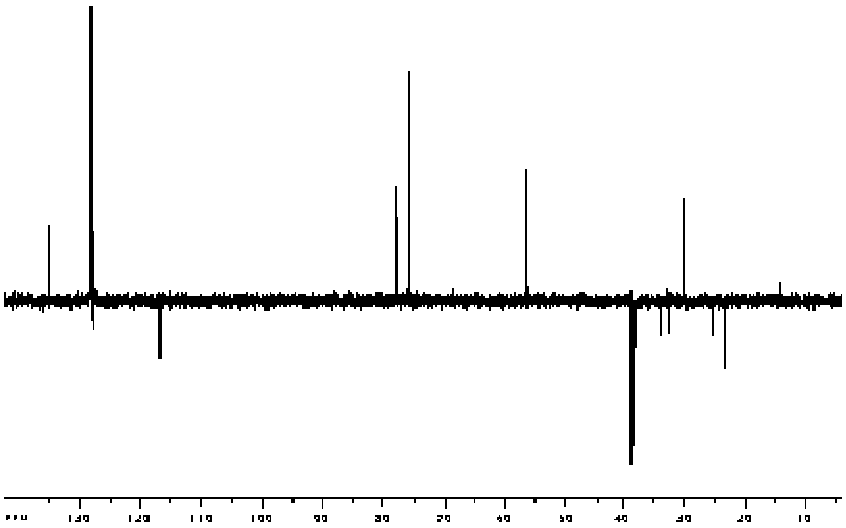

D - COSY

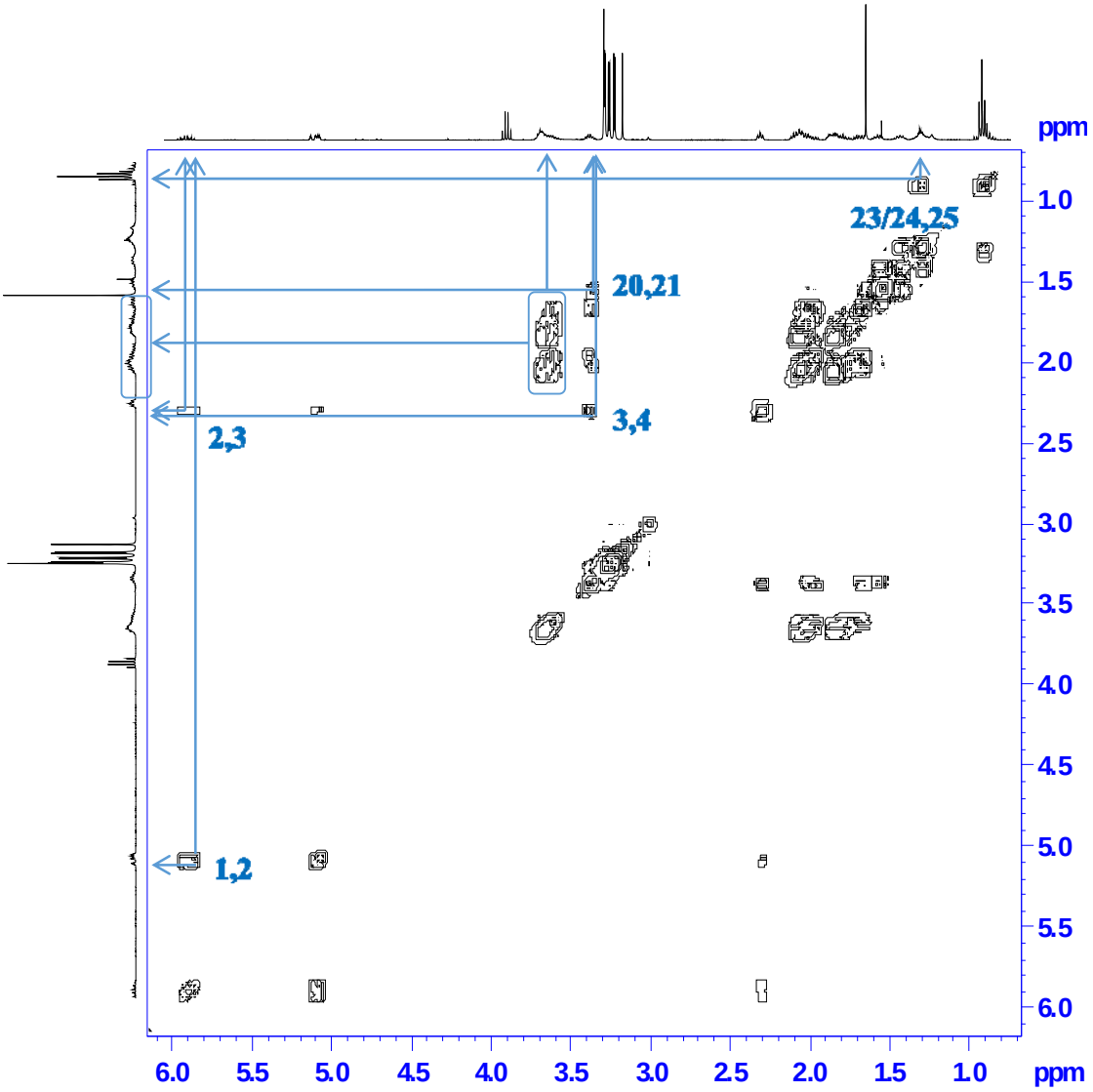
ppm
1.0
1.5
2.0
2.5
3.0
3.5
4.0
4.5
5.0
5.5
6.0
23/24,25
20,21
3,4
2,3
1,2
6.0
5.5
5.0
4.5
4.0
3.5
3.0
2.5
2.0
1.5
1.0
ppm

E – HMQC

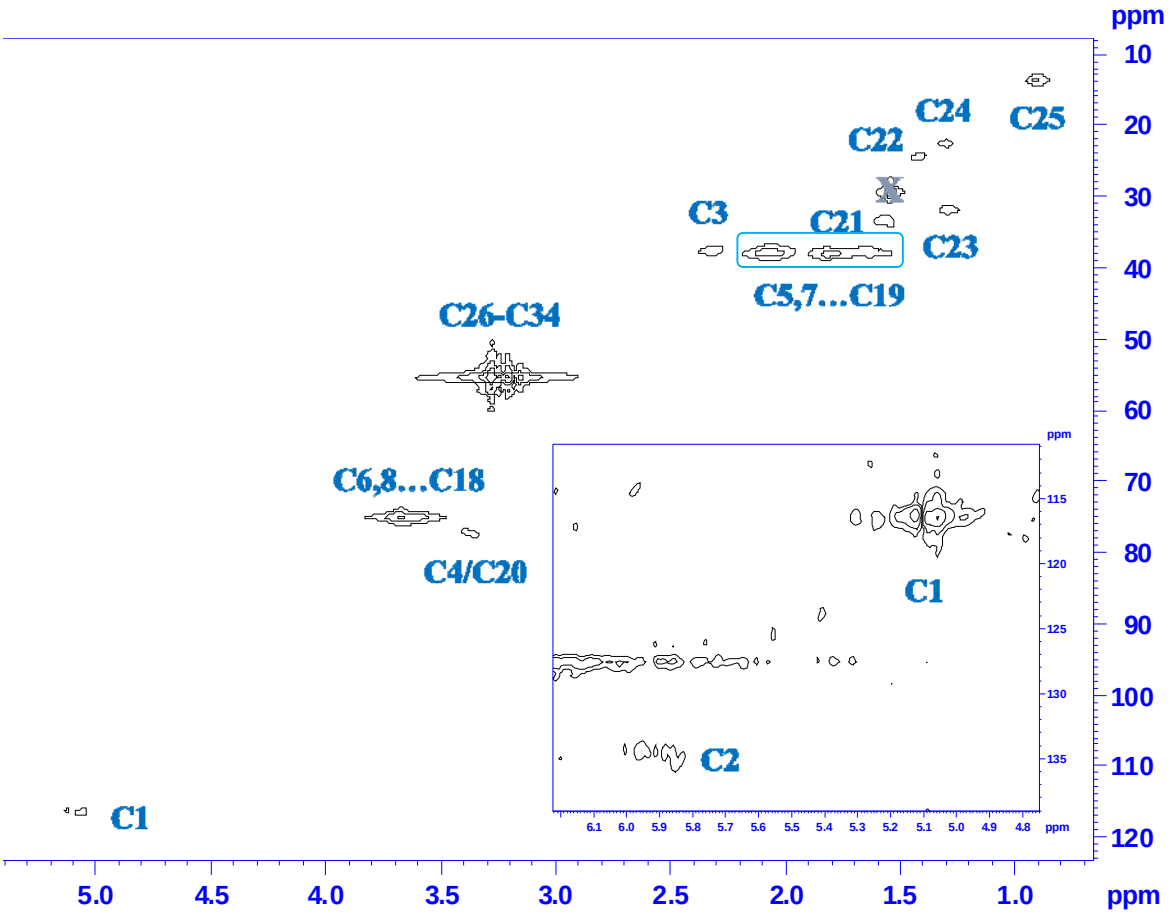
ppm
10
20
30
40
50
60
70
80
90
100
110
120
C24
C25
C22
C3
C21
C23
C5,7...C19
C26-C34
C6,8...C18
C4/C20
C1
C2
C1
5.0
4.5
4.0
3.5
3.0
2.5
2.0
1.5
1.0
ppm

F – HMBC

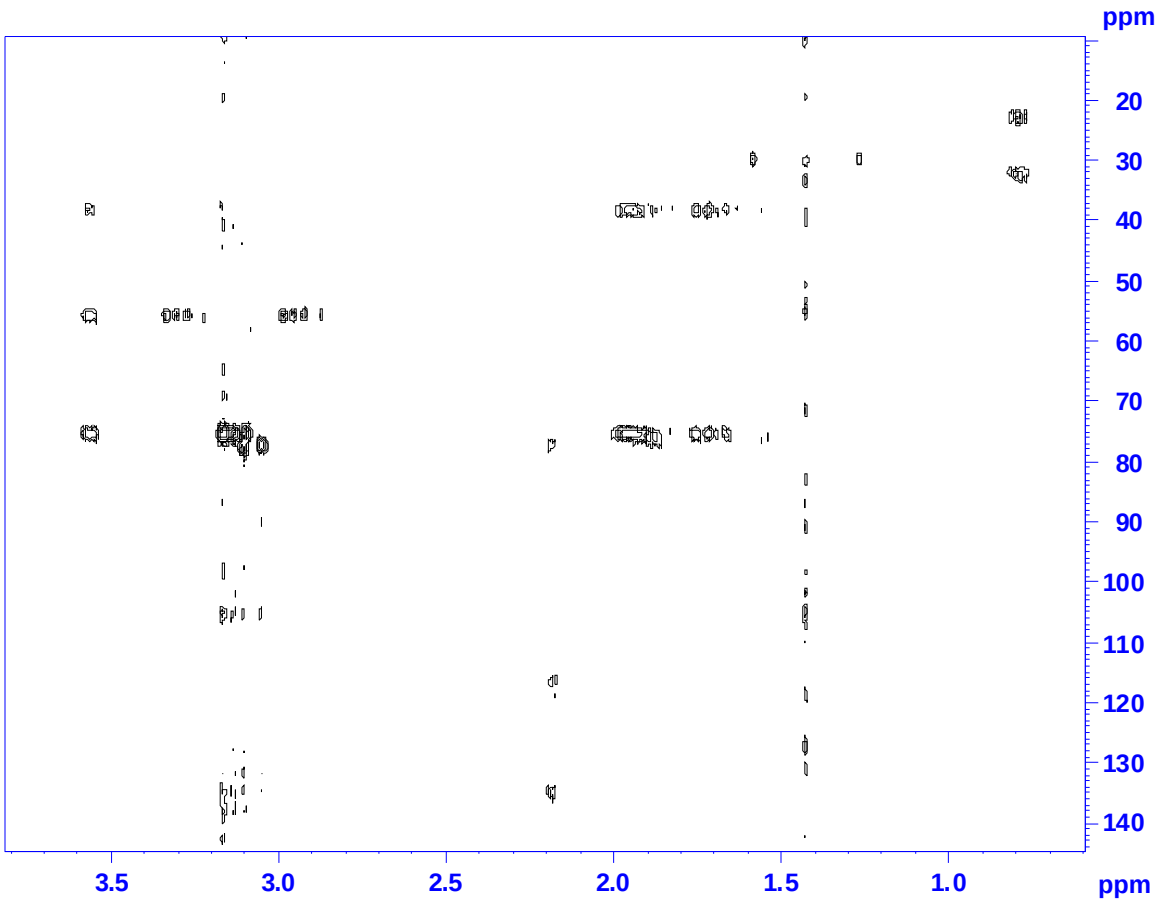

*A2.2.3. PMA **4** $^1$H-NMR in $C_6D_6$*

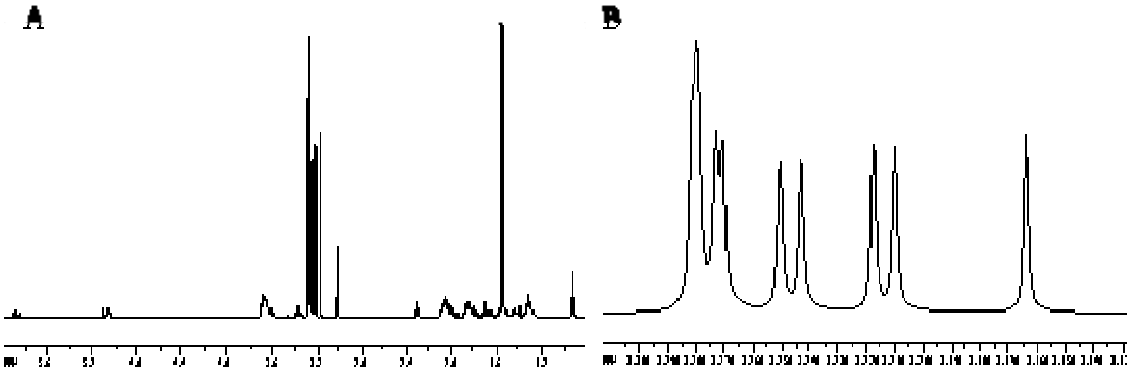


*A2.2.4. PMA **5** $^1$H-NMR in $C_6D_6$*

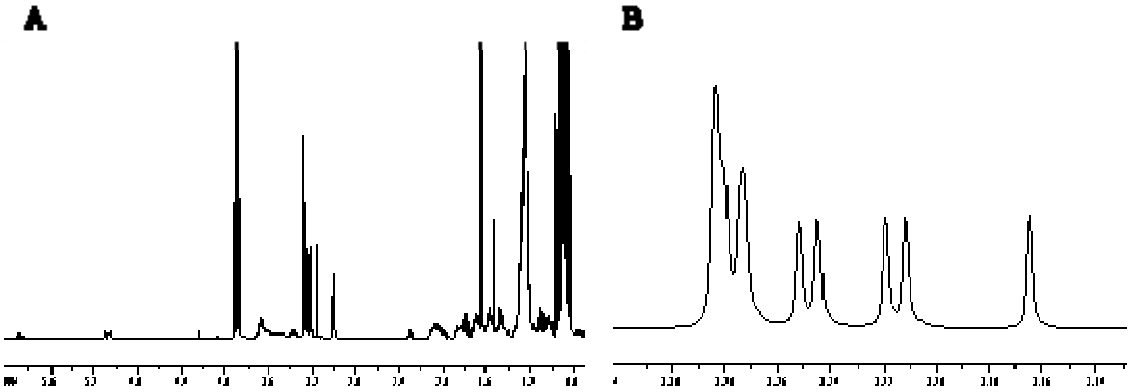

## A2.3. Mass Spectral Data for PMAs from *A. ovalisporum*

### *A2.3.1. MS of PMA **1***

A

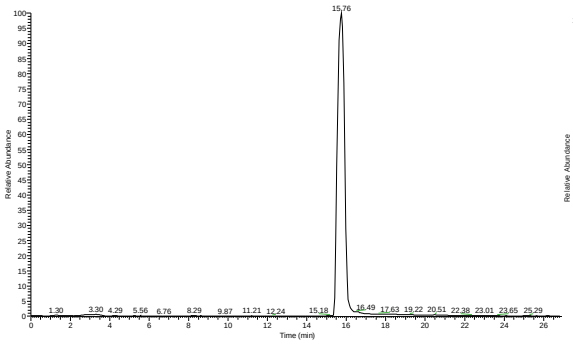


B

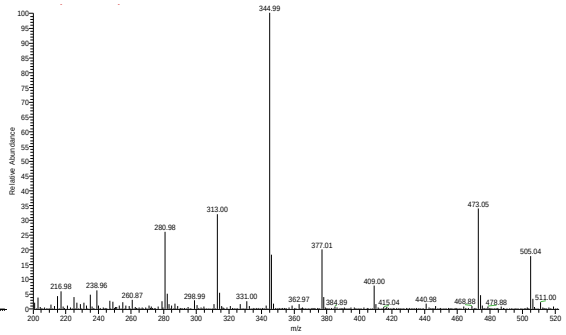


### *A2.3.2. MS of PMA **2***

A

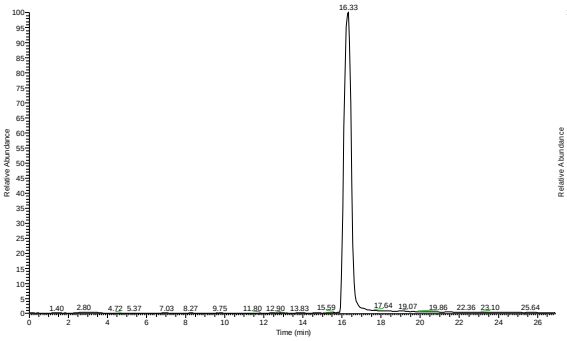


B

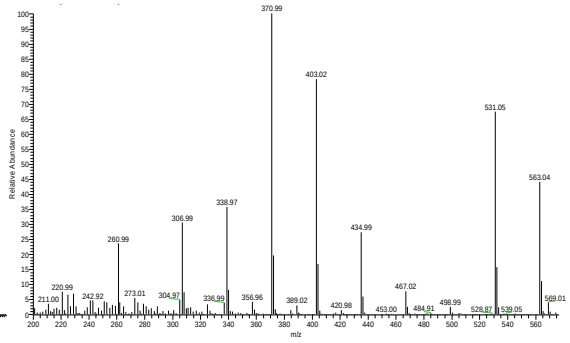


### *A2.3.3. MS of PMA **3***

A

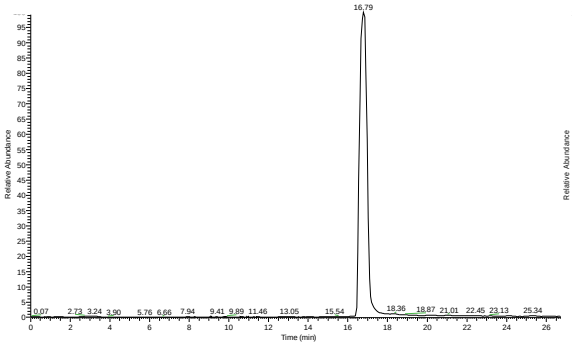


B

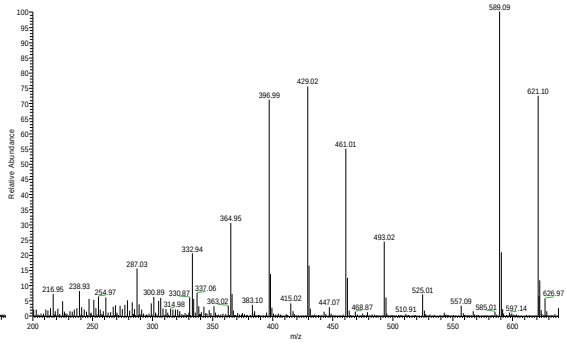

*A2.3.4. MS of PMA **4***

A B

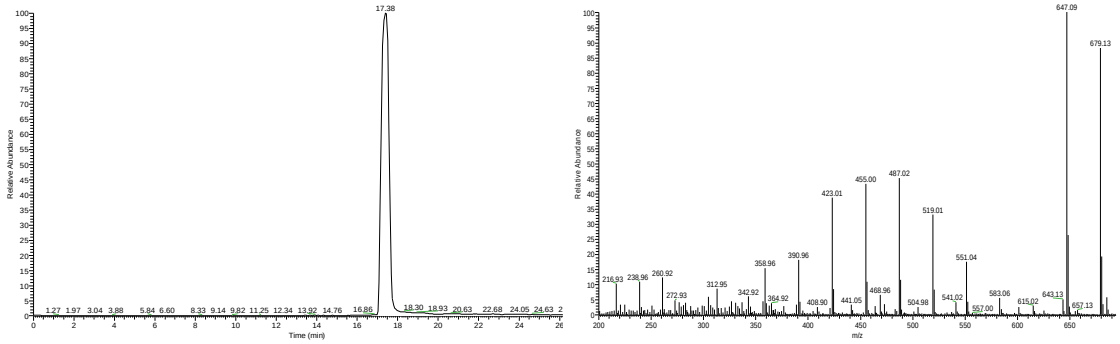


*A2.3.5. MS of PMA **5***

A B

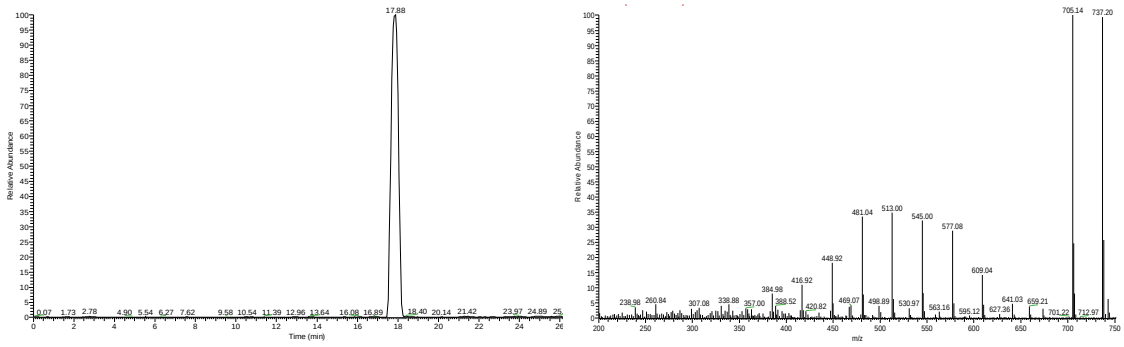


*A2.3.6. MS of PMA **6***

A B

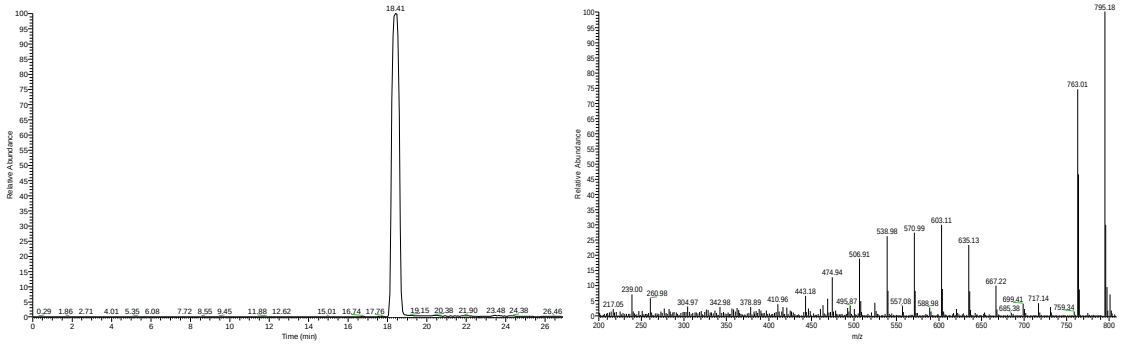

## A2.4. Cylindro AQS PMAs observed from the HRESIMS

A

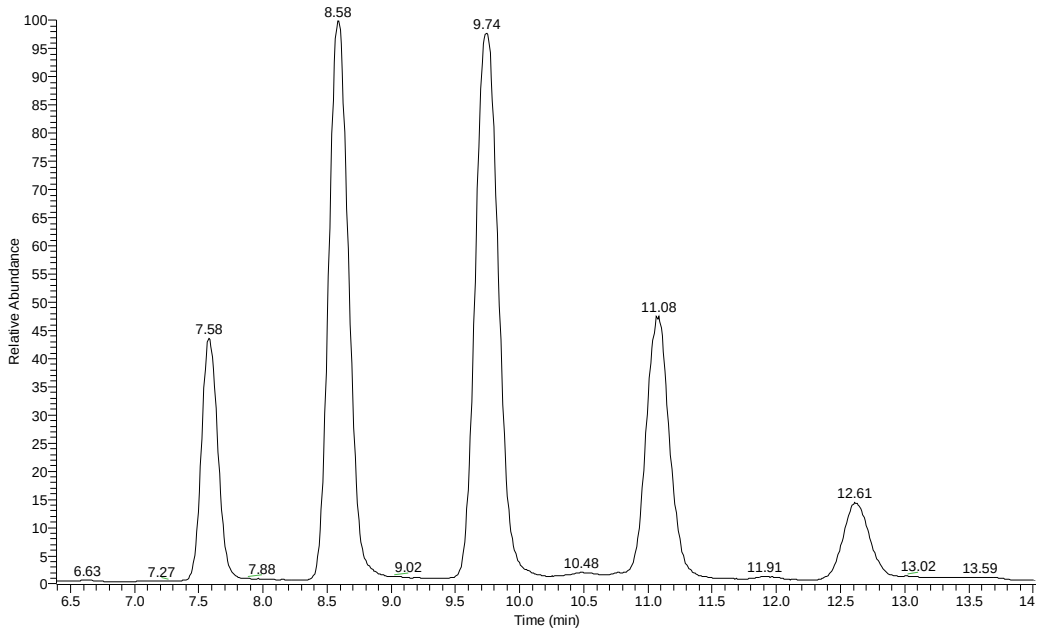


B

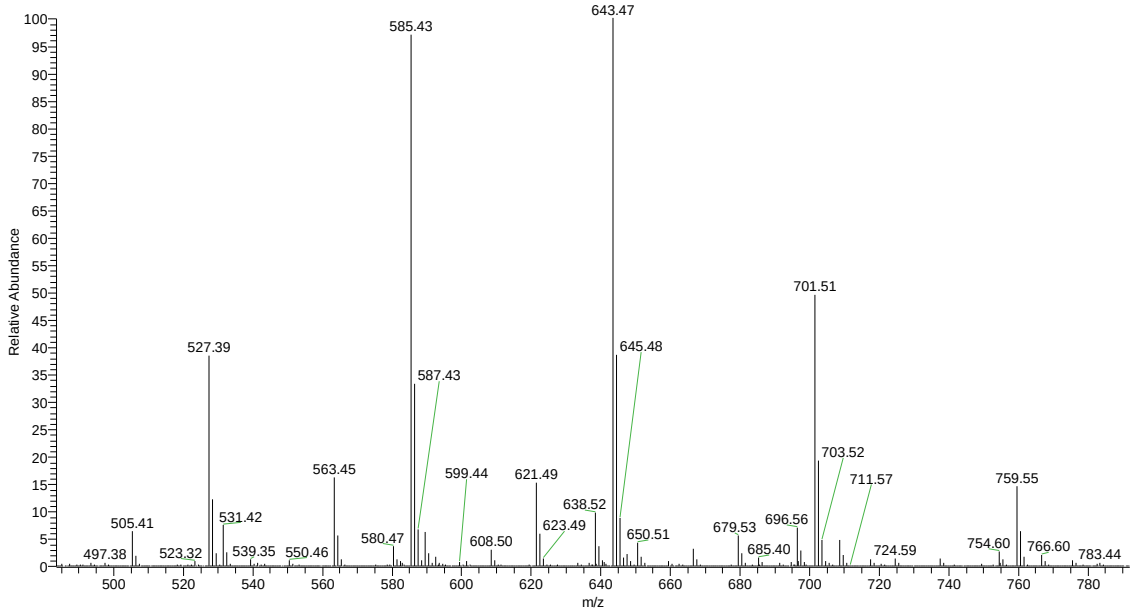

**A5.1. CAQS Carotenoid 1 (*m/z* 744)**

A) UV-Vis spectrum from the HPLC-PDA run isocratically at 65% acetonitrile in water.

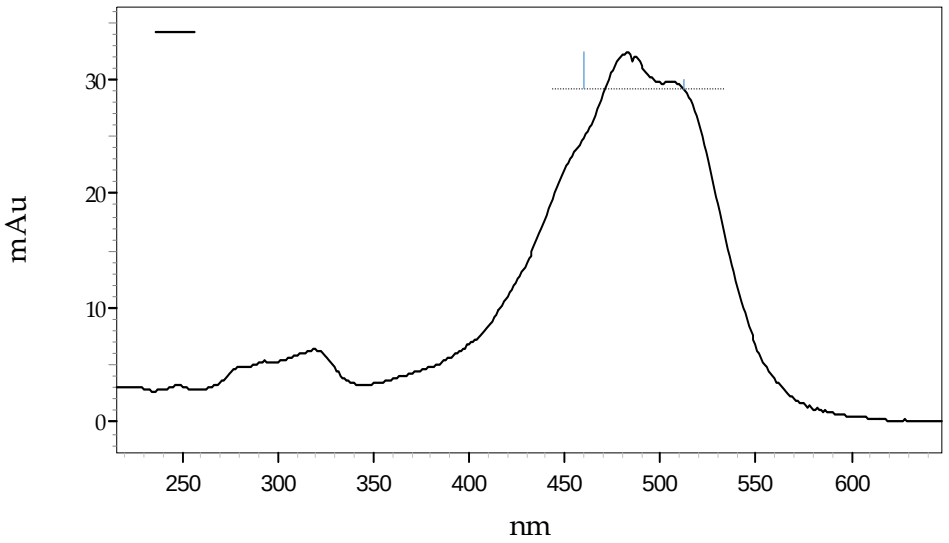


B) MS/MS of Carotenoid 1 (Molecular ion peak *m/z* 744)

MS/MS 744

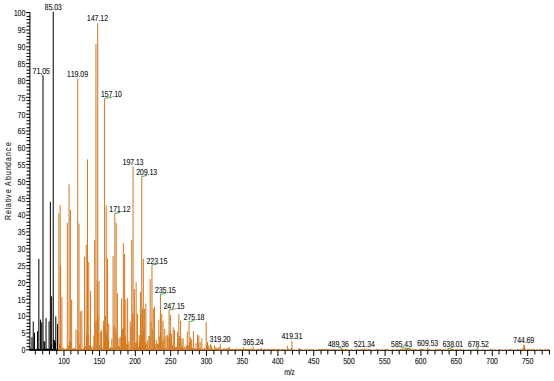


MS/MS 581

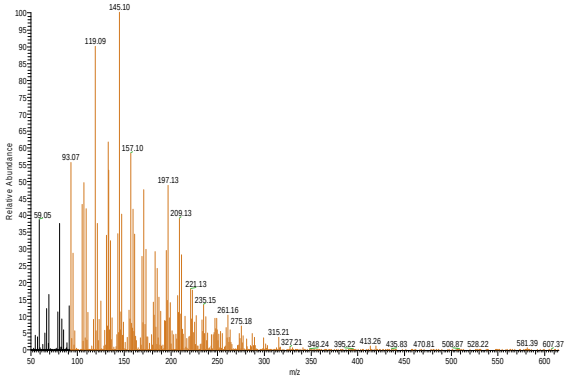

## A6.1. CMEX Carotenoid 3 (*m/z* 746)

A) HPLC-UV/Vis spectrum of the bioactive peak from the 100% MeOH fraction. The solvent system used for the HPLC run was 65% acetonitrile in water (isocratic).

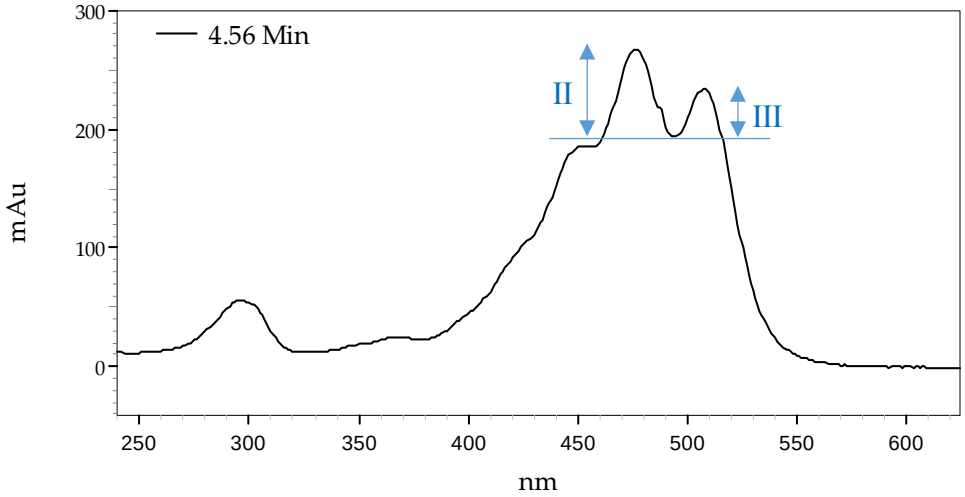


B) MS/MS of the bioactive peak (*m/z* 746)

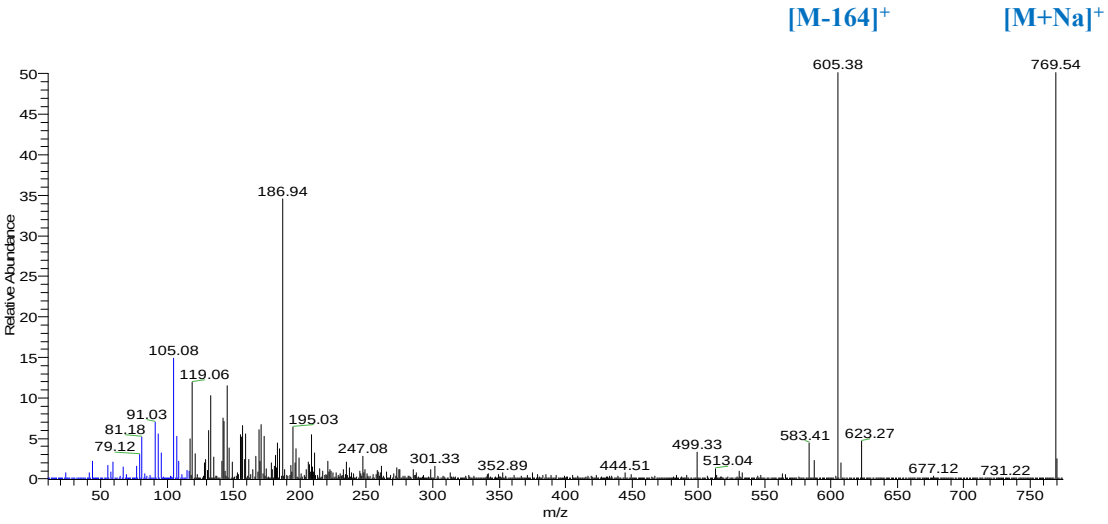

**A6.2. CMEX (Carotenoid 3;** Louda method)

A) Total chromatogram of methanol fraction from CMEX which the proposed aphanizophyll peak at 11.32mins circled.

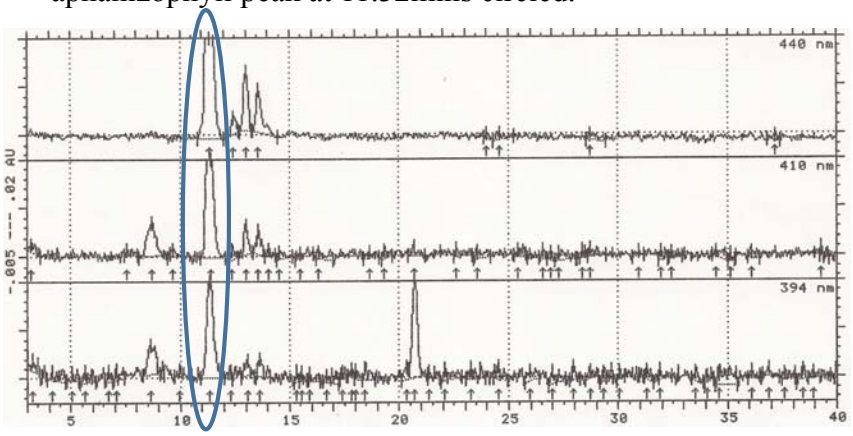


B) UV-spectrum of the proposed aphanizophyll peak at 11.32mins [UV-vis: 451, 476, 507nm, %III/II 56]

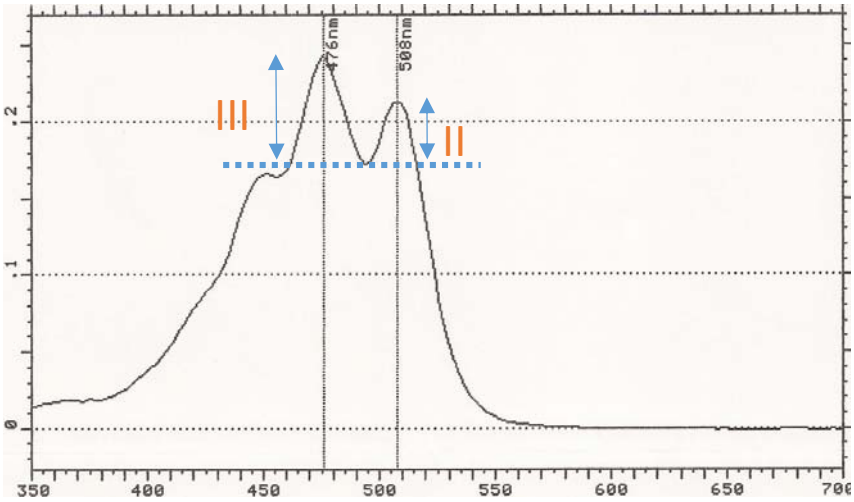

**A6.3. MC 81-11 (LC-MS of bioactive fractions from TLC band 2 and 3, 24-26mins)**

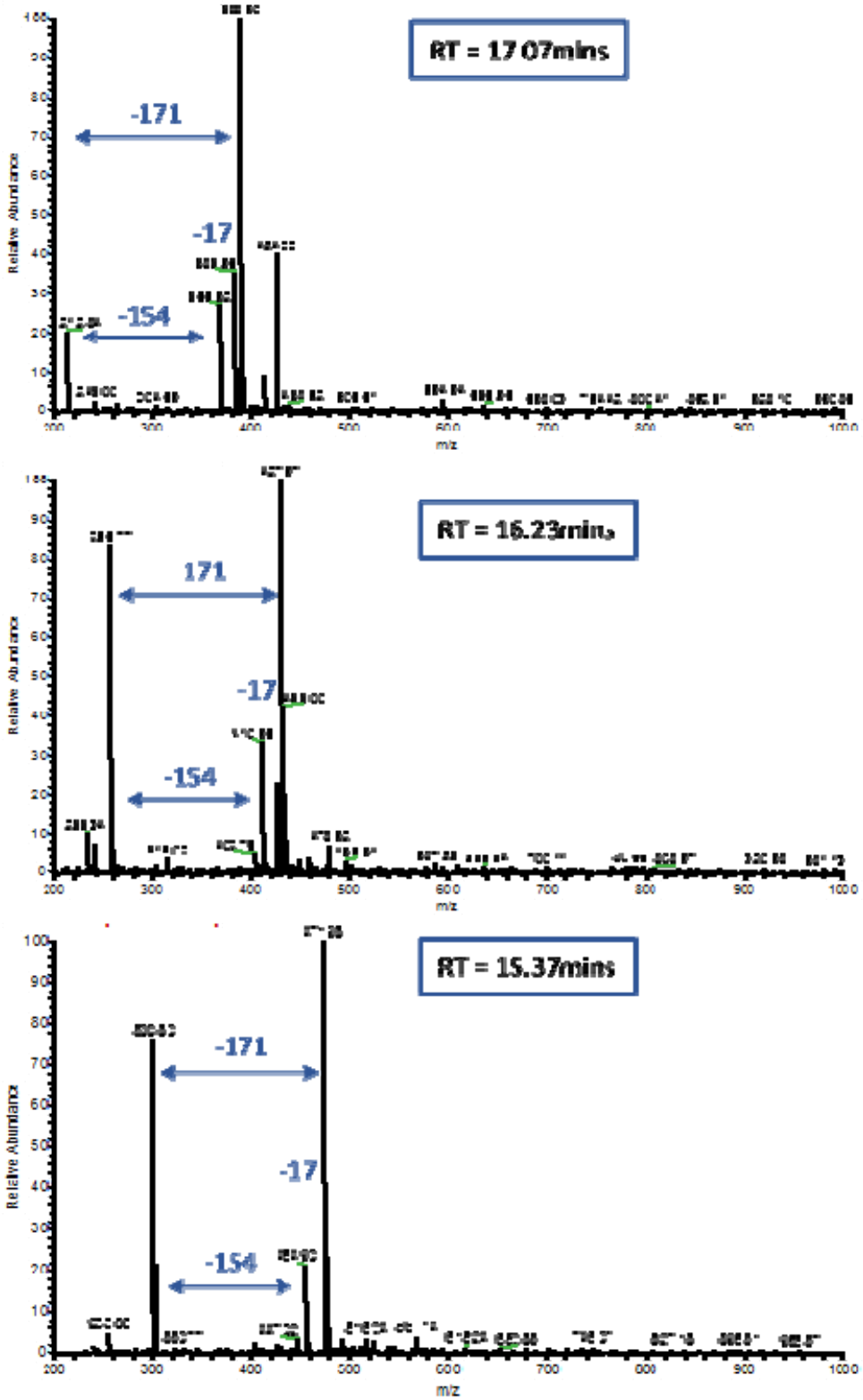

# VITA

ASHA JAJA-CHIMEDZA

Born, Kingston, Jamaica

## EDUCATION

| | |
|---|---|
| 2001-2005 | B.S. Chemistry<br>Florida Agricultural & Mechanical University<br>Tallahassee, Florida |
| 2007-2009 | M.Sc. Chemistry<br>Florida International University<br>Miami, Florida |
| 2009-Present | Doctoral Candidate<br>Florida International University<br>Miami, Florida |
| | Teaching Assistant<br>Florida International University<br>Miami, Florida |

## PUBLICATIONS AND PRESENTATIONS

Jaja-Chimedza, A.; Saez, C.; Gantar, M.; Gibbs, P.; Berry, J. Isolation of Polymethoxy-1-Alkenes as Toxic, Lipophilic Metabolites from Cultures of the Freshwater Cyanobacterial Species, *Cylindrospermopsis raciborskii*. *Journal of Natural Products*. In preparation.

Jaja-Chimedza, A.; Gantar, M.; Gibbs, P.; Schmale, M.; Berry, J. 2012 Polymethoxy-1-alkenes from *Aphanizomenon ovalisporum* inhibit vertebrate development in the zebrafish (*Danio rerio*) embryo model. *Marine Drugs*. 10(10), 2322-2336

Jaja-Chimedza, A.; Gantar, M.; Mayer, G.; Gibbs, P.; Berry, J. 2012 Effects of cyanobacterial lipopolysaccharides from microcystis on glutathione-based detoxification pathways in the zebrafish (*Danio rerio*) embryo. *Toxins* (Basel). 4(6), 390-404.

Berry, J.; Jaja-Chimedza, A.; Dávalos-Lind, L.; Lind, O. 2012 Apparent bioaccumulation of cylindrospermopsin and paralytic shellfish toxins by finfish in Lake Catemaco

(Veracruz, Mexico). *Food Addit Contam Part A Chem Anal Control Expo Risk Assess*. 29(2), 314-321.

Asha Jaja-Chimedza, Patrick Gibbs, Miroslav Gantar, John Berry. Contribution of Lipophilic Toxins to the Toxicity of Toxigenic Strains of Freshwater Cyanobacteria. (Oral) 2nd Gordon Research Seminar on Mycotoxins and Phycotoxins. Easton, MA, June 15-16, 2013.

Asha Jaja-Chimedza, Patrick Gibbs, Miroslav Gantar, John Berry. Contribution of Lipophilic Toxins to the Toxicity of Toxigenic Strains of Freshwater Cyanobacteria. (Poster and Oral) 16th Gordon Research Conference on Mycotoxins and Phycotoxins. Easton, MA, June 16-21, 2013.

Asha Jaja-Chimedza, Patrick Gibbs, Miroslav Gantar, John Berry. Inhibition of Vertebrate Development in Zebrafish (*Danio rerio*) Embryos Exposed to Polymethoxy-1-alkenes Isolated from Freshwater Cyanobacteria. (Oral) 15th International Conference on Harmful Algae. Changwon Gyeongnam, Korea, October 29 – Novermber 2, 2012.

Asha Jaja-Chimedza and John Berry. Apparent Lipophilic Toxins from a Microcystis Strain Isolated from the Great Lakes. (Poster) *6th Symposium on Harmful Algae in the US*. Austin, TX, November 13-18, 2011.

Asha Jaja-Chimedza. Purification and Characterization of Isotactic Polymethoxy Alkenes from Known Toxigenic Strains of Cyanobacteria. (Oral) *33rd Annual Southeastern Phycological Colloquy*. Miami, FL, October 14, 2011

Asha Jaja-Chimedza, Patrick Gibbs, John Berry. Cyanobacterial Developmental Toxins: Identification, Isolation, and Characterization. (Poster) *2010 Joint Annual Meeting of the American Society of Pharmacognosy & the Phytochemical Society of North America*. St. Petersburg, FL, July 10-14, 2010.